# JET PROPULSION

*Journal of the*
AMERICAN ROCKET SOCIETY
*Rocketry . . . . Jet Propulsion Sciences . . . . . Astronautics*



VOLUME 24 MARCH-APRIL 1954 NUMBER 2



IAF CONGRESS, AUG. 2–8 INNSBRUCK, AUSTRIA SEE PAGE 124

## Scope of JET PROPULSION

JET PROPULSION, the Journal of the American Rocket Society, is devoted to the advancement of the field of jet propulsion through the publication of original papers disclosing new knowledge and new developments. The term "jet propulsion" as used herein is understood to embrace all engines that develop thrust by rearward discharge of a jet through a nozzle or duct; and thus it includes systems utilizing atmospheric air and underwater systems, as well as rocket engines. JET PROPULSION is open to contributions, either fundamental or applied, dealing with specialized aspects of jet and rocket propulsion, such as fuels and propellants, combustion, heat transfer, high temperature materials, mechanical design analyses, flight mechanics of jet-propelled vehicles, astronautics, and so forth. JET PROPULSION endeavors, also, to keep its subscribers informed of the affairs of the Society and of outstanding events in the rocket and jet propulsion field.

## Limitation of Responsibility

Statements and opinions expressed in JET PROPULSION are to be understood as the individual expressions of the authors and do not necessarily reflect the views of the Editors or the Society.

## Subscription Rates

| | |
|---|---|
| One year (six bimonthly issues) | $10.00 |
| Foreign countries, additional postage | add .50 |
| Single copies | 1.75 |
| Special issues, single copies | 2.50 |
| Back numbers | 2.00 |

## Change of Address

Notices of change of address should be sent to the Secretary of the Society at least 30 days prior to the date of publication.

## Information for Authors

### *Preparation of Manuscripts*

Manuscripts must be double spaced on one side of paper only with wide margins to allow for instructions to printer. Submit two copies: original and first carbon. Include a 100–200 word abstract of paper. The title of the paper should be brief to simplify indexing. The author's name should be given without title, degree, or honor. A footnote on the first page should indicate the author's position and affiliation. Include only essential illustrations, tables, and mathematics. References should be grouped at the end of the manuscript; footnotes are reserved for comments on the text. Use American Standard symbols and abbreviations published by the American Standards Association. Greek letters should be identified clearly for the printer. References should be given as follows: For Journal Articles: Title, Authors, Journal, Volume, Year, Page Numbers. For Books: Title, Author, Publisher, City, Edition, Year, Page Numbers. Line drawings must be made with India ink on white paper or tracing cloth. Lettering on drawings should be large enough to permit reduction to standard one-column width, except for unusually complex drawings where such reduction would be prohibitive. Photographs should be clear, glossy prints. Legends must accompany each illustration submitted and should be listed in order on a separate sheet of paper.

### *Security Clearance*

Manuscripts must be accompanied by written assurance as to security clearance in the event the subject matter of the manuscript is considered to lie in a classified area. Alternatively, written assurance that clearance is unnecessary should be submitted. Full responsibility for obtaining authoritative clearance rests with the author.

### *Submission of Manuscripts*

Manuscripts should be submitted in duplicate to the Editor-in-Chief, Martin Summerfield, Professor of Aeronautical Engineering, Princeton University, Princeton, N. J.

### *Manuscripts Presented at ARS Meetings*

A manuscript submitted to the ARS Program Chairman and accepted for presentation at a national meeting will automatically be referred to the Editors for consideration for publication in JET PROPULSION, unless a contrary request is made by the author.

### *To Order Reprints*

Prices for reprints will be sent to the author with the galley proof, and orders should accompany the corrected galley when it is returned to the Managing Editor.


# JET PROPULSION

*Journal of the*
AMERICAN ROCKET SOCIETY







JET PROPULSION, the Journal of the American Rocket Society, published bimonthly by the American Rocket Society at 20th and Northampton Streets, Easton, Pa., U.S.A. The Editorial Office is located at the Engineering Societies Building, 29 West 39th Street, New York 18, N. Y. Price $1.75 per copy, $10.00 per year. Entered as second-class matter at the Post Office at Easton, Pa., under the Act of March 3, 1879.

# HOW TO KICK OFF A ROCKET
## in the right direction

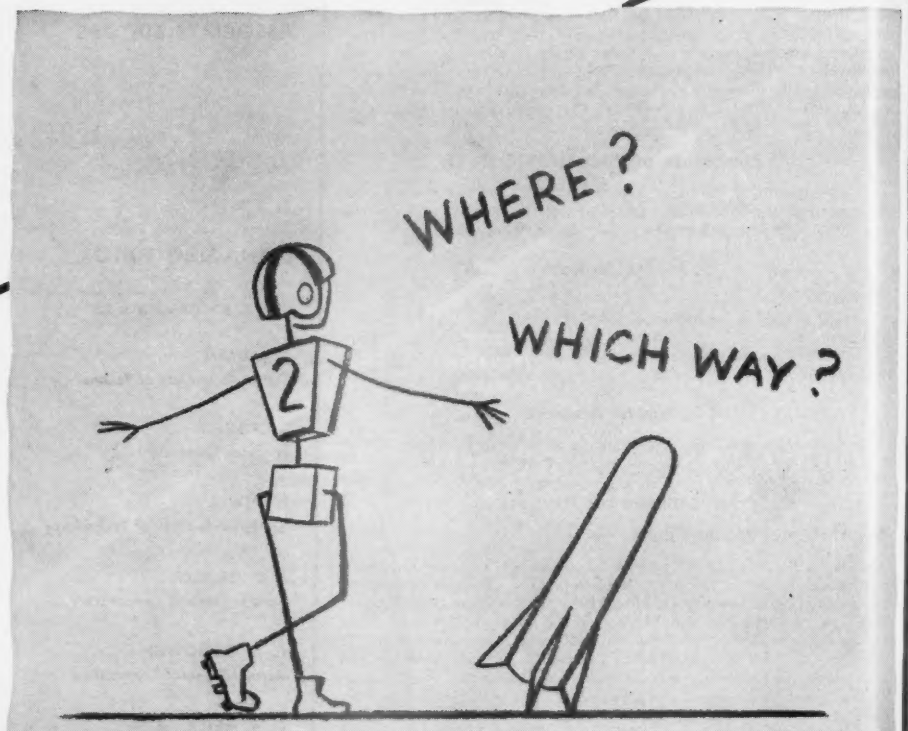


**...and FORD was asked to find the answer**

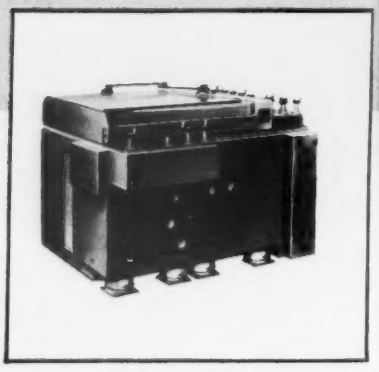

Load! Aim! Launch! And off goes a rocket from shipboard . . . but not without precise devices that start the rocket in the right direction. Devices . . . such as Ford Instrument has manufactured for the Armed Forces since 1915. For from the vast engineering and production facilities of the Ford Instrument Company, come the mechanical, hydraulic, electro-mechanical, magnetic and electronic instruments that bring us our "tomorrows" today. Control problems of both Industry and the Military are Ford specialties.

14

**You can see why a job with Ford Instrument offers young engineers a challenge. If you can qualify, there may be a spot for you in automatic control development at Ford. Write for brochure about products or job opportunities. State your preference.**

FORD

**FORD INSTRUMENT COMPANY**
**DIVISION OF THE SPERRY CORPORATION**
**31-10 Thomson Avenue, Long Island City 1, N. Y.**

# RYAN builds ROCKET MOTORS for 3000 mile-per-hour missiles

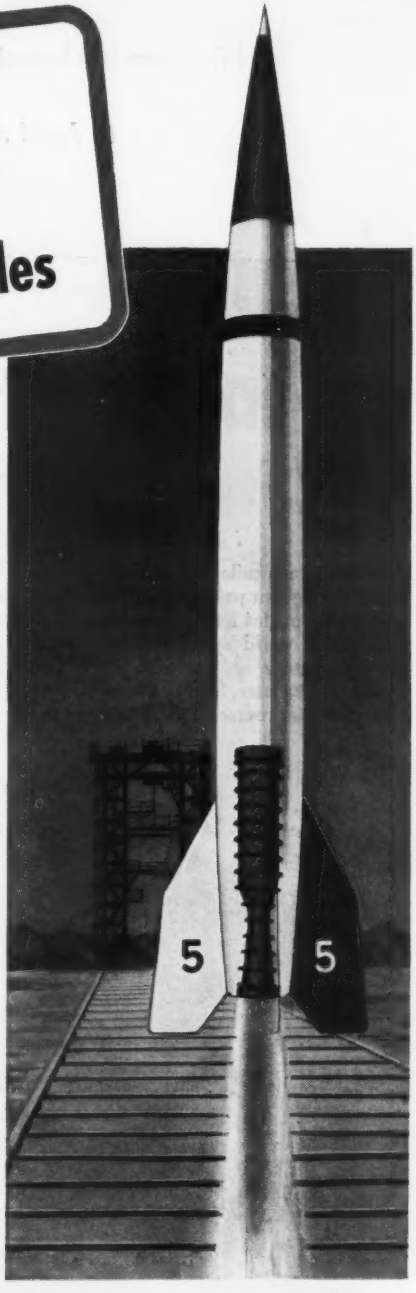


IMAGINE a motor powerful enough to propel a missile at speeds exceeding 3000 mph . . . so powerful that its developed thrust can amount to tens of thousands of pounds. One of Ryan's most challenging current assignments is the complete production of such a motor for an Army Ordnance surface-to-surface missile.

There was a many-sided problem of fabrication, welding and machining that Ryan had to solve in connection with rocket motor manufacture. Because a rocket motor is capable of burning as much as a ton of fuel a minute at temperatures up to 5000 degrees F., terrific internal pressures are created that must be contained in a very compact package of complex construction and exacting dimensions.

The solution was found in perfecting new techniques for forming, welding and machining the special alloy materials. Ryan devised new methods of controlling work to very close tolerances; ingenious electric resistance and arc welding processes and a better furnace brazing system . . . plus intricate machine operations that had to be jewel-like in precision.

Ryan's proved ability in the production of complete rocket motors is due in large measure to its long experience in building the "hot end" of jet and piston engines. Its versatility in many specialized fields is an important advantage in each new assignment, for it enables every division to draw on 31 years of first hand experience in the most advanced phases of aviation engineering and production.

Thus, each year more unique technical engineering and production projects are awarded Ryan . . . an integrated company with superior abilities in meeting the challenges of today's high-speed air age.

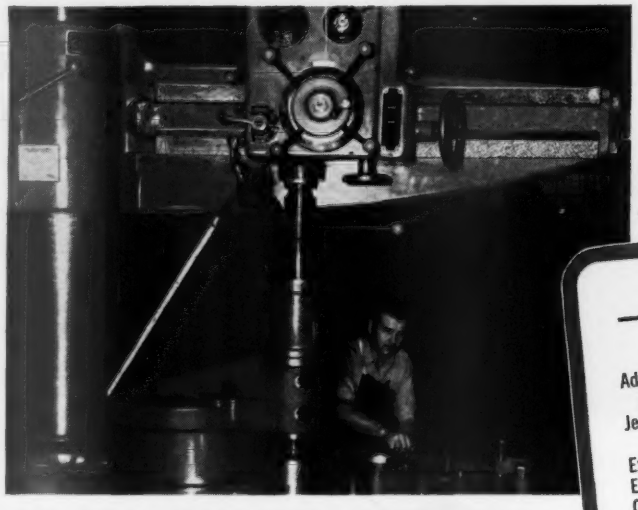

**RYAN** SPECIALIZED INGENIOUS VERSATILE

Advanced-type Aircraft and Components
Jet and Rocket Engines and Components
Exhaust Systems for Aircraft
Electronics Equipment
Ceramics for "Hot Parts"
Weapons Systems Design and Management
Aircraft and Power Plant Research
Metallurgical Engineering
Thin-Wall Ducting
Firebee Pilotless Jet Planes

PIONEERS IN EACH ★ LEADERS IN ALL

**RYAN AERONAUTICAL COMPANY**
Factory and Home Offices: Lindbergh Field, San Diego 12, California
OTHER OFFICES: WASHINGTON, D.C.; DAYTON, OHIO; SEATTLE, WASH.; NEW YORK CITY

*First carrier-based airplane*

*to hold a world's speed record*

753.4 m.p.h.

*the U.S. Navy's*

# Douglas F4D Skyray

Streaking each mile in *less* than 5 seconds, during four passes at a 3-kilometer course, a Douglas F4D Skyray returned the official world speed record to the United States.

Two weeks later, Skyray blazed into a 100-kilometer course, cracked all records by an even wider margin. Now in production for the Navy, this delta wing jet interceptor adds terrific climb and firepower to its speed—plus the ease of handling needed in carrier landings. The Douglas F4D Skyray has now passed its initial carrier tests, in service will guard our fleets against the fastest of modern jet bombers.

Performance of the Navy's F4D Skyray is another example of Douglas leadership in aviation. Faster and farther with a bigger payload is always the basic rule of Douglas design.


*Be a Naval Aviator—*
*write Nav. Cad.*
*Washington 25, D.C.*

**Depend on *DOUGLAS*** **First in Aviation**

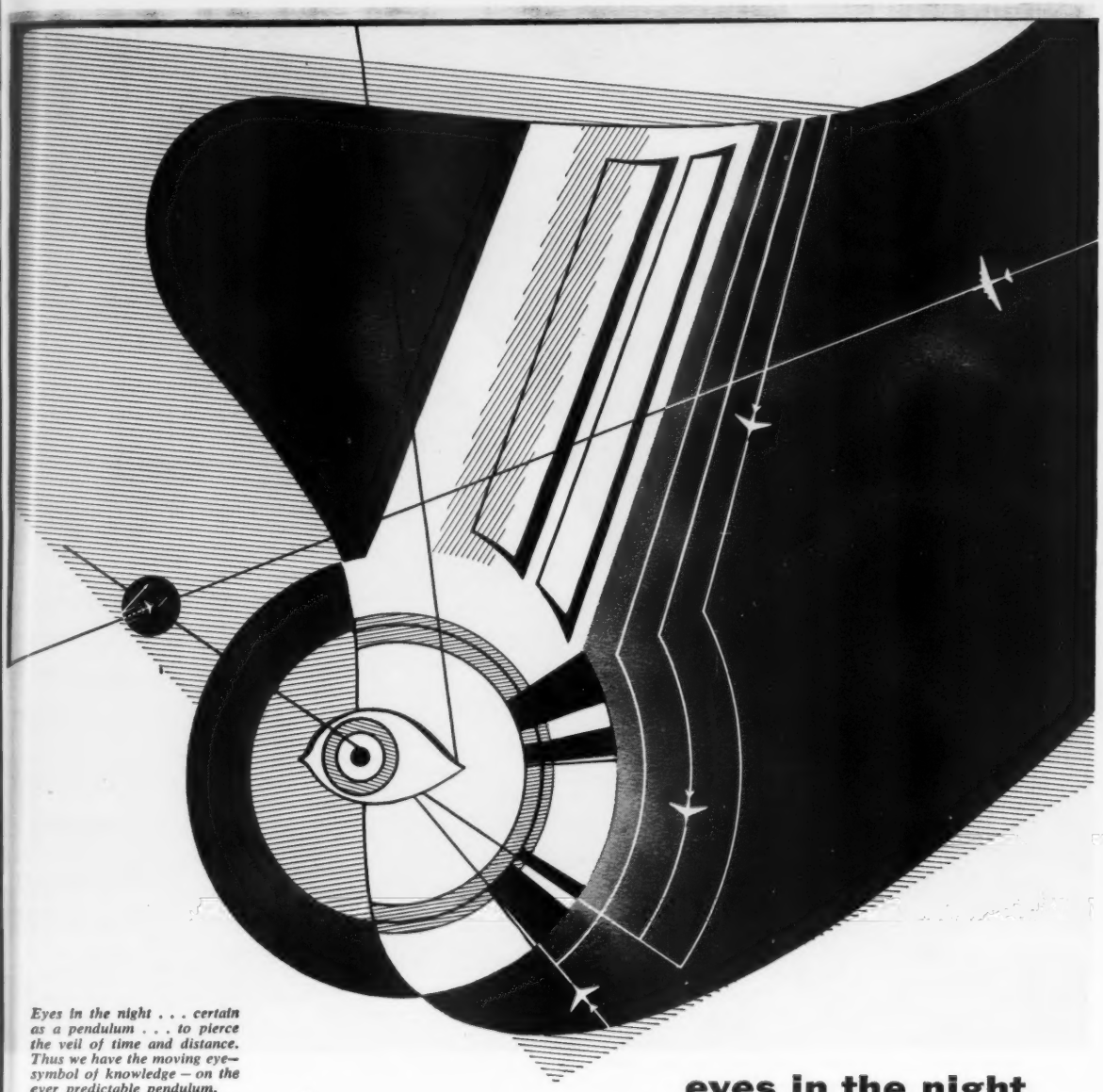

*Eyes in the night . . . certain as a pendulum . . . to pierce the veil of time and distance. Thus we have the moving eye—symbol of knowledge — on the ever predictable pendulum.*

## eyes in the night

The victory over time and darkness is certain with Kollsman instruments. Certain because of our quarter century dedication to accuracy in controls and instrumentation.

Today our activities encompass four fields:

**AIRCRAFT INSTRUMENTS AND CONTROLS**
**OPTICAL PARTS AND DEVICES**
**MINIATURE AC MOTORS**
**RADIO COMMUNICATIONS AND NAVIGATION EQUIPMENT**

Our manufacturing and research facilities . . . our skills and talents, are available to those seeking solutions to instrumentation and control problems.

**kollsman** INSTRUMENT CORP.

ELMHURST, NEW YORK • GLENDALE, CALIFORNIA • SUBSIDIARY OF *Standard* COIL PRODUCTS CO. INC.

# Air Strike....Submarine Style

**Guided missiles launched from submarines promise to be major offensive weapons in case of war. A missile of this type travels to its distant destination under unerring electronic orders. The brain center for such missiles will be typical of the electronic systems developed and manufactured by Arma Corporation.**

**In close collaboration with the Armed Forces since 1918, and more recently with the Atomic Energy Commission, Arma has contributed much in basic research, design, development and manufacture to the advancement of electronic and electromechanical weapon control, navigation, and other precision remote control systems. There is every reason to believe that engineering background and techniques—first used successfully in these devices —will see widespread industrial applications.** ***Arma Corporation, Brooklyn, N. Y.; Mineola, N. Y. Subsidiary of American Bosch Corporation.***

**ARMA** ADVANCED ELECTRONICS FOR CONTROL

MARCH-APRIL 1954

VOLUME 24 NUMBER 2

JET PROPULSION
Journal of the
AMERICAN ROCKET SOCIETY

Editor-in-Chief

MARTIN SUMMERFIELD

# Ramjet Diffusers at Supersonic Speeds[1]

FRANCIS H. CLAUSER[2]

The Johns Hopkins University, Baltimore, Md.

**By using a few basic principles of compressible flows, it is shown that even simple ducts will show interesting properties at supersonic speeds. This knowledge is applied to the diffuser problem and a picture is given of the pressure recoveries and drags to be expected and of the hysteresis phenomena that will occur. A discussion is given of the behavior of the flow in a ramjet, including some of the problems of aerodynamic control. It is shown that the recovery of simple diffusers at high Mach numbers is poor, and ways of using more complex diffusers to improve the efficiencies are discussed. A final section is devoted to a consideration of some of the flow instabilities that can occur in ramjets.**

## Behavior of a Simple Duct at Supersonic Speeds

IN DISCUSSING the problem of introducing and expelling air from missiles and aircraft at supersonic speeds, I believe it is instructive to start with the simplest kind of a duct and investigate its characteristics, seeing if it offers flow phenomena of interest. We start with a section of cylindrical pipe oriented with its axis parallel to a supersonic airstream. We imagine that the pipe is so constructed that its internal area can be reduced, as shown by the dotted lines in Fig. 1.

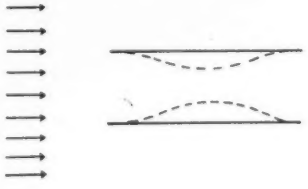

FIG. 1. SCHEMATIC DIAGRAM OF A SIMPLE DUCT

For the moment we keep the picture as simple as possible by neglecting skin friction and assuming that the internal flow is uniform across any normal cross section.

For the unrestricted pipe, the flow goes through at the speed of the free stream. If the internal area is reduced, the velocity of the flow, in contrast to the subsonic case, goes down as is known from elementary analysis in compressible fluids. As the area reduction is carried farther, the Mach number at the throat decreases until the limiting value of $M = 1$ is reached. Throughout this process, the mass flow has been constant and equal to product of the free stream density and velocity times the entrance area. However, if the internal area is reduced to less than its value when $M = 1$ at the throat, this condition of constant mass flow is no longer possible. The minimum area acts as a "choke" or throttle, reducing the flow through the duct. This reduction is communicated to the oncoming flow by a compression wave originating at the throat and traveling upstream in the duct. It is clear that this compression wave cannot remain stationary in the duct. It quickly develops into a shock wave and the resulting entropy increase of the fluid passing through it lowers the pressure at the minimum section (but does not change the corresponding velocity or temperature). The resulting decrease in density causes a further reduction in mass flow. As a consequence, a second compression wave is formed which overtakes and coalesces with the first wave, moving upstream in the duct to a position of higher Mach number. This process will be repeated until the shock wave is expelled at the entrance and forced far enough upstream so that a portion of the oncoming flow can spill around the lips to take care of the reduced flow through the duct (see Fig. 2).

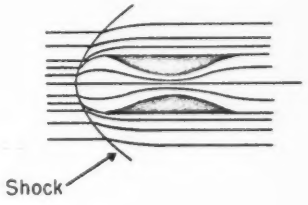


FIG. 2. FLOW PATTERN WHEN DUCT IS CHOKED

If the internal area continues to be reduced, the shock wave does not increase in intensity but moves forward enough to allow a greater amount of spillage around the lips.

Now let us imagine the procedure to be reversed, i.e., the throat area to be increased. The question arises: When the throat area exceeds the value at which the choking first occurs (and the shock appears), is the shock swallowed in the duct from whence it came? It is apparent that it does not because the reduced density fluid passing through the throat cannot permit the shock to retreat to the entrance down which it must be swallowed. In fact, the internal area must be increased by the inverse ratio of the lowered throat density before the shock will be swallowed and the regime of constant mass flow re-established.

Let us re-examine the above by considering the pressure distribution of the fluid as it passes through the duct. When there is no reduction in the internal area, the pressures are equal to the free stream value throughout the duct, as shown

[1] EDITOR'S NOTE: This paper is based on a lecture given originally at the Symposium on Supersonic Aerodynamics held at The Johns Hopkins University, December 6, 1945. It was selected by the editors for publication at this time in response to suggestions that have been received from ARS members to the effect that a general introduction to the ramjet diffuser, nonmathematical yet advanced in viewpoint, would be a welcome addition to the literature.

[2] Chairman, Department of Aeronautics.

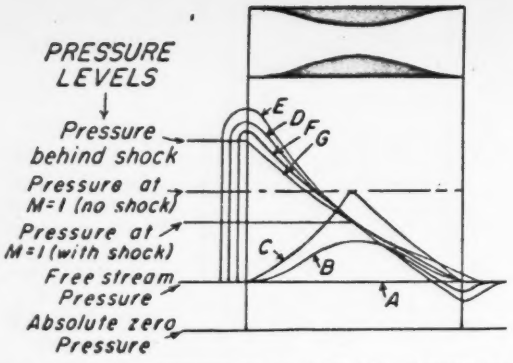


FIG. 3 PRESSURE DISTRIBUTION IN DUCT FOR VARIOUS FLOW PATTERNS

by line A in Fig. 3. When the area reduction is moderate, the pressure rises to a maximum and falls as shown by B. When the area is reduced so that $M = 1$ at the throat, the pressure is given by C. With further reduction in area, the pressures no longer follow this pattern. Instead, a shock forms in front and the pressures become nonsymmetrical as shown by D. It will be noticed that there is an abrupt rise in pressure through the shock, a further subsonic compression to the entrance of the duct, then an expansion through the velocity of sound at the minimum section to supersonic velocities in the rear. The pressure at the minimum section, corresponding to $M = 1$, is lower than it was before the shock appeared because of the entropy rise through the shock. This causes the flow to reach the exit at less than free-stream pressure and compression must take place in the exit jet. Continued reduction of the internal area simply exaggerates this pressure distribution without changing its pattern as exemplified by E.

If, now, the area is increased beyond its value corresponding to D, the pressure pattern will not immediately return to the symmetrical case typified by C and B but will continue on the nonsymmetrical sequence F and G. At G, the area has been increased to such an extent that the shock wave has moved back to the mouth of the entrance. Any further increase in area allows the wave to move back into the duct where it becomes unstable. The procedure of originally forming the shock will be reversed and the shock swallowed by the duct. However, the shock disappearance occurs at a different area than that at which it appeared.

An interesting phenomenon takes place at the exit during the sequence EDFG. As mentioned previously, when the shock first appears D, the flow arrives at the exit with a pressure lower than free stream and compression must take place in the exit jet. However, in the process of increasing the throat area, it turns out that a condition F is reached, before the shock disappears, for which the expansion from throat to exit is so small that the fluid arrives at the exit with free-stream pressure. In the limiting case G, the exit pressure is always above free stream and expansion will take place in the exit jet. Here we have the interesting phenomenon of flow experiencing an entropy rise and yet rejoining the isentropic external flow, at an increased pressure.

When we examine the pressure distributions, we see that under our assumptions the duct has no drag for the cases A, B, and C because the pressures are symmetrical and have no resultant rearward component. However, when the shock appears in cases D, E, F, and G, higher pressures act on the forward facing areas than on the rearward facing areas, resulting in a large drag. One frequently sees statements in connection with tests of ducted models that a shock wave in front causes high external drag. I believe that the observed drag increase is really atrributable primarily to the internal flow and not the effect of the shock on the external flow.

## Hysteresis of Entry Flow

In our consideration of flow in a simple duct, we have noticed that there is a hysteresis in the flow pattern as the throat area is changed. This is probably best illustrated by the graphs of Fig. 4 showing mass flow and drag as a function of the throat area.

When the throat area is equal to the entrance area, we start at the point A, and as the throat is reduced we travel to B. During this time the drag has been zero and the mass flow constant. At B, we have $M = 1$ in the throat and the shock appears ahead of the duct. The mass flow drops and the drag rises to C. A further reduction in area takes us to the point D. Upon reversing the procedure and increasing the area, the conditions do not follow the line from C to B, but the area must be increased to E before the shock retreats to

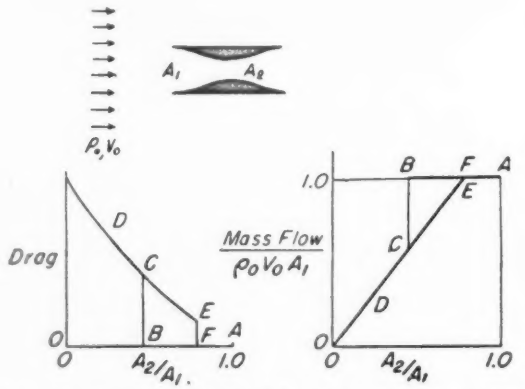


FIG. 4 HYSTERESIS OF DRAG AND MASS FLOW IN A SIMPLE DUCT

the mouth of the duct. The shock then disappears and we go to F, back on the original curve from A to B. It is clear that BCEF is hysteresis loop and that we must know the previous history as well as the present geometry to ascertain the flow conditions existing in the duct.

Under our previous assumptions of no friction and uniform flow across any duct section, it is a straightforward procedure to compute the mass flows and drags for several Mach numbers, as well as the area ratios and pressure ratios as a function of Mach number. This has been done and the results presented on the four accompanying graphs of Fig. 5.

The first graph shows internal drag coefficient versus the ratio of throat area to entrance area for the Mach numbers 1, 2, 3, 4. It will be noticed that the drags are quite high, being of the same order as the external drag for projectiles.

The second graph presents mass flow coefficient versus area ratio for the same set of Mach numbers. It shows clearly the large reductions in mass flow that occur when the shock appears at high Mach numbers. Both the drag curves and the mass flow curves illustrate how rapidly the region of hysteresis broadens out with increasing Mach number. This indicates that at Mach numbers only a little above 1, a small amount of unsteadiness in the airstream causes the flow pattern to shift from one type to the other, in some cases even obscuring the existence of a hysteresis phenomenon. However, at higher Mach numbers each flow pattern has wide ranges of stable existence; so much so that major changes in duct geometry are required to go from one pattern to the other.

The third graph presents the ratio of throat area to entrance area for which the shock appears and disappears as a function of Mach number. It shows how great the constriction must be to produce a shock at high Mach numbers and how slight the constriction permissible to insure that no shock is present.

The fourth graph shows how much the pressure is reduced

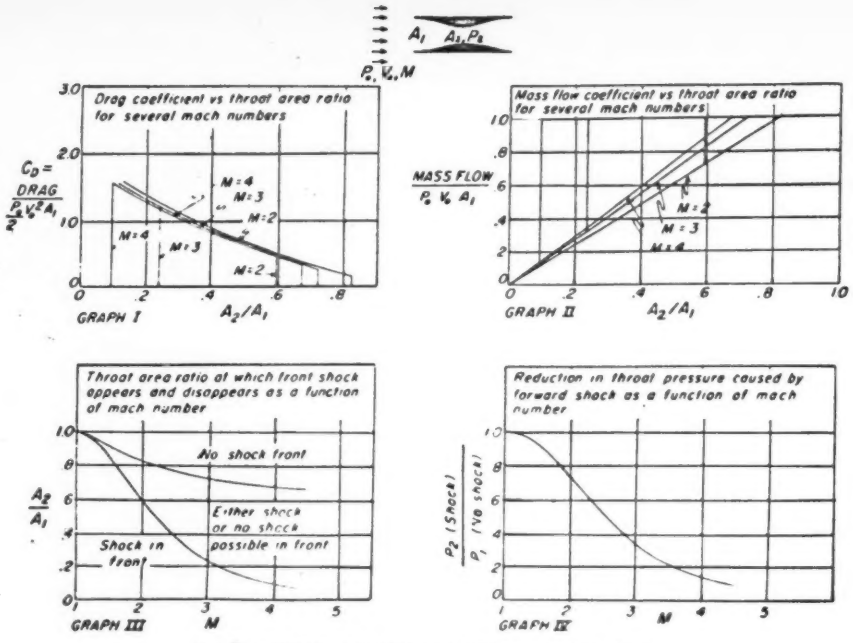


FIG. 5 SUMMARY OF PERFORMANCE OF A SIMPLE DUCT

at the throat by the presence of the shock wave. This curve can also be interpreted as the ratio of the maximum pressure recovery possible behind the shock to the recovery if the compression were reversibly adiabatic. It shows quite clearly the enormous losses incurred if the shock is present at high Mach numbers.

## Behavior of Ducts at Different Speeds

In all of our previous discussion we have varied the throat area of the duct in a constant Mach number stream. Let us now observe the behavior of a fixed duct as the Mach number is changed. This is the case of interest in actual missile or aircraft work. We begin our observation at the instant when the missile is accelerating through the Mach number one. We see from the third graph that if the throat is constricted at all, the only possible flow pattern is with the shock wave in front. This is highly significant, because it means that a duct system, with even the slightest constriction, enters the supersonic regime with a shock wave in front. Consequently, no fixed geometry duct of this type could be expected to operate with shock free flow using a throat area designed to reduce the Mach number to nearly one at operating speed unless the missile is first overspeeded until the shock is swallowed and then allowed to return to the operating speed (a maneuver not frequently possible in practice).

It is interesting to compare the results predicted by the simplified theory given above with some results actually observed in practice. The first experiments made on such a simple duct were those by Ferri (1)[3]. He was investigating a two-dimensional biplane proposed by Busemann, who arrived at a conclusion similar to ours (by different reasoning) that an internal flow system (in his case, two-dimensionally disposed to form wings) could have very small drags because of the nearly symmetrical fore and aft pressure distribution. However, when first proposed, it was not realized that the nonsymmetrical pressure distribution with shock in front was also possible and that this latter case is the one present when the supersonic regime is first entered. Ferri's model, tested at a Mach number of approximately 2, had an area ratio of 0.705, which is in the region of hysteresis. Consequently, when the tunnel was brought up to speed, the observed flow pattern was always the one with the shock present and not the one predicted by Busemann, which proved somewhat disconcerting. Later it was found that by spreading the two wings apart (increasing the ratio $A_2/A_1$) the shock could be made to disappear suddenly and the Busemann-type flow established.

The drag of the biplane was measured for each of the types of flow possible and it was found that $C_D = 0.298$ when the shock was present ahead of the model. Our simple theory, neglecting friction, predicts a value of $C_D = 0.30$. A reasonable estimate for skin friction ($C_f = 0.003$) increases the predicted value of $C_D$ to 0.329 (the ratio of wetted area to frontal area is 9.6:1). This agreement is considered encouraging. When no shock was present, the drag dropped to about $1/7$ of the value with shock. Since this low drag can be largely accounted for by skin friction, this result also indicates no significant disagreement with theory.

An interesting discrepancy between our conclusions, based on the assumption of uniform flow across any section and the actual two-dimensional flow, can be seen in the schlieren

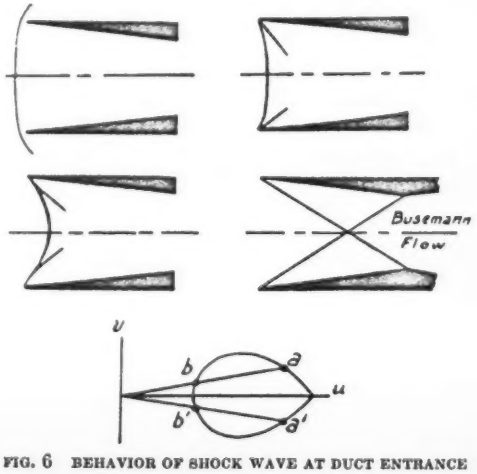


FIG. 6 BEHAVIOR OF SHOCK WAVE AT DUCT ENTRANCE

[3] Numbers in parentheses refer to the References on page 94.

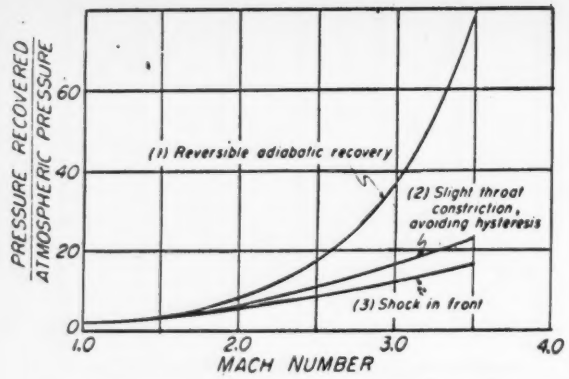


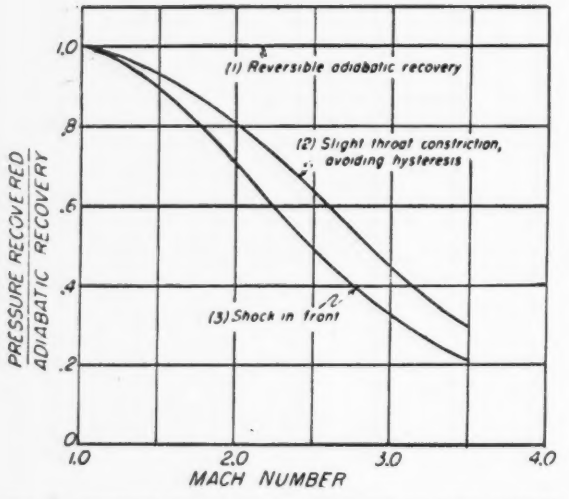


FIG. 7 PRESSURE RECOVERY AS A FUNCTION OF MACH NUMBER

photographs of Ferri, drawings of which are reproduced in Fig. 6. We predicted that when the shock had retreated to the mouth of the entrance it would become unstable and be swallowed. Actually, the shock wave retreats a considerable distance inside the entrance before it is swallowed. The normal shock curves into diagonal shocks at the ends and the entire system is swallowed when very little of the normal shock is left. These extremal diagonal shocks correspond to the "second" solutions, $b$ and $b'$ of the shock polar. The interior portions of the shock wave correspond to the portion of the shock polar between $b$ and $b'$. After this system is swallowed, the completely supersonic flow predicted by Busemann is established with diagonal shocks corresponding to the "first" solutions, $a$ and $a'$ of the shock polar.

## Diffusers for Supersonic Ramjets

At this point, we attempt to apply some of the results of our previous discussion to the problem of obtaining efficient pressure recovery in an air intake for a supersonic ram jet. A glance at Fig. 7 shows that the maximum possible recoveries at high Mach numbers are remarkably large, being of the order of 20 or more times atmospheric pressure. This is in contrast to the more familiar subsonic pressure rises which are only a fraction of an atmosphere. The figure also shows how

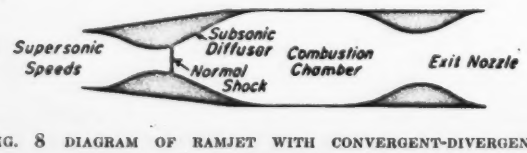


FIG. 8 DIAGRAM OF RAMJET WITH CONVERGENT-DIVERGENT DIFFUSER

much the maximum pressure recoveries are lowered by the presence of a normal shock wave ahead of the intake at high Mach numbers. Consequently, we are tempted to consider the arrangement shown in Fig. 8.

The air is decelerated in a simple converging entrance to a Mach number a little above 1 at the throat. The transition to subsonic Mach numbers is by means of a normal shock maintained in the diverging portion as shown (if the shock is in the converging portion, it is unstable as we have seen previously). Since the normal shock takes place at lower Mach numbers where the losses are small, this arrangement can provide acceptable recoveries if the subsonic diffusion losses are kept low. However, this arrangement is not without its problems. First, the normal shock must be maintained in its position behind the throat. This can be accomplished either by varying the exit throat area (the final exit area cannot be used for this control because in its usable range it has no effect on the combustion chamber pressure) or by varying the density of the exhaust gases by the heat released in the combustion chamber. If the combustion chamber pressure is decreased by these controls, the normal shock will move back in the diffuser to a point of higher Mach number and its loss will rapidly increase. If the chamber pressure is increased, the shock will move into the throat and, if overcontrolled, will pass through the throat and out the converging section to assume a position ahead of the entrance, nullifying the advantage of this arrangement. If the control is reversed and the chamber pressure lowered, the shock will not be swallowed, as we have seen from our previous discussion. What occurs is that the air will accelerate in the converging section to $M = 1$ at the throat and a second shock will form in the diffuser. The only way to remove the forward shock is either to speed up the vehicle or provide some means of varying the ratio of throat area to entrance area. Neither expedient can be said to be convenient.

This forward shock condition is encountered not only when the throat shock is inadvertently regurgitated, but is sure to be present after the supersonic regime is first entered by the vehicle. It is again encountered when the question of the stability of the flow is considered. In order to maintain low loss, the shock must be positioned near the throat where its stability is not great. The inevitable huffing and puffing of the combustion process will repeatedly force the shock out the intake. After each expulsion the process of swallowing

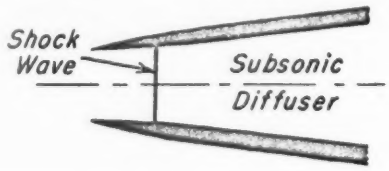


FIG. 9 DIVERGENT DIFFUSER FOR LOW SUPERSONIC MACH NUMBER

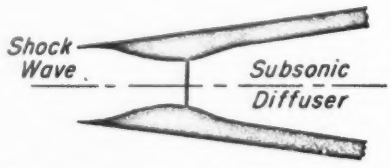


FIG. 10 CONVERGENT-DIVERGENT DIFFUSER FOR INTERMEDIATE SUPERSONIC MACH NUMBERS

the shock must be repeated. All things considered, this arrangement does not appear to have too bright a future.

The foregoing suggests that, in practice, intakes may be classed in three Mach number ranges.

1 In the range of $1<M<1.5$, simple diverging entrances such as the one shown in Fig. 9 may be used. In this Mach number range, the pressure loss through the shock will be

about 10 per cent or less. This simple diverging entrance avoids all hysteresis phenomena and eliminates the necessity of changing entrance geometry to swallow the shock. The greatest recoveries possible with this entrance are given by curve 3 of Fig. 7.

2 In the range $1.5<M<1.7$, entrances may be used in which a converging-diverging nozzle is used (Fig. 10), but the constriction is so slight that at operating speed, hysteresis is always avoided. Reference to the third graph of Fig. 5 shows that the constriction will be about 10 per cent. This modest area reduction proves sufficiently beneficial so that the maximum recoveries in this higher Mach number range are as great as those of the simple entrance in the lower range. When used at speeds lower than the design speed, this entrance will probably have a shock in front most of the time, but at these lower speeds, the shock losses are small enough to cause no trouble. This type of entrance has been tested by Kantrowitz and Donaldson (2) and the preliminary results show that it can be successfully used. The greatest recoveries possible with this entrance are given by curve 2 of Fig. 7.

3 In the range $M>1.7$ it is desirable to use entrances having more complex supersonic flow patterns which are designed to avoid the troubles we encountered in our high efficiency converging-diverging entrance. We shall discuss such entrances at greater length in the following paragraphs.

## Diagonal Shock Diffusers

In our original discussion of flow in a simple duct, we postulated a simple one-dimensional flow. This postulate has been retained throughout the above discussion and this retention has forced us to overlook some very useful means of decelerating a supersonic stream efficiently. The unidimensional postulate permitted only normal shock waves which are unacceptably inefficient at high Mach numbers. However, if we consider the possibility of using diagonal shock waves, this proves to be a fruitful field of investigation. We find that a single diagonal shock wave can reduce the Mach number from 2.5 to 2.0 with only a 5 per cent loss in recoverable pressure. If we place a slightly constricted entrance in the flow behind a diagonal shock, as shown in Fig. 11, the limiting recoveries are about 81 per cent. If a diverging entrance alone is used the limiting recoveries are about 50 per cent.

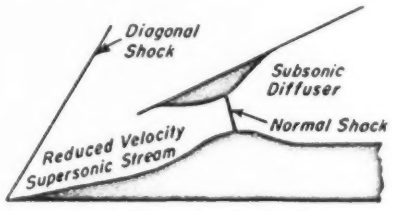


FIG. 11 DIFFUSER USING DIAGONAL SHOCK

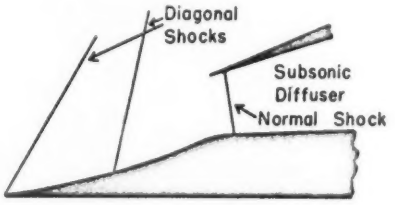


FIG. 12 DIFFUSER USING MULTIPLE DIAGONAL SHOCKS

A slightly constricted entrance by itself gives limiting recoveries of about 62%. The advantage of using the diagonal shock is quite apparent.

With such gains possible, it appears worth while to consider using multiple diagonal shocks, possibly followed by a simple diverging entrance as shown in Fig. 12. At $M = 2.5$, this will not improve the recovery greatly; however, at higher Mach numbers this procedure can be used quite effectively to maintain high levels of efficiency, as shown by Fig. 13. This was taken from a paper by Oswatitsch (3). It shows the limiting recoveries for multiple diagonal shocks and illustrates clearly the advantage of their use at high Mach numbers.

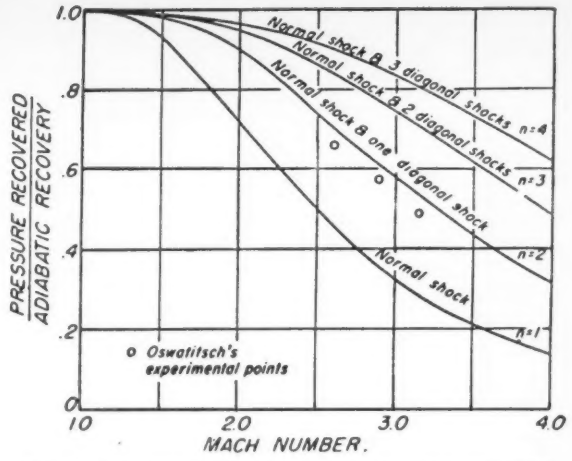


FIG. 13 PRESSURE RECOVERY OF DIAGONAL SHOCK DIFFUSERS

This type of entrance was first discussed by Ferrari, Oswatitsch, and Busemann. During World War II, tests were made in Germany at the Kaiser Wilhelm Institut, Göttingen, The Hermann Göring Institut, Braunschweig, and the Wasserbau Versuchsanstalt, Kochelsee, and the results indicated that superior efficiencies could be attained in practice. A few of Oswatitsch's results are indicated in Fig. 13. In all of the afore-mentioned tests, the entrance was constructed with circular symmetry by revolving the entrances shown above about the straight side parallel to the airstream.

The great disadvantage that this type of entrance appears to possess is the difficulty of keeping the drag within reasonable limits. High recoveries and low drags are somewhat incompatible. It will be remembered that the drag of a given surface element increases approximately as the square of its angle of inclination. On the other hand, high recoveries dictate large angles of inclination of the entrance. Some improvement can be had by reducing the projected area of the lower lip with the shocks focusing at the tip of the upper lip, as shown in Fig. 14. It is also helpful to curve the upper lip as shown. However, this must be done with care to prevent difficulties in the subsonic diffuser. In spite of these refinements, the drags are still large.

In searching for a means of reducing the drag, the question arises: If multiple diagonal shocks are used, do they all need to come from the same surface, or can they come from opposite surfaces, as shown in Fig. 15? The reduction in frontal area and drag is immediately apparent. it will be

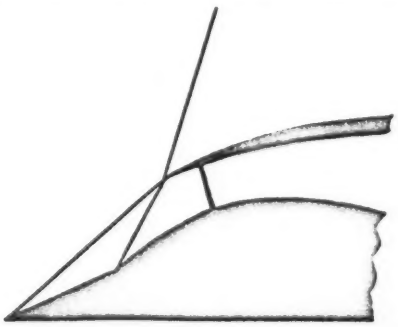

FIG. 14 DIAGONAL SHOCK ENTRY WITH CURVED DIFFUSER

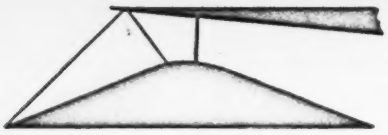

FIG. 15 DIFFUSER USING REFLECTED DIAGONAL SHOCK

remembered that the important parameter in determining hysteresis is the ratio of entrance area to throat area (when this ratio is one, as in the simple diverging entrance, no hysteresis is experienced). This type of entrance is evidently somewhat inferior in this respect to the higher drag entrances discussed above.

In examining the above entrance, it might be suspected that the interaction of the second diagonal shock with the sizable boundary layer of the lower lip might cause trouble. However, this is not the case because the tendency is to diminish the thickness of this boundary layer rather than cause separation. Such cases were encountered by Ferri (1). He found that when the shock does not intersect the boundary layer at the kink in the surface, the boundary layer distorts so that at its outer surface the kink is obligingly moved to the shock intersection point, as shown in Fig. 16. This helpful role of the boundary layer prevents the shock wave from being reflected by the solid surface and followed or preceded by an expansion fan when the shock does not exactly intersect the kink as designed.

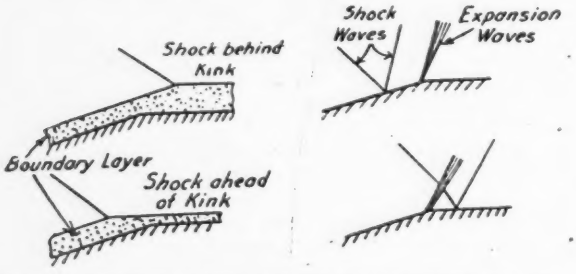


FIG. 16 SCHEMATIC DIAGRAM OF SHOCK-WAVE BOUNDARY-LAYER INTERACTION

Having gone this far in the use of diagonal shock waves to improve the pressure recovery characteristics of supersonic intakes, it is only natural to ask about the possibility of using diagonal compression waves, as shown in Fig. 17. In this case the extended lip is smoothly curved and isentropic compression takes place without shock losses. A glance at Fig. 13 shows that such an entrance would have a useful application at very high Mach numbers where the number of diagonal shocks required to obtain good recoveries would be so great that they would be almost indistinguishable from a uniform fan of compression waves. The low losses possible with this configuration makes its use attractive at lower Mach numbers as well.

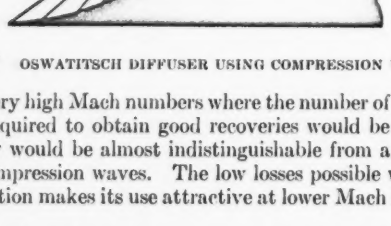

FIG. 17 OSWATITSCH DIFFUSER USING COMPRESSION WAVES

Oswatitsch made early tests on the entrance (see Fig. 17) which makes use of a fan of compression waves rather than discrete diagonal shocks. No unexpected difficulties were encountered. However, at the Mach numbers of his tests (about 2.9), Oswatitsch felt that the compression waves offered little gain over multiple diagonal shocks, and the former has the construction difficulty of a very fine point.

## Unstable Flow in Ramjets

At this point, we turn our attention to the effects of the entrance on the internal characteristics of a ramjet, and in particular the role the entrance can play in promoting oscillations in such a system. There are many ways in which a ramjet can have dynamic coupling that will produce oscillations, particularly as its control and fuel metering systems become more complex. Only a few simple examples will be treated here to illustrate the possible difficulties that can be encountered.

Our first example considers a ramjet operating with a simple diverging entrance. The ramjet is to be ignited in flight, but when tried this cannot be successfully accomplished. The test data have shown that the mixture strength is too lean at the instant of ignition. To remedy this, the fuel flow has been considerably increased. The burner now ignites properly but combustion temperatures increase the back pressure of the exit nozzle so much that air flow is reduced to about one third of its value before ignition. The mixture strength now becomes so very rich the fire is extinguished and the cycle begins over again for as long as the ignition system is left on.

In our second example, we suppose that the ramjet is equipped with a slightly constricted entrance in which the throat is large enough to avoid hysteresis. The fuel for the ramjet is supplied by constant flow nozzles which, by design or accident, are delivering an amount of fuel in excess of stoichiometric proportions. The exit throat, normally adjusted so that a normal shock would be just behind the entrance throat (as shown in Fig. 18), is actually constructed slightly smaller. This forces the shock wave through the throat and out in front. As soon as this occurs, the air flow diminishes because of the greater losses through the shock in front, causing a decrease in the air to fuel ratio and the temperature of combustion. This in turn decreases the back pressure of the exit nozzle, allowing the shock to be swallowed. However, in the beginning we saw that this condition was unstable and started the cycle of oscillation.

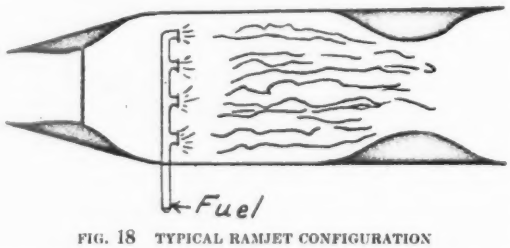


FIG. 18 TYPICAL RAMJET CONFIGURATION

For our last example we consider a ramjet missile having an entrance with a large constriction. It is operated in the range of hysteresis. If we suppose that the burner used operates poorly on lean mixtures and that the drag is less than anticipated in the design calculations, then we have the following possible sequence of events. After acceleration to design speed, a shock wave is present in front of the entrance. However, the thrust still exceeds the drag and the missile continues to accelerate with the drag, increasing only slightly more rapidly than the thrust. The missile reaches a Mach number at which the shock is swallowed. This results in a large air flow because of both the increased recovery and the high Mach number. The mixture ratio becomes quite lean and the burner operates poorly or not at all. The thrust decreases abruptly and the missile decelerates to a Mach number where the forward shock reappears, starting the cycle over again.

(*Continued on page 94*)

# Ignition and Combustion in a Laminar Mixing Zone[1]

FRANK E. MARBLE[2] and THOMAS C. ADAMSON, JR.[3]

California Institute of Technology, Pasadena, Calif.

**The analytic investigation of laminar combustion processes which are essentially two- or three-dimensional present some mathematical difficulties. There are, however, several examples of two-dimensional flame propagation which involve transverse velocities that are small in comparison with that in the principal direction of flow. Such examples occur in the problem of flame quenching by a cool surface, flame stabilization on a heated flat plate, combustion in laminar mixing zones, etc. In these cases the problem may be simplified by employing what is known in fluid mechanics as the boundary-layer approximation, since it was applied first by Prandtl in his treatment of the viscous flow over a flat plate. Physically it consists in recognizing that if the transverse velocity is small, the variations of flow properties along the direction of main flow are small in comparison with those in a direction normal to the main flow. The analytic description of the problem simplifies accordingly. The present analysis considers the ignition and combustion in the laminar mixing zone between two parallel moving gas streams. One stream consists of a cool combustible mixture, the second is hot combustion products. The two streams come into contact at a given point and a laminar mixing process follows in which the velocity distribution is modified by viscosity, and the temperature and composition distributions by conduction, diffusion, and chemical reaction. The decomposition of the combustible stream is assumed to follow first-order reaction kinetics with temperature dependence according to the Arrhenius law. For a given initial velocity, composition, and temperature distribution, the questions to be answered are: (1) Does the combustible material ignite; and (2) how far downstream of the initial contact point does the flame appear and what is the detailed process of development. Since the hot stream is of infinite extent, it is found that ignition always takes place at some point of the stream. However, when the temperature of the hot stream drops below a certain value, the distance required for ignition increases so enormously that it essentially does not occur in a physical apparatus of finite dimension. The complete development of the laminar flame front is computed using an approximation similar to the integral technique introduced by von Kármán into boundary layer theory.**

## Nomenclature

$A$ = activation energy, cal/mole/°K
$c_p$ = specific heat at constant pressure, cal/gm/°K
$D$ = binary diffusion coefficient, cm²/sec
$f$ = dimensionless stream function
$P_r$ = Prandtl number = $c_p\mu/\lambda$
$Q$ = rate at which heat is added per unit volume, cal/sec/unit vol
$q$ = average heat release per unit mass of fuel gas, cal/gm
$R$ = universal gas constant, cal/mole/°K
$S_c$ = Schmidt number = $\mu/\rho D$
$T$ = local stream temperature, °K
$u$ = local axial stream velocity, cm/sec
$v$ = local transverse stream velocity, cm/sec
$\beta$ = boundary of thermal zones
$\Delta$ = boundary of diffusion zones
$\delta$ = boundary of velocity boundary layer
$\vartheta$ = dimensionless temperature = $T/T_2$
$\vartheta_a$ = dimensionless activation energy = $A/RT_2$
$\kappa$ = local relative mass concentration of combustible gas
$\Lambda$ = velocity ratio = $u_2/u_1$
$\lambda$ = coefficient of thermal conductivity, cal/cm/sec/°K
$\mu$ = dynamic viscosity, gm/cm/sec
$\nu$ = kinematic viscosity, cm/sec = $\mu/\rho$
$\rho$ = density, gm/cm³
$\tau$ = characteristic time of the chemical reaction

## Introduction

ANALYTIC studies of combustion in flowing gaseous mixtures (1, 2, 3)[4] are confined, for the most part, to the plane one-dimensional flame front. The reason for this is not entirely because of the relative simplicity of this problem but also because, due to the very small thickness of the laminar combustion zone at ordinary pressures, many actual situations are well approximated by the plane flame front in spite of the fact that the actual flame front is curved.

There exist some problems, however, in which the physical situation may in no way be approximated by a plane flame front. For example, the thermal quenching of a gaseous mixture near a cool wall (4) or the thermal ignition near a heated wall essentially involve two-dimensional fields. Likewise, combustion processes in free jets and combustion under conditions of mixing between two gaseous streams require considerations beyond the one-dimensional flame theory. In many problems associated with thermal jet-propulsion systems and rocket motors, the circumstance arises where a flowing stream of combustible mixture is ignited by contact and mixing with another stream of hot gas or products of combustion. Such a process is certainly of importance near the injector of a rocket motor, in the flow and combustion of gas through the small ports of turbojet cans, and plays a definite and vital role in the flame stabilization on bluff bodies. This, in common with the other two-dimensional problems which have been mentioned, has the property that, for large stream velocities the variations of temperature, composition, and velocity are much larger in the direction normal to the stream than they are parallel to the direction of flow. In fluid mechanics, problems exhibiting this characteristic are treated by the so-called boundary layer approximation which simplifies the description of the problem by deleting certain variations along the direction of flow in comparison with those across the flow. An extension of this idea to flow with combustion allows an analytic treatment of this entire class of problems. The present treatment is restricted to laminar flow processes, in particular that of the ignition and development of a flame front in the laminar mixing zone between parallel streams of combustible gas and hot products of combustion.

Presented at the 8th ARS National Convention, New York, N. Y., December 3, 1953.

[1] This investigation was carried out, in part, under the financial sponsorship of the Ordnance Corps, U. S. Army.

[2] Associate Professor, the Daniel and Florence Guggenheim Jet Propulsion Center.

[3] Research Engineer, Jet Propulsion Laboratory.

[4] Numbers in parentheses refer to the References on page 94.

After discussing the physical and chemical relations which apply to the problem and simplifying the equations through extension of the boundary layer concept, the initial portion of the mixing zone is investigated where the heat evolved through chemical reaction is yet small and the problem may be solved through a perturbation to the solution for mixing without combustion. Then using the integral technique introduced by von Kármán into the study of the boundary layer, the development of combustion is traced approximately from ignition through development of the plane laminar flame front.

The authors have benefited from their many opportunities of discussing this work with Professor H. S. Tsien, through whose advice the problem has become much clearer and greatly simplified. They are most grateful for his patient and continued interest in the analysis.

## Formulation of the Combustion Problem

The problem of combustion in a laminar mixing zone may be formulated by considering two semi-infinite streams of gas flowing steadily parallel to the $x$-axis, one of a combustible mixture at temperature $T_1$ flowing with a velocity $u_1$, the other consisting of combustion products at a temperature $T_2$, less than the adiabatic flame temperature for the combustible mixture, moving with a velocity $u_2$. Suppose the two streams begin to mix at $x = 0$. Then if no reaction takes place the process is simply one where the velocity profile develops in a well-known manner (Fig. 1) and the temperature

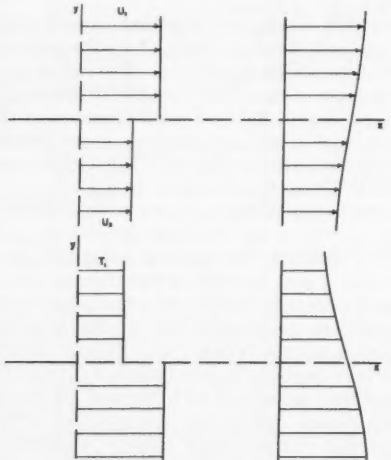

FIG. 1 VELOCITY AND TEMPERATURE PROFILES FOR A MIXING REGION WITHOUT CHEMICAL REACTION

profile grows in a somewhat similar fashion. In addition, diffusion takes place between the two streams of different gaseous composition, the combustible gas from the upper stream diffuses into the hot combustion products of the lower stream. Likewise products of combustion diffuse from the lower stream to dilute the combustible upper stream.

Now when the combustible stream reacts chemically, producing heat in the process, the change in the resulting flow is most easily observed from the development of the temperature profiles. As indicated in Fig. 2, the first noticeable modification will be the small increase in temperature caused by reaction of the gas which has diffused into the hot stream. The temperature increase takes place predominantly in the hotter part of the stream because of the extreme importance of the ambient temperature in promoting reaction. At a later stage the temperature profile is sufficiently distorted to produce a "bulge" where the local temperature exceeds that of the hot gas stream. From this point forward, the strongest

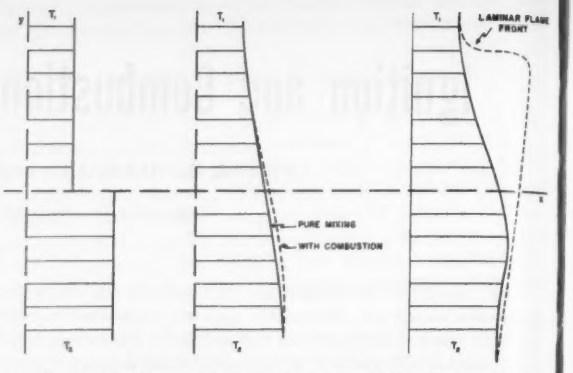


FIG. 2 TEMPERATURE PROFILES AND DEVELOPMENT OF LAMINAR FLAME IN MIXING REGION WITH CHEMICAL REACTION

reaction takes place above the maximum temperature point, due to the fact that the greater concentration of combustible gas is exposed to the higher temperatures, and consequently the point of maximum temperature moves toward the upper stream. Eventually this zone of reaction develops into a thin region resembling the laminar flame front and propagates at the appropriate speed. Since the mixing zone grows roughly as $\sqrt{x}$, it is clear that the reaction zone will move out of the laminar mixing region into the undisturbed combustible mixture and hence develops into a true plane laminar flame front. If the velocities of the two gas streams are such that laminar flame makes a very small angle with the $x$-axis, that is, if $u_1 \gg$ laminar flame speed, then the boundary layer approximation is applicable throughout the region of flame development.

Three physical processes are involved in this problem: (A) The fluid mechanical development of the laminar mixing zone between the two streams through viscous action; (B) the development of the temperature field through conduction between the two streams and heat generated by chemical action; (C) molecular diffusion of each gaseous component into the other stream together with annihilation of combustible gas and generation of combustion products through chemical action. The first of these processes is described by the equations of motion for a viscous compressible fluid. Under the boundary layer assumptions only the dynamic equilibrium in the direction of flow need be considered. Furthermore, it is well known that due to the low value of the laminar burning speed, the pressure variations are negligible. Therefore the pressure field is uniform and, denoting by $\bar{u}$, $\bar{v}$ the velocity components in the $\bar{x}$, $\bar{y}$ directions, the equation of motion is

$$\rho\bar{u}\frac{\partial\bar{u}}{\partial\bar{x}} + \rho\bar{v}\frac{\partial\bar{u}}{\partial\bar{y}} = \frac{\partial}{\partial\bar{y}}\left(\mu\frac{\partial\bar{u}}{\partial\bar{y}}\right) \quad [1]$$

Here $\mu$ is the viscosity of the gas so that if it is assumed that the molecular weights of combustible and combustion products are the same[5], the viscosity is simply proportional to $T$, the local gas temperature. Now since the gas velocities are very small in comparison with the velocity of sound, the density $\rho$ depends only upon the local gas temperature, in fact $\rho \sim 1/T$. The two velocity components and the density are related further through the equation of continuity, expressing the conservation of mass as

$$\frac{\partial}{\partial\bar{x}}(\rho\bar{u}) + \frac{\partial}{\partial\bar{y}}(\rho\bar{v}) = 0 \quad [2]$$

Now since the density is a function only of the temperature,

[5] The three simplifying assumptions underlying this choice of gas properties are: (1) The molecular weights of both gases are equal so that the molecular weight of the mixture is independent of concentrations; (2) the gases are composed of Maxwellian molecules so that $\mu$, for example, behaves as $T$; (3) the Eucken correction for thermal conduction holds for the mixture.

it is particularly convenient to employ the Howarth transformation which introduces a new vertical scale (5, 6)

$$y = \int_0^{\bar{y}} \frac{\rho}{\rho_1}\, d\bar{y} \quad \ldots\ldots [3]$$

where $\rho_1$ is the density of the combustible free stream. Calling the new coordinate system $x$, $y$ where $x = \bar{x}$, and new velocity components $u = \bar{u}, v = \frac{\rho}{\rho_1}\bar{v} + \bar{u}\int_0^{\bar{y}} \frac{\partial}{\partial \bar{x}}\left(\frac{\rho}{\rho_1}\right) d\bar{y}$, it is easy to show that the modified flow satisfies the boundary layer relations for a corresponding incompressible flow problem

$$\frac{\partial u}{\partial x} + \frac{\partial v}{\partial y} = 0 \quad \ldots\ldots [4]$$

$$u\frac{\partial u}{\partial x} + v\frac{\partial u}{\partial y} = \nu\frac{\partial^2 u}{\partial y^2} \quad \ldots\ldots [5]$$

where $\nu = \mu_1/\rho_1$ is the kinematic viscosity of the combustible stream. Formally then the velocity field $u$, $v$ is independent of the temperature and composition fields and may be determined separately. The calculation of the real field $\bar{u}$, $\bar{v}$, however, requires knowledge of the temperature field to invert the transformation given by Equation [3].

The temperature field is described by the energy equation (7,8) which equates the convection of thermodynamic enthalpy with the transmission by conduction and the heat generation by chemical reaction. Then assuming the value of $c_p$, specific heat at constant pressure, to be the same for all gas compositions and independent of temperature, the differential relation is, neglecting the pressure variation

$$\rho\bar{u}\frac{\partial c_p T}{\partial \bar{x}} + \rho\bar{v}\frac{\partial c_p T}{\partial \bar{y}} = \frac{\partial}{\partial \bar{y}}\left(\lambda\frac{\partial T}{\partial \bar{y}}\right) + Q \quad \ldots\ldots [6]$$

where $Q$ is the rate at which heat is being added per unit volume at a point $\bar{x}$, $\bar{y}$, and $\lambda$ is the thermal conductivity of the gases which will be assumed proportional to the local temperature. The heat addition rate $Q$ is determined by the heat of reaction $q$,[6] the local mass concentration of the reacting molecules $\kappa$, and the rate at which molecules of fuel are transformed into molecules of combustion products. This rate is usually accepted by chemists to be of the form $(1/\tau)e^{-A/RT}$, the Arrhenius factor, where $\tau$ is the characteristic time associated with a transformation, $A$ the activation energy which measures the kinetic energy a molecule must possess in order to react successfully, and $R$ the universal gas constant. For a unimolecular reaction, the rate of chemical transformation is simply the product of the local density of combustible gas with the Arrhenius factor, that is, $\kappa\rho(1/\tau)e^{-A/RT}$. Thus the rate of heat addition by chemical reaction is simply

$$Q = q\rho\kappa\frac{1}{\tau}e^{-A/RT} \quad \ldots\ldots [7]$$

It is again convenient to apply the Howarth transformation to the energy equation so that it will be written in terms of the same quantities as the momentum equation.

$$u\frac{\partial T}{\partial x} + v\frac{\partial T}{\partial y} = \frac{\nu}{P_r}\frac{\partial^2 T}{\partial y^2} + \frac{q}{c_p\tau}\kappa e^{-A/RT} \quad \ldots\ldots [8]$$

where $P_r \equiv c_p\mu_1/\lambda_1$ is the Prandtl number of the gases, which is constant. For nonvanishing temperature the heat evolved through chemical reaction vanishes only if the local concentration of combustible matter vanishes. This fact leads to the formal difficulty that a gas which flows from $x = -\infty$ is completely reacted unless a condition is added to disconnect the flow from $x = -\infty$. The identical problem arises in the study of the one-dimensional laminar flame and has recently been discussed by von Kármán (3). In the present work it will be treated in a manner similar to that which von Kármán has employed for one-dimensional flame propagation.

Finally the distributions of combustible gas and products of combustion must be determined through the conservation relations for the chemical species. There are two species and hence two conservation laws; however, it is clear that the two must sum to the gross continuity relation, Equation [2], and hence only one is independent. It is convenient to consider the mass concentration $\kappa$ of the combustible gas. The movement of this gas differs from that of the complete gas only by the diffusion velocity and the combustible mixture is destroyed locally according to the reaction rate. Then with good approximation

$$\rho\bar{u}\frac{\partial \kappa}{\partial \bar{x}} + \rho\bar{v}\frac{\partial \kappa}{\partial \bar{y}} = \frac{\partial}{\partial \bar{y}}\left(\rho D\frac{\partial \kappa}{\partial \bar{y}}\right) - \rho\frac{\kappa}{\tau}e^{-A/RT} \quad \ldots\ldots [9]$$

If the Howarth transformation is again carried out, and the Schmidt number $S_c = \mu/\rho D$ assumed to be constant, then the conservation of combustible material may be written

$$u\frac{\partial \kappa}{\partial x} + v\frac{\partial \kappa}{\partial y} = \frac{\nu}{S_c}\frac{\partial^2 \kappa}{\partial y^2} - \frac{\kappa}{\tau}e^{-A/RT} \quad \ldots\ldots [10]$$

Equations [4], [5], [8], and [10] now describe the simplified combustion process which takes place in an equivalent incompressible flow. By virtue of the Howarth transformation the momentum and continuity equations may be treated independently of the temperature and composition fields and hence constitute a conventional mixing problem. The energy relation and equation for conservation of combustible material must be solved simultaneously, employing knowledge of the velocity field. Since the equations are nonlinear it is clear that solutions may be expected in only certain cases or certain regions and only approximate solutions may be obtained with any generality. Because of the importance of the ignition region, a solution will be obtained for the early portion of the mixing zone. Then, by means of an approximate treatment, the complete course of development of a laminar flame front will be examined.

## Initial Development of the Combustion Zone

During the first portion of the combustion process, where the heat added by the chemical reaction is yet small, the velocity, temperature, and composition fields differ only slightly from those which would occur in the absence of chemical action. The fields without combustion may be computed easily, and consequently the variation due to combustion may be treated as a perturbation.

If the reaction were taking place at a temperature $T$ and concentration $\kappa$, the combustible material would be consumed at a rate $\kappa(1/\tau)e^{-A/RT}$. Due to the strong influence of the Arrhenius factor, the initial reaction takes place where $T$ is nearly $T_2$ and the concentration $\kappa$ is very small. The actual value of $\kappa$ where the reaction takes place most rapidly may be estimated by computing the maximum value of the local reaction rate. Thus

$$\frac{d\kappa}{dy}\frac{1}{\tau}e^{-A/RT} + \frac{\kappa}{\tau}\frac{A}{RT}\frac{1}{T}\frac{dT}{dy}e^{-A/RT} = 0$$

But the temperature distribution $(T_2 - T)/(T_2 - T_1)$ is identical with the concentration distribution $\kappa(y)$ when the Prandtl and Schmidt numbers are equal. Then

$$\frac{d\kappa}{dy}\Big/\frac{dT}{dy} = \frac{-1}{T_2 - T_1}$$

and taking account of the fact that the reaction takes place where $T \approx T_2$, the local concentration is approximately

[6] In view of the assumptions concerning the constancy of molecular weight and $c_p$, $q$ is to be interpreted as the average heat release per unit mass of the fuel gas.

$$\kappa = \left[\frac{A}{RT_2}\left(1 - \frac{T_1}{T_2}\right)\right]^{-1}$$

Consequently the local rate at which combustible matter is consumed is

$$\frac{1}{\frac{A}{RT_2}(1 - T_1/T_2)}\,\frac{1}{\tau}\,e^{-A/RT_2}$$

and the total heat release which takes place over a length $x$ is proportional to

$$\frac{x}{u_2\tau}\,\frac{e^{-A/RT_2}}{\frac{A}{RT^2}(1 - T_1/T_2)} \quad \ldots\ldots\ldots\ldots\ldots [11]$$

since the reaction takes place predominantly where the gas velocity is nearly $u_2$. Then so long as $x$ is such that the total heat addition is small, a perturbation procedure is in order. Therefore it is appropriate to define a characteristic length associated with combustion, $l = \frac{\tau u_2}{RT_2}A\,(1 - T_1/T_2)e^{-A/RT_2}$, which may be employed to make the formulation dimensionless; denote $\xi = x/l$.

Because of its important role in the early stages of combustion, the temperature $T_2$ of the hot stream is conveniently chosen as the characteristic temperature; denote $T/T_2 = \vartheta$, $T_1/T_2 = \vartheta_1$, and $A/RT_2 = \vartheta_a$. The energy and diffusion equations then may be written simply as

$$u\frac{\partial\vartheta}{\partial x} + v\frac{\partial\vartheta}{\partial y} = \frac{\nu}{P_r}\frac{\partial^2\vartheta}{\partial y^2} + \frac{q}{c_pT_2}\frac{\kappa}{\tau}e^{-\vartheta_a/\vartheta} \quad \ldots\ldots [12]$$

and

$$u\frac{\partial\kappa}{\partial x} + v\frac{\partial\kappa}{\partial y} = \frac{\nu}{S_c}\frac{\partial^2\kappa}{\partial y^2} - \frac{\kappa}{\tau}e^{-\vartheta_a/\vartheta} \quad \ldots\ldots\ldots [13]$$

Now the momentum equation has a simple similarity solution regardless of the structure of the rest of the field. For, choosing a stream function $\psi(x, y)$ such that $u = \partial\psi/\partial y$, $v = -\partial\psi/\partial x$, it is easily shown that $\psi = \sqrt{u_1\nu x}f(\eta)$ where $\eta = y\sqrt{u_1/\nu x}$ and $f(\eta)$ satisfies the differential equation.

$$2f''' + ff'' = 0 \quad \ldots\ldots\ldots\ldots\ldots [14]$$

with boundary conditions $f'(\infty) = 1$, $f'(-\infty) = \frac{u_2}{u_1} = \Lambda$, and $f''(\infty) = f''(-\infty) = 0$. In the absence of chemical reaction Equations [12] and [13] also have simple solutions. The differential equations reduce directly to

$$\frac{2}{P_r}\vartheta^{(0)\prime\prime} + f\vartheta^{(0)\prime} = 0 \quad \ldots\ldots\ldots\ldots\ldots [15]$$

and

$$\frac{2}{S_c}\kappa^{(0)\prime\prime} + f\kappa^{(0)\prime} = 0 \quad \ldots\ldots\ldots\ldots\ldots [16]$$

with boundary conditions $\vartheta^{(0)}(\infty) = T_1/T_2 = \vartheta_1$, $\vartheta^{(0)}(-\infty) = 1$, $\vartheta^{(0)\prime}(\infty) = \vartheta^{(0)\prime}(-\infty) = 0$; and similarly $\kappa^{(0)}(\infty) = 1$, $\kappa^{(0)}(-\infty) = 0$, $\kappa^{(0)\prime}(\infty) = \kappa^{(0)\prime}(-\infty) = 0$.

The presence of chemical action destroys the elementary similarity of this simple mixing problem so that the solutions $\vartheta$ and $\kappa$ cannot be functions of $\eta$ alone, but the distance $x$ must also enter. Then, for example, if $\vartheta$ depends upon both $\eta$ and $x$, Equation [12] becomes

$$\frac{1}{P_r}\frac{\partial^2\vartheta}{\partial\eta^2} + \frac{f}{2}\frac{\partial\vartheta}{\partial\eta} - f'x\frac{\partial\vartheta}{\partial x} = -\frac{q}{c_pT_2}\kappa\left(\frac{\kappa}{u_1\tau}e^{-\vartheta_a/\vartheta}\right) \ldots [17]$$

which reduces directly to Equation [15] when $q = 0$, for then the dependence upon $x$ is unnecessary. By writing Equation [17] in the form

$$\frac{1}{P_r}\frac{\partial^2\vartheta}{\partial\eta^2} + \frac{f}{2}\frac{\partial\vartheta}{\partial\eta} - f'\xi\frac{\partial\vartheta}{\partial\xi} = -\frac{q}{c_pT_2}\Lambda\kappa\xi\vartheta_a(1 - \vartheta_1)e^{-\vartheta_a\left(\frac{1}{\vartheta} - 1\right)} \ldots [18]$$

then so long as

$$\frac{xe^{-\vartheta_a}}{u_2\tau\vartheta_a(1 - \vartheta_1)} \equiv \xi \ll 1$$

the appropriate expression for $\vartheta$ is

$$\vartheta = \vartheta^{(0)}(\eta) + \vartheta^{(1)}(\eta)\xi + \vartheta^{(2)}(\eta)\xi^2 + \vartheta^{(3)}(\eta)\xi^3 + \ldots \quad \ldots [19]$$

The situation is quite similar for the equations describing the conservation of combustible matter, for Equation [13] may be written

$$\frac{1}{S_c}\frac{\partial^2\kappa}{\partial\eta^2} + \frac{f}{2}\frac{\partial\kappa}{\partial\eta} - f'\xi\frac{\partial\kappa}{\partial\xi} = \Lambda\kappa\xi\vartheta_a(1 - \vartheta)e^{-\vartheta_a\left(\frac{1}{\vartheta} - 1\right)} \ldots [20]$$

so that likewise it is appropriate to express

$$\kappa = \kappa^{(0)}(\eta) + \kappa^{(1)}(\eta)\xi + \kappa^{(2)}(\eta)\xi^2 + \kappa^{(3)}(\eta)\xi^3 + \ldots \quad \ldots [21]$$

It is obvious that $\vartheta^{(0)}(\eta)$ and $\kappa^{(0)}(\eta)$ satisfy Equations [15] and [16], respectively, for the pure mixing problem, while the relations to be satisfied by $\vartheta^{(n)}(\eta)$ and $\kappa^{(n)}(\eta)$ follow upon substitution into Equations [18] and [20], respectively, according to the classical perturbation technique. The first-order perturbation gives simply

$$\frac{1}{P_r}\frac{d^2\vartheta^{(1)}}{d\eta^2} + \frac{f}{2}\frac{d\vartheta^{(1)}}{d\eta} - f'\vartheta^{(1)} = -\frac{q}{c_pT_2}\Lambda\kappa^{(0)}\vartheta_a(1 - \vartheta_1)e^{-\vartheta_a\left(\frac{1}{\vartheta^{(0)}} - 1\right)} \ldots [22]$$

$$\frac{1}{S_c}\frac{d^2\kappa^{(1)}}{d\eta^2} + \frac{f}{2}\frac{d\kappa^{(1)}}{d\eta} - f'\kappa^{(1)} = \Lambda\kappa^{(0)}\vartheta_a(1 - \vartheta_1)e^{-\vartheta_a\left(\frac{1}{\vartheta^{(0)}} - 1\right)} \ldots [23]$$

where it is necessary that these perturbations and their derivatives vanish at $\eta = \pm\infty$.

The perturbation solution may be worked out for various special cases, the simplest of which is that where the velocities of the two streams are equal, that is, where $\Lambda = 1$. Then the stream function is just $f = \eta$, and it is easily demonstrated that the distributions of temperature and composition in the absence of combustion are just

$$\frac{\vartheta^{(0)}(\eta) - \vartheta_1}{1 - \vartheta_1} = \frac{1}{2}\left[1 - erf\left(\frac{1}{2}\sqrt{P_r}\,\eta\right)\right] \quad \ldots\ldots [24]$$

$$\kappa^{(0)}(\eta) - 1 = \frac{1}{2}\left[1 - erf\left(\frac{1}{2}\sqrt{S_c}\,\eta\right)\right] \quad \ldots\ldots\ldots [25]$$

where $erf(z) = (2/\sqrt{\pi})\int_0^z e^{-t^2}\,dt$. These are well-known solutions of the simple heat conduction and diffusion problems. The first-order perturbation equation for temperature distribution, Equation [22], may now be written as

$$\frac{1}{P_r}\frac{d^2\vartheta^{(1)}}{d\eta^2} + \frac{\eta}{2}\frac{d\vartheta^{(1)}}{d\eta} - \vartheta^{(1)} = -\frac{q}{c_pT_2}\kappa^{(0)}\vartheta_a(1 - \vartheta_1)e^{-\vartheta_a\left(\frac{1}{\vartheta^{(0)}} - 1\right)} \quad \ldots [26]$$

where $\vartheta^{(0)}(\eta)$ is given by Equation [24]. The homogeneous equation has two linearly independent solutions which may be written in the form

$$\mathfrak{C}_1(\eta) = \sqrt{P_r}\eta e^{-\frac{P_r}{4}\eta^2} + \left(\frac{1}{2} + \frac{P_r}{4}\eta^2\right)2\sqrt{2\pi}\left[erf\left(\frac{\sqrt{P_r}}{2}\eta\right) - 1\right] \ldots [27]$$

$$\mathcal{K}_2(\eta) = \sqrt{P_r}\eta e^{-\frac{P_r}{4}\eta^2} + \left(\frac{1}{2} + \frac{P_r}{4}\eta^2\right) 2\sqrt{2\pi}\left[erf\left(\frac{\sqrt{P_r}}{2}\eta\right) + 1\right] \quad \ldots [28]$$

Then constructing the appropriate Green's function as

$$G(\eta, \bar{\eta};\ P_r) = \left\{ \begin{array}{l} \dfrac{-1}{4\sqrt{\pi P_r}}\, \mathcal{K}_1(\eta)\mathcal{K}_2(\bar{\eta}) e^{\frac{P_r}{4}\bar{\eta}^2};\ \eta \geq \bar{\eta} \\ \dfrac{-1}{4\sqrt{\pi P_r}}\, \mathcal{K}_1(\bar{\eta})\mathcal{K}_2(\eta) e^{\frac{P_r}{4}\bar{\eta}^2};\ \eta \leq \bar{\eta} \end{array} \right\} \quad \ldots\ldots [29]$$

the solution of Equation [26] may be written explicitly as

$$\vartheta^{(1)}(\eta) = P_r \frac{q}{C_p T_2}\, \vartheta_a(1 - \vartheta_1) \int_{-\infty}^{\infty} G(\eta, \bar{\eta};\ P_r)\kappa^{(0)}(\bar{\eta}) e^{-\vartheta_a\left(\frac{1}{\vartheta^{(0)}} - 1\right)} d\bar{\eta} \ldots [30]$$

It is clear from Equation [23] that the first-order perturbation for the concentration may be obtained in a similar manner as

$$\kappa^{(1)}(\eta) = -S_c \vartheta_a(1 - \vartheta_1) \int_{-\infty}^{\infty} G(\eta, \bar{\eta};\ S_c)\kappa^{(0)}(\bar{\eta}) e^{-\vartheta_a\left(\frac{1}{\vartheta^{(0)}} - 1\right)} d\bar{\eta} \ldots [31]$$

where, as indicated, the Schmidt number now replaces the Prandtl number in Green's function.

This form is very suitable for numerical computation since Green's function and the rest of the integrand are easily calculable. The integration has been carried out for the particular case where $P_r = 0.91$, $S_c = 1.00$, $\vartheta_1 = 0.286$, $\vartheta_a = 23.96$, $\frac{q}{c_p T_2} = 1.29$, and $T_1 = 300°\text{K}$, where physical parameters are approximately those of the fuel azomethane. The resulting temperature profiles are given in Fig. 3 where it is clearly shown that the maximum perturbation occurs well below the center line of the mixing zone. This is due to the relatively preponderant effect of the stream temperature in increasing the reaction rate, so that although the concentration is low, the temperature is sufficiently high to react almost immediately that combustible which has diffused into this region. The temperature profiles show that very early a bulge is formed where the temperature exceeds that of the hot stream. This region continues to grow, working its way toward the combustible stream. The tendency is therefore for the initial reaction to develop into a flame since the temperatures continually increase with $x$.

The principal question is how long a time or, more realistically, how great a distance is required before the combustion takes place. The simplest significant length to measure is the value of $x$ at which the temperature profile first exhibits a vertical tangent; that is, where the local temperature has increased sufficiently to form a "bulge" in the profile. Fortunately this point may be determined analytically, for considering only the first perturbation, it is clear that

$$\frac{\partial \vartheta}{\partial \eta} \approx \frac{d\vartheta^{(0)}}{d\eta} + \xi \frac{d\vartheta^{(1)}}{d\eta} = 0 \quad \ldots\ldots [32]$$

Furthermore the smallest value of $\xi$ at which this condition may be satisfied is the dimension of interest and will be denoted $\xi_i$. It is necessary also that $d\xi/d\eta = 0$ at $\xi_i$, so that

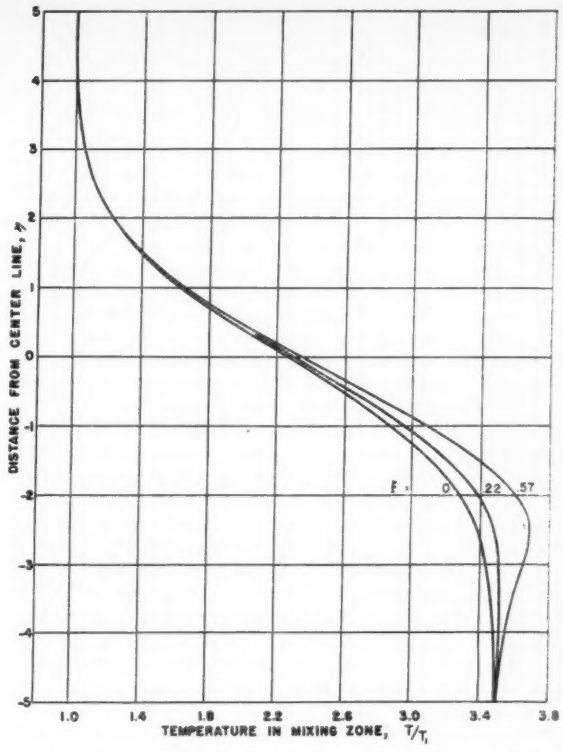


FIG. 3 DETAILED DEVELOPMENT OF TEMPERATURE PROFILES DURING THE EARLY STAGES OF REACTION

calculating from Equation [32]

$$\frac{d^2\vartheta^{(0)}}{d\eta^2} + \xi_i \frac{d^2\vartheta^{(1)}}{d\eta^2} = 0$$

But now applying the differential relations for $\vartheta^{(0)}(\eta)$ and $\vartheta^{(1)}(\eta)$, given by Equation [15] and Equation [22], respectively, it follows that the value $\eta_i$ for which a vertical slope in the temperature is first observed is given by the simple algebraic relation

$$\vartheta^{(1)}(\eta_i) = \frac{q}{C_p T_2}\, \kappa^{(0)}(\eta_i)\vartheta_a(1 - \vartheta_1) e^{-\vartheta_a\left(\frac{1}{\vartheta^{(0)}(\eta_i)} - 1\right)} \ldots\ldots [33]$$

Then, according to Equation [32], the value of $\xi_i$ is just

$$\xi_i = -\left(\frac{d\vartheta^{(0)}}{d\eta} \Big/ \frac{d\vartheta^{(1)}}{d\eta}\right)_{\eta_i} \ldots\ldots [34]$$

Now the expressions involved in Equations [33] and [34] are not simple to handle, but fortunately the values of $\eta_i$ which are involved may be seen, from Fig. 3, to be $\ll -0$, so that good approximation may be made using asymptotic expansions for $\vartheta^{(1)}(\eta)$ and for the right-hand member of Equation [33]. For example, when the Prandtl number is less than unity, the asymptotic expressions for $\kappa^{(0)}(\eta)$ and $\vartheta^{(1)}(\eta)$ at large negative values of $\eta$ are

$$\kappa^{(0)}(\eta) \sim \frac{-1}{\sqrt{\pi}\sqrt{S_c}} \frac{e^{-\frac{S_c}{4}\eta_2}}{\eta} \left\{1 - \frac{2}{S_c\eta^2} + \ldots\right\} \qquad \vartheta^{(1)}(\eta) \sim \frac{-2}{\sqrt{\pi P_r}} \frac{q}{c_p T_2}\, \vartheta_a(1 - \vartheta_1) \left\{\frac{4}{S_c^{3/2}} \frac{e^{-\frac{S_c}{4}\eta^2}}{\eta^5}\left(1 + \frac{P_r}{2}\eta^2\right) \times \left(1 - \left[\frac{1}{S_c} + \frac{1}{P_r}\right]\frac{12}{\eta^2} + \ldots\right) + \frac{e^{-\frac{P_r}{4}\eta^2}}{\eta^3}\left(1 - \frac{12}{P_r\eta^2} + \ldots\right)\left(C_1 - \frac{2}{\sqrt{S_c}} \frac{P_r}{S_c - P_r} e^{-\frac{\eta^2}{4}(S_c - P_r)}\right)\right\} \ldots [35]$$

where

$$C_1 = -\int_{-\infty}^{\infty} \mathcal{K}_1(\bar{\eta})\kappa^{(0)}(\bar{\eta}) e^{-\vartheta_a\left(\frac{1}{\vartheta^{(0)}} - 1\right)} e^{\frac{P_r}{4}\bar{\eta}^2} d\bar{\eta}$$

Then from Equation [33] it follows that the value of $\eta_i$ is determined by the relation

$$\frac{8}{P_r S_c \eta_i^4}\left(1+\frac{P_r}{2}\eta_i^2\right)\left(1-\left[\frac{1}{S_c}+\frac{1}{P_r}\right]\frac{12}{\eta_i^2}+\ldots\right)+\frac{2\sqrt{S_c}}{P_r}\frac{e^{\frac{\eta_i^2}{4}(S_c-P_r)}}{\eta_i^2}\left(1-\frac{12}{P_r\eta_i^2}+\ldots\right)\left(C_1-\frac{2P_r e^{-\frac{\eta_i^2}{4}(S_c-P_r)}}{(S_c-P_r)\sqrt{S_c}}\right)=$$

$$1-\frac{2}{S_c\eta_i^2}+\ldots\ldots\ldots [36]$$

After numerical solution for $\eta_i$, the value of $\xi_i$ is obtained through direct substitution into Equation [34], that is

$$\xi_i=\frac{\sqrt{P_r}}{2}\frac{\eta_i^2}{\vartheta_a(1-\vartheta_1)}\left\{\left(C_1-\frac{2P_r e^{\frac{-\eta_i^2}{4}(S_c-P_r)}}{(S_c-P_r)\sqrt{S_c}}\right)\left(1-\frac{6}{P_r\eta_i^2}+\ldots\right)-\frac{8}{\eta_i^2}\frac{e^{\frac{-\eta_i^2}{4}(S_c-P_r)}}{S_c^{3/2}}\left(1-\frac{12}{\eta_i^2}\left[\frac{1}{S_c}+\frac{1}{P_r}\right]\right)\right\}^{-1}\ldots [37]$$

where the asymptotic expansions have been used for $d\vartheta^{(1)}/d\eta$. Now the principal variation of $x_i$ is due to the exponential term so that it is clear that as the temperature of the hot stream decreases, the detachment distance of the combustion zone increases exponentially. Using the same values of the parameters as those employed in constructing the temperature profiles, the detachment distance $x_i$ has been computed for a range of hot stream temperatures. Calculations incidentally showed that $\eta_i$ was about $-6$, thereby justifying the use of asymptotic expansions in its evaluation. It appears from Fig. 4 that the value of $x_i$ increases enormously as the hot stream becomes cooler. Therefore it is seen that although this process of combustion in a laminar mixing zone shows no distinct blowoff, the flame detachment becomes so great for low stream temperature that it exceeds the physical dimensions of any apparatus.

Because the initial reaction occurs at such large negative values of $\eta$, it is a simple matter to extend the analysis to the case where $\Lambda \neq 1$ by employing the asymptotic expansions of the solution for the velocity field. However, this additional consideration modifies Equation [35] only to the order $(e^{-\frac{\eta^2}{4}})^2$, and therefore Equation [37] is valid, to the present approximation, for any value of $\Lambda$ that is not too small.

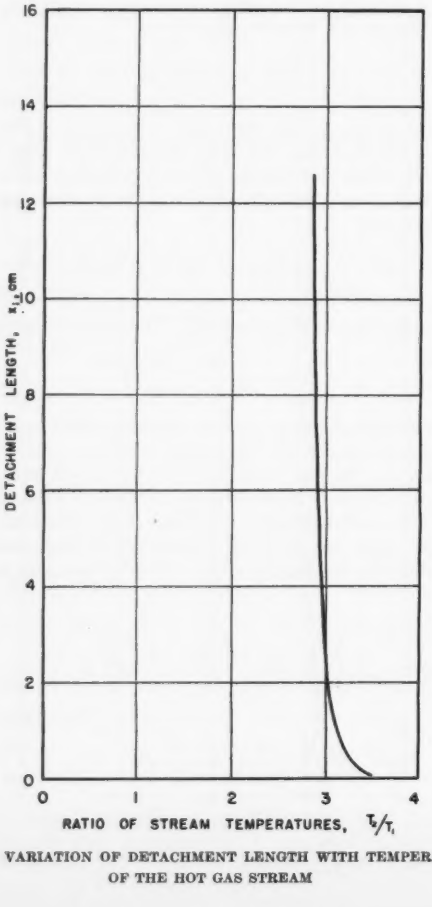


FIG. 4 VARIATION OF DETACHMENT LENGTH WITH TEMPERATURE OF THE HOT GAS STREAM

## Development of the Laminar Flame

The perturbation scheme employed in discussing the initial combustion zone is, of course, inappropriate for following the transition to a laminar flame front. However, since the initial region is known from the foregoing analysis, an approximate procedure is employed in extending the solution throughout the remainder of the flame zone. The technique that allows best use of the information which has so far been accumulated is the integral method introduced by von Kármán into the study of laminar and turbulent boundary layers. In this method the differential equations are integrated across the stream utilizing a descriptive knowledge of the distribution of velocity, temperature, etc. The resulting ordinary differential equations then describe the manner in which the geometric widths of assumed profiles vary along the direction of flow. Extension of von Kármán's integral method to problems of combustion simply necessitates addition of the integrated equations for species conservation to those for momentum and energy employed in the analysis of compressible boundary layer.

Since the success of the method is directly related to the reasonable choice of approximate profiles, it is necessary to be assured that profiles selected exhibit the essential physical characteristics. The velocity distribution is probably the simplest, since after the Howarth transformation it is independent of temperature or composition variations. The two fluid streams are initially separate and it is convenient to describe them by separate integral relations. The streamline which divides the two fluids is not straight but deflects during the mixing process. This deflection is negligibly small, however, and the division will be taken at the line $y = 0$; the velocity $u_0$ is constant along this streamline (9). Now let $\delta_1$ represent the extent of the mixing zone into the combustible mixture and $-\delta_2$ the extent into the hot combustion products. The momentum integral for the upper stream is then obtained by integrating the momentum equation, Equation [5], over the range $0 \leq y \leq \delta_1$, in the conventional manner (10), to obtain

$$\frac{d}{dx}\int_0^{\delta_1(x)}\frac{u}{u_1}\left(1-\frac{u}{u_1}\right)dy=\nu\frac{\partial}{\partial y}\left(\frac{u}{u_1}\right)_{y=0}\ldots\ldots [38]$$

Similarly in the lower fluid region

$$\frac{d}{dx}\int_{-\delta_2(x)}^{0}\frac{u}{u_1}\left(\Lambda-\frac{u}{u_1}\right)dy=-\nu\frac{\partial}{\partial y}\left(\frac{u}{u_1}\right)_{y=0}\ldots [39]$$

The results of these two relations must match at the dividing line so that the viscous shear be continuous. Since all fluid properties are continuous at this point,

$$\frac{\partial}{\partial y}\left(\frac{u}{u_1}\right)_{y=0+} = \frac{\partial}{\partial y}\left(\frac{u}{u_1}\right)_{y=0-} \quad \ldots\ldots\ldots [40]$$

The energy integrals are established through Equation [12]; suppose the extent of the thermal layer above the $x$-axis is $\beta_1(x)$, while that below is $-\beta_2(x)$. It is convenient to make a division between the "upper" and "lower" streams along a line $\beta_0(x)$ above which the reaction rate may be neglected. If the temperature of the hot stream is not too great, this may be taken as the isotherm having a temperature $\vartheta = \vartheta_0$ corresponding to that of the dividing streamline ($y = 0$) in the absence of combustion. Then integrating over the region $y > \beta_0(x)$ gives

$$\frac{d}{dx}\int_{\beta_0(x)}^{\beta_1(x)} \frac{u}{u_1}(\vartheta_1 - \vartheta)\,dy - (\vartheta_0 - \vartheta_1)\frac{d}{dx}\int_0^{\beta_0(x)} \frac{u}{u_1}\,dy = \frac{\nu}{P_r U_1}\left.\frac{\partial \vartheta}{\partial y}\right|_{y=\beta_0(x)} \quad \ldots [41]$$

and for the region $y < \beta_0(x)$

$$\frac{d}{dx}\int_{-\beta_2(x)}^{\beta_0(x)} \frac{u}{u_1}(1 - \vartheta)\,dy - (1 - \vartheta_0)\frac{d}{dx}\int_0^{\beta_0(x)} \frac{u}{u_1}\,dy = -\frac{\nu}{P_r u_1}\left.\frac{\partial \vartheta}{\partial y}\right|_{y=\beta_0(x)} - \frac{q}{c_p T_2 u_1}\tau \int_{-\beta_2(x)}^{\beta_0(x)} \kappa e^{-\vartheta_a/\vartheta}\,dy \ldots [42]$$

For these equations the matching between the two regions expresses the physical fact that the heat conduction is continuous across $\beta_0(x)$, that is

$$\left.\frac{\partial \vartheta}{\partial y}\right|_{\beta_0+} = \left.\frac{\partial \vartheta}{\partial y}\right|_{\beta_0-} \quad \ldots\ldots\ldots\ldots\ldots [43]$$

Integration of the concentration relation [13], presents the additional complication that the concentration $\kappa(\beta_0)$ is not constant. Integration above the line $\beta_0(x)$ leads to the relation

$$\frac{d}{dx}\int_{\beta_0(x)}^{\Delta_1(x)} \frac{u}{u_1}(1 - \kappa)\,dy + (1 - \kappa(\beta_0))\frac{d}{dx}\int_0^{\beta_0(x)} \frac{u}{u_1}\,dy = \frac{\nu}{S_c u_1}\left.\frac{\partial \kappa}{\partial y}\right|_{\beta_0+} \quad \ldots [44]$$

and below the line $\beta_0(x)$

$$\frac{d}{dx}\int_{-\Delta_2(x)}^{\beta_0(x)} \frac{u}{u_1}\kappa\,dy - \kappa(\beta_0)\int_0^{\beta_0(x)} \frac{u}{u_1}\,dy = \frac{\nu}{S_c u_1}\left.\frac{\partial \kappa}{\partial y}\right|_{\beta_0-} - \frac{1}{\tau u_1}\int_{-\Delta_2(x)}^{\beta_0(x)} \kappa e^{-\vartheta_a/\vartheta}\,dy \ldots [45]$$

where $\Delta_1(x)$ and $-\Delta_2(x)$ are the thicknesses of the diffusion zone in the upper and lower streams respectively. The continuity of diffusive transport of combustible matter at $\beta_0(x)$ gives the matching relation

$$\left.\frac{\partial \kappa}{\partial y}\right|_{\beta_0+} = \left.\frac{\partial \kappa}{\partial y}\right|_{\beta_0-} \quad \ldots\ldots\ldots\ldots\ldots [46]$$

The perturbation analysis of the previous section disclosed the fact that the temperature profiles have a different character accordingly as the value of $x$ is less than or greater than $x_i$ where a temperature maximum first appears. To illustrate the manner in which this fact exhibits itself in the present approximate treatment, consider the situation where the Prandtl number is less than the Schmidt number so that the diffusion of combustible matter into the lower stream takes place more slowly than the increase of the thermal boundary layer thickness, that is, $\beta_2 > \Delta_2$ for the initial reaction zone. Clearly then, the reaction takes place most rapidly at the highest temperature and consequently near the boundary $\Delta_2$ of the diffusion zone. In spite of the low concentration of combustible material, the temperature increases in this region causing a reduction in thickness $\beta_2$ of the lower thermal layer. In order that a combustion wave develop, it is necessary that the reaction eventually take place at a high temperature so that the thermal layer must decrease in thickness at a rate exceeding that at which the diffusion layer decreases due to consumption of combustible. Consequently the diffusion layer must exceed the thickness of the thermal layer after sufficient distance has been covered. As soon as this occurs, there exists a zone of reaction in the region where the temperature of the gas already is equal to $T_2$ and hence the local temperature will exceed $T_2$. This corresponds to the first appearance of a maximum in the temperature profile which was observed in the perturbation calculation, and consequently it is clear that $\Delta_2 = \beta_2$ at a distance $x_i$ downstream. Furthermore, a bifurcation occurs in the thermal layer thickness at $x_i$, and for $x > x_i$; one branch lies above the maximum temperature, the other at the edge of the lower thermal zone, below the maximum. It is only the lower branch which possesses a particular physical significance. Therefore, although an approximation to the velocity and concentration profiles may be obtained which is valid over the whole mixing region, the temperature profile must be approximated differently accordingly as the point in question lies upstream or downstream of the distance where a maximum is first obtained in the temperature profile.

It is both convenient and reasonably accurate to represent the various profiles by appropriate portions of trigonometric functions. For example, Lock (9) has employed this approximation in one method of treating the viscous layer between two parallel streams of gas. For the velocity profile the distribution will be

$$\frac{u}{u_1} = \frac{u_0}{u_1} + \left(1 - \frac{u_0}{u_1}\right)\sin\frac{\pi}{2}\frac{y}{\delta_1};\quad y > 0$$

$$= \frac{u_0}{u_1} + \left(\frac{u_2}{u_1} - \frac{u_0}{u_1}\right)\sin\frac{\pi}{2}\left(\frac{y}{-\delta_2}\right);\quad y < 0 \ldots [47]$$

The concentration distribution is also relatively simple except that it must be written with respect to the concentration $\kappa(\beta_0)$ and with respect to the limit $\beta_0(x)$ of the combustion zone. Therefore

$$\kappa = \kappa(\beta_0) + (1 - \kappa(\beta_0))\sin\frac{\pi}{2}\left(\frac{y - \beta_0}{\Delta_1 - \beta_0}\right);\quad y > \beta_0$$

$$= \kappa(\beta_0) - \kappa(\beta_0)\sin\frac{\pi}{2}\left(\frac{y - \beta_0}{-\Delta_2 - \beta_2}\right);\quad y < \beta_0 \ldots\ldots [48]$$

Now for the region $x < x_i$ the temperature profile may also be approximated in this elementary manner

$$\vartheta = \vartheta_0 + (\vartheta_1 - \vartheta_0)\sin\frac{\pi}{2}\left(\frac{y - \beta_0}{\beta_1 - \beta_0}\right);\quad y > \beta_0$$

$$= \vartheta_0 + (1 - \vartheta_0)\sin\frac{\pi}{2}\left(\frac{y - \beta_0}{-\beta_2 - \beta_0}\right);\quad y < \beta_0 \ldots [49]$$

but for $x > x_i$ it must be possible for the profile to show a maximum temperature. To accomplish this in a relatively simple manner it is sufficiently realistic to assume that for any value of $x$, the maximum temperature occurs at the lower boundary of the diffusion zone, that is, where $y = -\Delta_2(x)$. The maximum temperature is then just $\vartheta(-\Delta_2)$ and the temperature profiles are

$$\vartheta = \vartheta_0 + (\vartheta_1 - \vartheta_0)\sin\frac{\pi}{2}\left(\frac{y - \beta_0}{\beta_1 - \beta_0}\right);\quad y > \beta_0$$

$$= \vartheta_0 + (\vartheta(-\Delta_2) - \vartheta_0)\sin\frac{\pi}{2}\left(\frac{y - \beta_0}{-\Delta_2 - \beta_0}\right);\quad -\Delta_2 < y < \beta_0$$

$$= \frac{\vartheta(-\Delta_2) + 1}{2} - \frac{\vartheta(-\Delta_2) - 1}{2}\cos\frac{\pi}{2}\left(\frac{-y - \beta_2}{-\Delta_2 - \beta_2}\right);\quad -\beta_2 < y < -\Delta_2 \ldots [50]$$

Substitution of these profiles into the preceding six integral equations yields six simultaneous ordinary differential equations for the functions $\delta_1(x)$, $\delta_2(x)$, $\Delta_1(x)$, $\Delta_2(x)$, $\beta_1(x)$, and $\beta_2(x)$. As an illustration it is instructive to use the same example employed in the perturbation analysis, that is, where $u_1 = u_2 \equiv u$. Then only four functions are involved, $\delta_1(x)$ and $\delta_2(x)$ being absent since no shearing stresses are present. Furthermore the temperature $\vartheta_0$ is just $(\vartheta_1 + 1)/2$, since it is that value which would occur at the interface in the absence of combustion. From the trigonometric relations themselves it is easily shown that $\beta_0(x) = \frac{1}{2}(\beta_1 - \beta_2)$ while the concentration along $\beta_0(x)$ is $\kappa(\beta_0) = (\beta_0 + \Delta_2)/(\Delta_1 + \Delta_2)$. Upon evaluation of the integrals in Equations [41], [42], [44], and [45], the following differential equations are obtained for the region $x < x_i$, after some simplification

$$\frac{d}{dx}(\Delta_1 + \Delta_2) = \frac{\pi^2}{2(\pi - 2)} \frac{\nu}{S_c u} \left(\frac{1}{\kappa(\beta_0)(1 - \kappa(\beta_0))}\right)\left(\frac{1}{\Delta_1 + \Delta_2}\right) - \frac{4}{\pi - 2} \frac{\kappa(\beta_0)(\Delta_1 + \Delta_2) I}{(1 - \vartheta_1) u \tau e^{-\vartheta_a}}$$

$$\frac{d}{dx}(\kappa(\beta_0)) = \frac{\pi^2}{4(\pi - 2)} \frac{\nu}{S_c u} \frac{1 - 2\kappa(\beta_0)}{\kappa(\beta_0)(1 - \kappa(\beta_0))} \frac{1}{(\Delta_1 + \Delta_2)^2} + \frac{2\kappa(\beta_0)}{\pi - 2}\left[\frac{\frac{q}{c_p T_2} + 1 - \vartheta_1}{1 - \vartheta_1} \kappa(\beta_0) - 1\right] \frac{I}{(1 - \vartheta_1) u \tau e^{\vartheta_a}}$$

$$\frac{d}{dx}(\beta_1 - \beta_0) = \frac{\pi^2}{2(\pi - 2)} \frac{\nu}{P_r u} \frac{1}{(\beta_1 - \beta_0)} - \frac{4}{\pi - 2} \frac{q}{c_p T_2 (1 - \vartheta_1)} \kappa^2(\beta_0)(\Delta_1 + \Delta_2) \frac{I}{(1 - \vartheta_1) u \tau e^{\vartheta_a}}$$

$$\frac{d\beta_0}{dx} = \frac{4}{\pi} \frac{q}{c_p T_2 (1 - \vartheta_1)} \kappa^2(\beta_0)(\Delta_1 + \Delta_2) \frac{I}{(1 - \vartheta_1) u \tau e^{\vartheta_a}} \quad \ldots\ldots [51]$$

where $I$ is a definite integral over the reaction zone given by

$$I = \int_{\vartheta_0}^{1} \sqrt{\frac{1 - \frac{\vartheta - \vartheta_0}{1 - \vartheta_0}}{1 + \frac{\vartheta - \vartheta_0}{1 - \vartheta_0}}} e^{-\vartheta_a\left(\frac{1}{\vartheta} - 1\right)} d\vartheta \quad \ldots\ldots [52]$$

Now since a numerical integration is obviously called for, it is necessary to investigate the behavior of the solutions to Equations [51] near the origin where integration must begin. The expansions are naturally in powers of $\xi$ and may be computed as

$$\frac{\Delta_1 + \Delta_2}{\sqrt{\frac{\nu x}{u}}} = \frac{2\pi}{\sqrt{S_c(\pi - 2)}}\left(1 - \frac{I\vartheta_a}{\pi - 2}\xi + \ldots\right)$$

$$\kappa(\beta_0) = \frac{1}{2} + \left(\frac{q}{c_p T_2(1 - \vartheta_1)} - 1\right)\frac{I\vartheta_a}{3(\pi - 2)}\xi + \ldots$$

$$\frac{\beta_0}{\sqrt{\frac{\nu x}{u}}} = \frac{2\pi}{\sqrt{S_c(\pi - 2)}} \frac{q}{c_p T_2(1 - \vartheta_1)} \frac{2I\vartheta_a}{3\pi}\xi + \ldots$$

$$\frac{\beta_1 - \beta_0}{\sqrt{\frac{\nu x}{u}}} = \frac{\pi}{\sqrt{P_r(\pi - 2)}}\left(1 - \sqrt{\frac{P_r}{S_c}} \frac{I\vartheta_a}{\pi - 2} \times \frac{q}{c_p T_2(1 - \vartheta_1)}\xi + \ldots\right) \quad \ldots [53]$$

Actually these expressions give a fairly accurate idea of the behavior of the mixing and reaction zones for $x < x_i$. For example, the value of $x_i$ itself, determined by the condition $\Delta_2(x_i) = \beta_2(x_i)$, may be calculated from these results by noting that since $\Delta_2 + \beta_2 = \kappa(\beta_0)(\Delta_1 + \Delta_2)$ and $\beta_2 + \beta_0 = \beta_1 - \beta_0$, the value of $x_i$ satisfies the relation $\beta_1(x_i) - \beta_2(x_i) = \kappa(\beta_0)[\Delta_1(x_i) + \Delta_2(x_i)]$. Then from Equations [53] it follows directly that

$$\xi_i = \frac{\sqrt{\frac{S_c}{P_r}} - 1}{\vartheta_a\left[\frac{q}{c_p T_2(1 - \vartheta_1)} - 1\right]}\left(\frac{3(\pi - 2)}{5I}\right) \quad \ldots\ldots [54]$$

The complete calculation is shown in Fig. 5 for this region for numerical values corresponding to azomethane which have been employed earlier. The results are essentially the same as those found by the perturbation analysis.

The differential relations which describe the development of combustion for $x > x_i$ are more involved than those describing the initial region due both to the more complex temperature profiles and to the initial conditions which must be used at $x = x_i$ where integration is started. Furthermore, there are now five of these differential equations and they may be written as

$$\frac{d}{dx}(\Delta_1 + \Delta_2) = \frac{\pi_2}{2(\pi - 2)} \frac{\nu}{S_c u} \frac{1}{\kappa(\beta_0)(1 - \kappa(\beta_0))} \frac{1}{\Delta_1 + \Delta_2} - \frac{4}{\pi - 2}(\beta_1 - \beta_0) \frac{I(\Delta_2, \beta_0)}{u\tau(1 - \vartheta_1) e^{\vartheta_a}}$$

$$\frac{d}{dx}(\beta_1 - \beta_0) = \frac{4 - \pi}{4\kappa(\beta_0)} \frac{\Delta_1 + \Delta_2}{\beta_1 - \beta_0} + \pi \times \left\{\frac{\pi^2}{2(\pi - 2)} \frac{\nu}{S_c u} \frac{1}{\kappa(\beta_0)(1 - \kappa(\beta_0))(\Delta_1 + \Delta_2)} \times \left[1 + 2\frac{S_c}{P_r}\frac{\pi - 2}{4 - \pi}(1 - \kappa(\beta_0))\right] + \frac{\pi^3}{2(\pi - 2)(4 - \pi)} \frac{\nu}{P_r u} \times \frac{1}{\beta_1 - \beta_0} - \frac{4}{\pi - 2} \frac{I(\Delta_2, \beta_0)}{u\tau(1 - \vartheta_1) e^{\vartheta_a}}(\beta_1 - \beta_0) \times \left[1 + \kappa(\beta_0) + \frac{4(\pi - 2)}{4 - \pi} \frac{q}{c_p T_2(1 - \vartheta_1)} \frac{\beta_1 - \beta_0}{\Delta_1 + \Delta_2}\right]\right\}$$

$$\frac{d\kappa(\beta_0)}{dx} = \frac{1}{2(\Delta_1 + \Delta_2)}\left\{(1 - \kappa(\beta_0))\frac{d}{dx}(\Delta_1 + \Delta_2) - \frac{d}{dx}(\beta_1 - \beta_0) + \frac{\pi^2}{2(\pi - 2)} \frac{\nu}{S_c u} \frac{1}{(\Delta_1 + \Delta_2)(1 - \kappa(\beta_0))} \times \left[\frac{S_c}{P_r} \frac{(\Delta_1 + \Delta_2)(1 - \kappa(\beta_0))}{(\beta_1 - \beta_0)} - 1\right]\right\}$$

$$\frac{d\beta_0}{dx} = \frac{\pi}{2} \frac{\nu}{P_r u} \frac{1}{(\beta_1 - \beta_0)} - \frac{\pi - 2}{\pi} \frac{d}{dx}(\beta_1 - \beta_0)$$

$$\frac{d}{dx}\left[(\beta_2 - \Delta_2)\left(\frac{\kappa(\beta_0)(\Delta_1 + \Delta_2)}{\beta_1 - \beta_0} - 1\right)\right] + 2\left[\frac{\kappa(\beta_0)(\Delta_1 + \Delta_2)}{\beta_1 - \beta_0} - 1\right]\left[\frac{d}{dx}(\kappa(\beta_0)(\Delta_1 + \Delta_2)) - \frac{d}{dx}(\beta_1 - \beta_0)\right] = 0 \quad \ldots [55]$$

where now

$$I(\Delta_2, \beta_0) = \int_{\vartheta_0}^{\vartheta(-\Delta_2)} \sqrt{\frac{1 - \frac{\vartheta - \vartheta_0}{\vartheta(-\Delta_2) - \vartheta_0}}{1 + \frac{\vartheta - \vartheta_0}{\vartheta(-\Delta_2) - \vartheta_0}}} e^{-\vartheta_a\left(\frac{1}{\vartheta} - 1\right)} d\vartheta \quad \ldots [56]$$

The development of the combustion zone into a laminar flame front was calculated by numerical integration of the differential Equations [51] and [55]. The resulting value of the gas temperature at $y = -\Delta_2$ is shown in Fig. 6 from the value $x = x_i$ on to the point where a normal flame front appears. The exponential increase of the maximum temperature is shown as the gas moves away from the point of initial mixing.

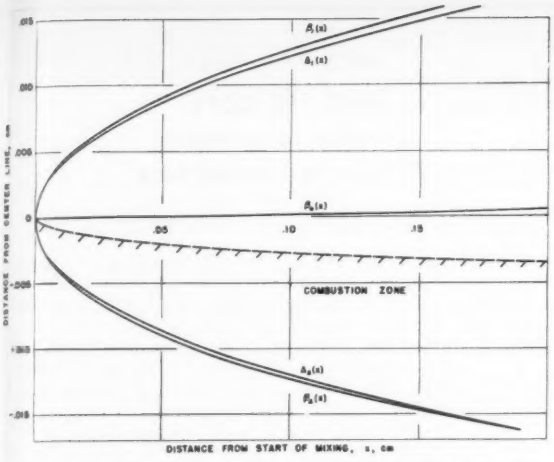


FIG. 5 GROWTH OF THICKNESSES OF TEMPERATURE AND COMPOSITION LAYERS IN THE INITIAL REACTION ZONE

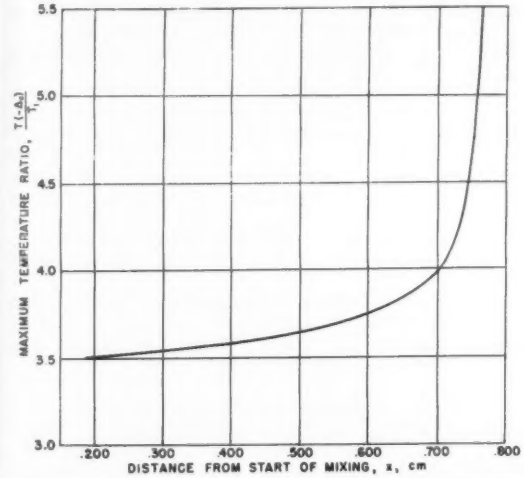


FIG. 6 INCREASE OF MAXIMUM GAS TEMPERATURE IN DIRECTION OF FLOW DURING THE LATER STAGES OF FLAME DEVELOPMENT

The detailed progress of the various regions and zones are traced in Fig. 7, in which the vertical scale is exaggerated, and demonstrates well the relatively sudden appearance of the laminar flame propagating into combustible mixture. This is indicated by the rapid convergence of the lines representing different temperatures and hence the appearance of strong temperature gradients. Also of interest is the observation (both from Fig. 6 and from Fig. 7) that the small perturbation analysis is probably adequate to describe the major portion of the reaction zone preceding the appearance of a laminar flame front. The temperature distribution profiles which occur near the end of the ignition zone, plotted in Fig. 8, show the rapidity with which the temperature gradient steepens to the laminar flame front. It is particularly striking that the major steepening of the gradient takes place in the last 10 per cent of the reaction zone.

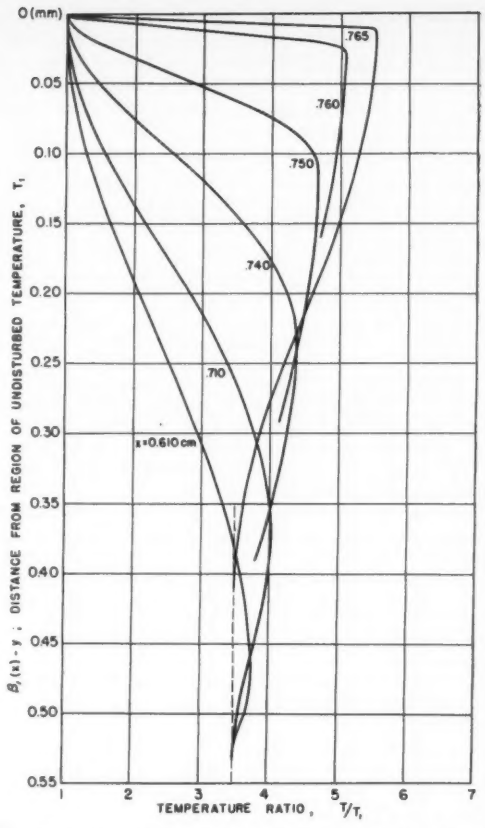


FIG. 8 TEMPERATURE PROFILES LEADING TO FINAL LAMINAR FLAME

## Concluding Remarks

Through application of a boundary layer type of analysis to the problem of ignition and combustion in the mixing zone between parallel streams of combustible gas and combustion products, some of the essential features have been deduced with relative ease. In particular, although the stream of combustible gas eventually ignites, the distance (or time) required is excessive where the temperature of the hot stream is too low. Then the flame develops so far downstream that it is essentially "blown off" any finite apparatus.

In a broader sense the analysis shows that a new class of combustion problems is open to investigation through extension of the usual boundary layer concepts. In addition

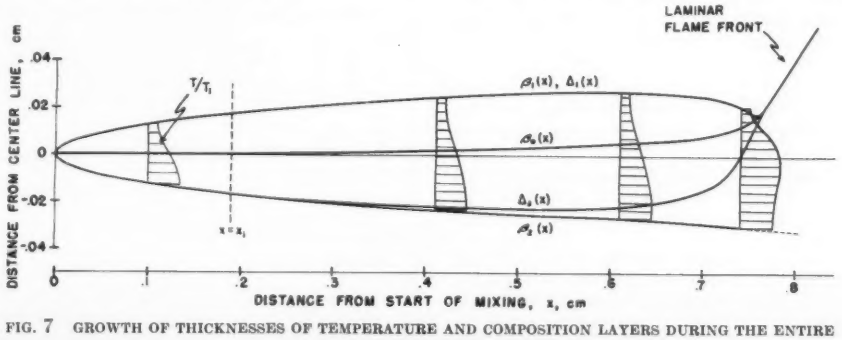


FIG. 7 GROWTH OF THICKNESSES OF TEMPERATURE AND COMPOSITION LAYERS DURING THE ENTIRE COURSE OF FLAME DEVELOPMENT

to the present one, this class includes such important problems as the theory of thermal quenching near a cool wall, the ignition and flame stabilization on a heated surface from which the boundary layer is unseparated, the erosive burning of solid propellent grains, and a great many others. There is no essential difficulty in proceeding to problems with axial symmetry and it seems quite possible that the process may be extended to include cases of turbulent mixing. Thus the theory of the plane laminar flame together with the description of such boundary layer regions as may be treated by the methods just described, seem to provide an adequate description of a relatively large group of problems which involve steady constant pressure deflagration.

### References


1 "Recherches Expérimentelles et Théoretiques sur la Combustion des Mélanges Gazeuses Explosifs," by E. Mallard and H. Le Chatelier, *Ann. mines*, Paris, vol. 8, series 4, 1883, p. 274.

2 "The Structure of the Reaction Zone in a Flame," by S. F. Boys and J. Corner, *Proceedings of the Royal Society of London*, vol. 197, series A, 1949, p. 90.

3 "The Thermal Theory of Constant Pressure Deflagration," by Theodore von Kármán and Gregorio Millan. Biezeno Anniversary Volume on Applied Mechanics, N. V. De Technische Uitgeverij H. Stam, Haarlem, Antwerpen, Djakarta, 1953, pp. 59–69.

4 "Thermal Theory of a Laminar Flame Front Near a Cold Wall," by Theodore von Kármán and Gregorio Millan. Fourth International Symposium on Combustion, Williams & Wilkins, Baltimore, 1953.

5 "Laminar Boundary Layers in Compressible Fluids," by A. Dorodnitzyn, C. R. Academy of Sciences, URSS, vol. 34, no. 8, 1952, pp. 213–219.

6 "Concerning the Effect of Compressibility on Laminar Boundary Layers and Their Separation," by P. L. Howarth, *Proceedings of the Royal Society of London*, vol. 194, series A, No. A1036, 1948, pp. 16–42.

7 "The Mathematical Theory of Non-Uniform Gases," by S. Chapman and T. G. Cowling, University Press, Cambridge, 2nd ed., 1942, pp. 218–258.

8 "The Kinetic Theory of Gases," by J. O. Hirschfelder, C. F. Curtiss, R. B. Bird, and E. L. Spotz, C. F. 1500A, University of Wisconsin, 1952, p. 88.

9 "The Velocity Distribution in the Laminar Boundary Layer Between Parallel Streams," by R. C. Lock, *Quart. J. Mechanics and Applied Mathematics*, vol. IV, pt. 1, 1951, pp. 42–63.

10 "Modern Developments in Fluid Mechanics," by S. Goldstein, Clarendon Press, Oxford, 1st ed., 1938, pp. 131–134.


## Ramjet Diffusers at Supersonic Speeds

(*Continued from page 84*)

The preceding examples have assumed fortuitous and sometimes improbable combinations of conditions to promote oscillations, but, as missile experts all know, Mother Nature has a perverse habit of assembling just such circumstances to confound the luckless experimenter. In the foregoing we have considered only simple configurations. The possibilities become almost unlimited when we introduce additional mechanisms such as fuel and/or area controls, each with its own lag and inertia characteristics. Then truly, Missiles Engineer, "there are more things in heaven and earth than are dreamt of in your philosophy."

### References and Collateral Reading


1 "Experiments at Supersonic Speed on a Biplane of the Busemann Type," by Antonio Ferri, Atti di Guidonia No. 37038, pp. 317–357, Oct. 11, 1940 (RTP Translation 1407).

2 "Preliminary Investigation of Supersonic Diffusers," by Arthur Kantrowitz and Coleman Donaldson, NACA Wartime Report L-713, May 1945.

3 "Pressure Recovery for Missiles with Reaction Propulsion at High Supersonic Speeds," by Klaus Oswatitsch, Bericht Nr. 1005, Kaiser Wilhelm Institut, Göttingen (translated as NACA TM 1140, June 1947).


(*Continued on page 112*)

# Low-Speed Combustion Aerodynamics

ROBERT A. GROSS[1] and ROBIN ESCH[2]

Combustion Aerodynamics Laboratory, Harvard University, Cambridge, Mass.

**The problem studied is the two-dimensional, low-speed, inviscid, steady flow field containing a finite length discontinuity which represents a flame. The flow takes place in unbounded space and has uniform parallel flow at infinity. It is shown that if the density ratio $\lambda$, the pressure ratio $p_2/p_1$ across the flamelike discontinuity, and $Q$, the heat of reaction are constant, the flow field is everywhere irrotational. For such cases the flow field can be described by classical potential theory where the flame discontinuity is represented by a source sheet. The fundamental equations for the flow field and the discontinuity are formulated for low Mach number flows. The source sheet equations are given in detail. Two approximate solutions to flow fields are presented; one is a finite length straight-line flame inclined at an angle to the free stream; the second is the V-flame shape. Dimensional considerations are discussed and some experimental results are reported.**

## Nomenclature

| | | |
|---|---|---|
| $a$ | = | local speed of sound |
| $f(\tau),g(\tau)$ | = | parametric quantities for flame shape |
| $h_0$ | = | stagnation enthalpy = h + $(q^2/2)$ |
| $\hat{i},\hat{j}$ | = | unit vectors in the $x$ and $y$ directions |
| $l$ | = | coordinate along source sheet |
| $L$ | = | length of source sheet |
| $M_1$ | = | flame-speed Mach number = $S/\sqrt{\gamma RT} = S/a$ |
| $\hat{n}$ | = | unit vector normal to flame discontinuity |
| $p$ | = | pressure |
| $\vec{q}$ | = | velocity |
| $\vec{q}_\infty$ | = | velocity at infinity |
| $Q$ | = | heat of reaction from combustion |
| $r$ | = | distance from a point in flow field to element of the discontinuity |
| $R$ | = | gas constant |
| $S$ | = | flame speed |
| $T$ | = | absolute temperature |
| $u$ | = | $x$ component of velocity |
| $v$ | = | $y$ component of velocity |
| $x,y$ | = | coordinates |
| $z$ | = | complex variable |
| $\gamma$ | = | ratio of specific heats |
| $\Gamma$ | = | source sheet strength per unit length of discontinuity |
| $\nabla$ | = | gradient operator |
| $\zeta,\eta$ | = | coordinates |
| $\theta$ | = | angle between flame discontinuity and $\vec{q}_\infty$ |
| $\lambda$ | = | density ratio = $\rho_1/\rho_2$ |
| $\mu$ | = | dipole strength |
| $\rho$ | = | density |
| $\sigma$ | = | entropy |
| $\phi$ | = | defined in Fig. 7 |
| $\Phi$ | = | real part of complex potential |
| $\psi$ | = | stream function |
| $\vec{\omega}$ | = | vorticity vector |

*Subscripts*

| | | |
|---|---|---|
| 1 | = | before flame front (reactants) |
| 2 | = | after flame front (products) |
| $n$ | = | normal component |
| $t$ | = | tangential component |
| $s$ | = | source sheet |

## Introduction

THE problem of determining the flow field associated with the burning of combustible fluids is an extremely complicated task. There appears to be little hope at present of solving the entire real problem which encompasses the realm of compressible viscous fluid dynamics, chemical kinetics, heat and mass transport, etc. To obtain a better understanding we desire solutions of simplified problems based upon the real phenomena. To be useful, these problems must be simple enough to permit analytical treatment yet must at least contain the essential features of the phenomena.

For many investigations in the field of aerothermodynamics it is reasonable to assume that the chemical reactions take place in such a short time and space that this region may be treated as a discontinuity in the flow field. The thickness of such reaction zones is of the order of 1 mm at atmospheric pressure. On either side of this discontinuity the flow may be considered as laminar, inviscid, and steady. Assuming the existence of a normal flame velocity permits us to compute and describe by known methods the flow phenomena occurring in many combustion problems.

In particular we shall consider here the case of two-dimensional, low-speed flows. By low speed we mean that the Mach number is so small that compressibility effects may be ignored. Thus, the reactants (upstream of the discontinuity) and the products (downstream of the discontinuity) are considered to be of constant, though different, densities. The fluid will be considered as an ideal gas.

## Fundamental Equations

The flow field may be considered as two regions separated by the flame discontinuity. We seek possible fluid motions in each region such that these regions are connected by conservation of mass and momentum across the discontinuity.

Two equations express the principles of conservation of mass and momentum. Under the simplifying assumptions previously mentioned, these equations are

$$\operatorname{div} \vec{q} = \frac{\partial u}{\partial x} + \frac{\partial v}{\partial y} = 0 \quad \ldots\ldots [1]$$

$$(\vec{q}\cdot\nabla)\vec{q} = -\frac{1}{\rho}\nabla p \quad \ldots\ldots [2]$$

where $\vec{q}$, $\rho$, and $p$ are the velocity, density, and pressure of the gas at the point $x,y$, and $u,v$ are the velocity components of $\vec{q}$ in the $x$ and $y$ directions, respectively, and $\nabla$ represents the gradient operator. Equations [1] and [2] must be satisfied everywhere in the reactant and product flow fields.

The condition to be satisfied across the discontinuity are that mass and momentum be conserved. Mass conservation yields

$$q_{2n} = \lambda S \quad \ldots\ldots [3]$$

Presented at the 8th ARS National Convention, New York, N. Y., December 3, 1953.

[1] Research Associate. Now associated with Fairchild Engine and Aircraft Corporation, Farmingdale, L. I., N. Y.

[2] Research Assistant.

where $q_{2n}$ is the velocity component normal to the discontinuity on the product side, $S$ is the flame speed or normal velocity component on the reactant side, and $\lambda$ is the density ratio of reactants to products

$$\lambda = \frac{\rho_1}{\rho_2} \quad [4]$$

The subscripts 1 and 2 refer to reactant and product sides of the discontinuity, respectively.

Momentum conservation equations tangential and normal to the discontinuity are

$$q_{1t} = q_{2t} \quad [5]$$

$$p_1 + \rho_1 S^2 = p_2 + \rho_2 q^2_{2n} \quad [6]$$

The kinematics of the discontinuity, expressed by Equations [3] and [5], are shown in Fig. 1. Defining the flame speed Mach number as

$$M_1^2 = \frac{S^2}{a^2} = \frac{S^2}{\gamma R T_1}$$

Equation [6] may be written as

$$\frac{p_2}{p_1} = 1 - \gamma(\lambda - 1)\, M_1^2 \quad [7]$$

where $\gamma$ is the ratio of specific heats. Tsien (1)[3] has set down the analogous equations for the compressible case, where one needs the addition of the energy conservation equation. The fact that for low-speed flows one may consider the flow as incompressible and the density ratio $\lambda$ as a constant leads to considerable simplifications.

Equations [1] and [2] plus the boundary conditions specify the reactant and product flow fields, while Equations [3], [5], and [7] connect these two fields across any flamelike discontinuity.

The reactant flow fields considered here will have uniform and parallel streamlines far upstream of the discontinuity. Therefore, the reactant flow field is irrotational everywhere. This follows from the theorem of Lagrange and the fact that there is a unique pressure density relationship. Thus

$$\vec{\omega} = \nabla \times \vec{q} = 0 \quad [8]$$

By introducing the stream function $\psi$ defined by

$$u = \frac{\partial \psi}{\partial y} \qquad v = -\frac{\partial \psi}{\partial x}$$

Equations [1] and [2] are satisfied for the irrotational reactant flow field if one finds a solution to Laplace's equation

$$\nabla^2 \psi_1 = \frac{\partial^2 \psi_1}{\partial x^2} + \frac{\partial^2 \psi_1}{\partial y^2} = 0 \quad [9]$$

Since the flame discontinuity can generate vorticity, it is necessary to examine what happens to $\vec{\omega}$ as the discontinuity is crossed. Tsien (1) has shown that in general, the combustion products are rotational.[4] To see why this is so, we make use of a theorem by Crocco (2). For steady inviscid flows, the equations of motion may be written as

$$\vec{q} \times \vec{\omega} = \nabla h_0 - T \nabla \sigma \quad [10]$$

or for two-dimensional flow (3)

$$\omega = \rho \left( T \frac{\partial \sigma}{\partial \psi} - \frac{\partial h_0}{\partial \psi} \right) \quad [10a]$$

[3] Numbers in parentheses refer to the References on page 101.

[4] It should be noted that the $\lambda$ defined by Tsien is different than that used in this paper.

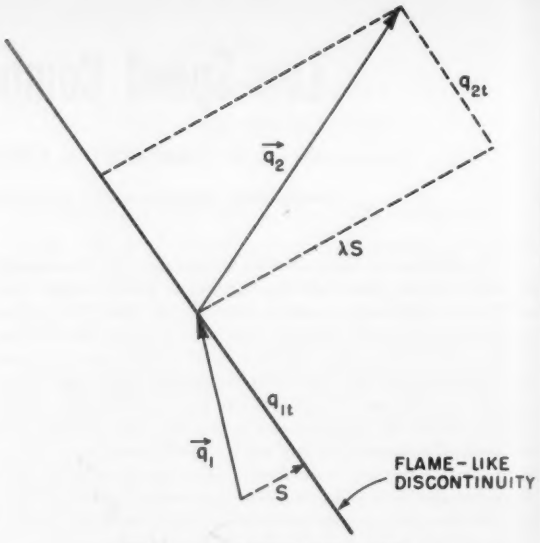


FIG. 1 FLAME FRONT KINEMATICS

where $h_0$ is the stagnation enthalpy, $T$ the temperature, and $\sigma$ the entropy. On the reactant flow side, $\omega_1 = 0$ and there are no entropy or total enthalpy gradients. The energy equation which relates the product and reactant flow field is

$$h_{0_1} + Q = h_{0_2} \quad [11]$$

where $Q$ is the thermal energy introduced into the flow at the discontinuity by means of the chemical reaction. This heat, released by combustion $Q$, may be considered as a constant.

The entropy change across the discontinuity can readily be computed

$$\sigma_2 - \sigma_1 = C_p \ln \lambda - C_v \ln \frac{p_2}{p_1} \quad [12]$$

The entropy change across the discontinuity is a function of the density and pressure ratios at that point. Thus, if $\lambda$ is not a constant (which is the case in compressible flow), or if the flame speed $S$, or the heat of reaction $Q$ is a variable along the flame front, the product flow is indeed rotational. This is the case whenever there are entropy or energy gradients in the flow field. The product flow field is therefore determined by

$$\nabla^2 \psi_2 = -\vec{\omega} \quad [13]$$

where the flame boundary values of $\vec{\omega}$ are given by Equations [10], [11], and [12].

It must be noted that the stream function $\psi$ in Equation [9] is different from that in Equation [13], since the density of the reactants is different from the products. The solution of Equations [9] and [13] coupled by the flame front Equations [3], [5], and [7] plus boundary conditions, is quite difficult. However, several special cases of interest have already been treated. Scurlock (4) has numerically solved the case of the flame shape and flow field in a two-dimensional combustion chamber of constant width. He neglects the pressure drop across the flame front, treats $\lambda$ as a constant, and reduces the problem to a quasi-one-dimensional calculation. Tsien (1) examined the same problem and showed that, with these same assumptions, the calculations could be made very much simpler. Tsien also examines the compressible case and treats the vorticity production by the flame front in detail. Ball (5) solved the same problem, including the pressure change at the flame front, by the relaxation technique.

## The Problem

Much of the present-day low-speed combustion research is done on burners in which the gas is flowing into essentially unbounded space. This combustible jet is often surrounded by moving secondary air to stabilize the flow. For example, at the Harvard Combustion Aerodynamics Laboratory, flames are produced in the combustible jet at a distance well above the nozzle in the combustion tunnel (see Fig. 2). The flame is thus burning in what is nearly equivalent to unbounded space. The primary (combustible) jet is surrounded by moving secondary air. The flow is nearly two-dimensional and steady. What we desire to find are analytical solutions to flow fields of the type which we observe under these experimental conditions.

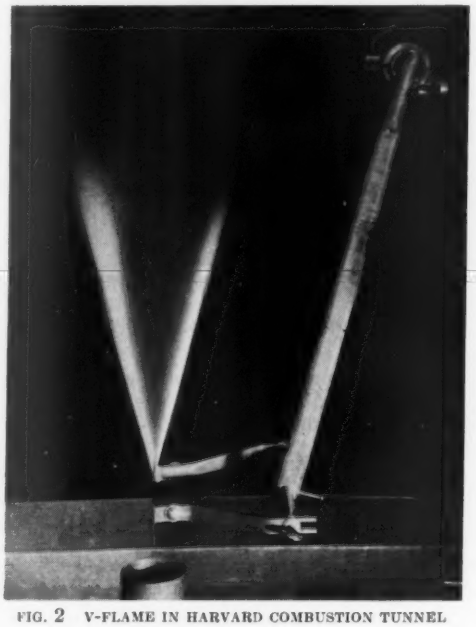

FIG. 2 V-FLAME IN HARVARD COMBUSTION TUNNEL

The problem thus consists of a two-dimensional, steady, inviscid flow in unbounded space. The flow field contains a combustible stream surrounded by secondary air. In actuality, the flame is stabilized on a thin wire or flat plate above the primary nozzle. The flow is low speed, with velocities well below 100 ft/sec. The reactants leave the nozzle with a uniform flat velocity distribution. Thus, Equation [9] determines the reactant flow field. Since the reactant flow field is irrotational, the vorticity of the product flow field is determined by Crocco's theorem expressed by Equation [10a]. Since there are no entropy gradients in the reactant flow, Equations [12] and [7] permit us to find the entropy gradients on the product side of the flame discontinuity. Equation [11] gives the stagnation enthalpy on the product side of the discontinuity. Therefore, Equation [10a] permits us to compute the vorticity on the product side of the flame front. However, we shall consider $\lambda$ and $Q$ as constant. If the flame speed Mach number is also a constant (implying constant flame speed and constant $T_1$) then the pressure ratio, $p_2/p_1$ is a constant. These three assumptions, that $\lambda$, $Q$ and $M_1$ are constant, are good ones for low-speed flows and they necessarily imply from Equation [10a] that the product flow field is irrotational. Therefore, the entire flow field is irrotational and the powerful tools of classical potential theory may be used.

It is interesting to note that one cannot neglect the pressure change across the discontinuity and still satisfy the mass conservation Equation [3]. The assumption of $p_2/p_1 = 1$ is quite good for high-speed flows where $\vec{q_1} \approx \vec{q_2}$ but cannot be used in low-speed flows. This small pressure change across the flame front arouses some interesting questions concerning the stability of such flamelike discontinuities, but we shall not treat such aspects here (6).

With $\lambda$, $Q$, and $p_2/p_1$ constant, the entire flow field is irrotational. The different density of the reactants and products still requires the use of separate $\psi$ functions. However, if one used a single $\psi$ function for both reactant and product fields, some interesting progress toward an approximate solution may be made. Thus, the entire flow field will be described by a single $\psi$ function and the influence of the flame discontinuity will be exactly accounted for by an appropriate source sheet. By considering the reactants and products to be of different densities, the use of a single $\psi$ function will introduce a difficulty along the two free streamlines which separate the products from the secondary air. However, this simplification permits us to arrive at an exact solution to the flow field everywhere except along these two free streamlines. Although this difficulty may be serious, this simplification does permit us to arrive at a solution which describes the type of aerodynamic influence that the flame exerts.

Thus the flow field is a solution to Equation [9] with uniform parallel flow at infinity. The flamelike discontinuity will be represented by an appropriate source sheet. An examination of Fig. 1 or Equations [3] and [5] will show that by choosing the source strength per unit length of the discontinuity to be

$$\Gamma = \frac{(\lambda - 1)S}{2\pi} \qquad [14]$$

the kinematic conditions across a flame front are satisfied. Each element of the source sheet will influence the remainder of the flow field. The solution of Laplace's Equation [9] in two dimensions, which gives the velocity induced by an element of the source sheet at a distance $r$, is

$$\Gamma \frac{dl}{r} = \frac{(\lambda - 1)S}{2\pi} \frac{dl}{r} \qquad [15]$$

Consider Fig. 3. An arbitrary shaped discontinuity is shown and it is specified by the parametric equations $x = f(\tau)$ and

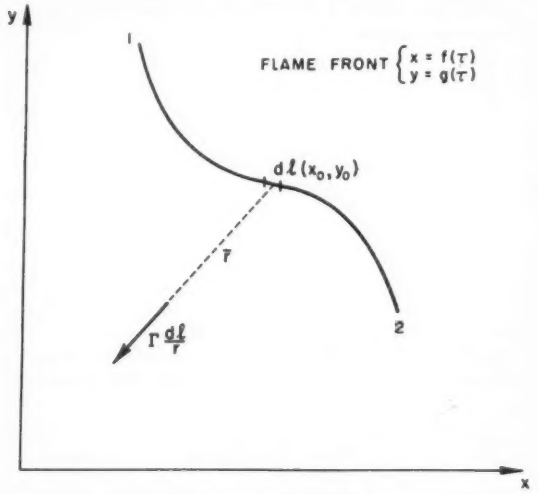


FIG. 3 SOURCE SHEET

$y = g(\tau)$. The flow field induced by the element of the source sheet $dl$ at the point $(\zeta,\eta)$ is given by

$$q_x = \frac{-\Gamma(x - \zeta)dl}{r^2}$$

$$q_y = \frac{-\Gamma(y - \eta)dl}{r^2} \qquad [16]$$

where

$$r^2 = (x - \zeta)^2 + (y - \eta)^2 \quad [17]$$

$$dl = \sqrt{f'(\tau)^2 + g'(\tau)^2}\, d\tau \quad [18]$$

The primes indicate differentiation with respect to $\tau$. The velocity induced by the entire source sheet at the point $(\zeta,\eta)$ is therefore given by

$$\vec{q}_s(\zeta,\eta) = \frac{-(\lambda - 1)}{2\pi} \int_1^2 \frac{S\sqrt{f'^2 + g'^2}}{r^2} \times [\hat{\imath}(f - \zeta) + \hat{\jmath}(g - \eta)]d\tau \quad [19]$$

where $\hat{\imath}$ and $\hat{\jmath}$ are the unit vectors in the $x$ and $y$ directions, respectively. Equation [19] gives the contribution to the velocity from the source sheet only. This induced velocity approaches zero as $r$ becomes very large. It is desired to have uniform parallel flow far from the discontinuity. Since Laplace's equation is linear, solutions may be added. The only boundary conditions to be satisfied are those at the discontinuity and at infinity; thus, addition of a uniform velocity is permissible. The complete velocity field is given by

$$\vec{q}(\zeta,\eta) = \vec{q}_s(\zeta,\eta) + \vec{q}_\infty \quad [20]$$

where $\vec{q}_\infty$ is the velocity at infinity.

The fact that the velocity component normal to the discontinuity on the reactant side must be equal to a preassigned quantity (the flame speed) has not yet been taken into account. Therefore, a constraint equation which limits the shapes of permissible flamelike discontinuities is given by

$$\vec{q}(x_0,y_0)\cdot\hat{n} = S \quad [21]$$

where $(x_0,y_0)$ represents a point on the discontinuity surface, and $\hat{n}$ is the unit vector normal to this surface. That is,

$$\hat{n} = \frac{-\hat{\imath}g'(\tau_0) + \hat{\jmath}f'(\tau_0)}{(f_0'^2 + g_0'^2)^{1/2}} \quad [22]$$

Designating the velocity at infinity as

$$\vec{q}_\infty = \hat{\imath}q_{x_\infty} + \hat{\jmath}q_{y_\infty}$$

the desired permissible flame shape constraint equation can be written out in detail. It is

$$S - \frac{f_0'q_{y\infty} - g_0'q_{x\infty}}{(f_0'^2 + g_0'^2)^{1/2}} = \lim_{\substack{\zeta\to f(\tau_0)\\ \eta\to g(\tau_0)}} \left\{ \frac{-(\lambda - 1)}{2\pi} \times \int_1^2 \frac{S\sqrt{f'(\tau)^2 + g'(\tau)^2}}{r^2\sqrt{f'(\tau_0)^2 + g'(\tau_0)^2}} \left[ -[f(\tau) - \zeta]\, g'(\tau_0) + [g(\tau) - \eta]f'(\tau_0) \right] d\tau \right\} \quad [23]$$

This is a nonlinear integrodifferential equation where the integral must take on preassigned values along the unknown function—namely, the shape of the discontinuity. The uniqueness of the problem is uncertain and appears to require additional physical conditions to be specified, such as stability, etc.

## Some Solutions

There are no known general techniques for finding a solution to equations such as [23]. However, one exact solution has been found. It is

$$x = a\tau \quad y = b\tau \quad \tau_1 \le \tau \le \tau_2$$

where $a$ and $b$ are constants. This solution represents a finite straight line inclined at a fixed angle relative to the velocity vector at infinity. By choosing the coordinate system so that $\vec{q}_\infty$ lies along the $y$-axis, the solution may be verified by substitution into Equation [23]. Thus

$$\frac{2\pi}{\lambda - 1}\left[1 - \frac{a}{(a^2 + b^2)^{1/2}}\left(\frac{q_\infty}{S}\right)\right] = \lim_{\substack{\zeta\to a\tau_0\\ \eta\to b\tau_0}} \left\{ \int_1^2 \frac{a\eta - b\zeta}{(a\tau - \zeta)^2 + (b\tau - \eta)^2}\, d\tau \right\}$$

Upon evaluating the integral and then taking the limit, the right side of the above equation approaches a value of $-\pi$. Therefore

$$\frac{a}{(a^2 + b^2)^{1/2}} = \sin\theta = \frac{\lambda + 1}{2}\left(\frac{S}{q_\infty}\right) \quad [24]$$

where $\theta$ is the angle between the discontinuity and the velocity vector at infinity. This same result may be obtained simply from the geometry at the flame front; see Fig. 8. This gives the straight-line flame-front discontinuity position in terms of the dimensionless quantities $\lambda$ and $S/q_\infty$.

Flame fronts that are extremely close to a straight line have been observed and, in fact, can be produced at will in the Harvard Combustion Tunnel. The details concerned with finding the equation of the streamlines for such a flame front are treated in Appendix 1. The result of this analysis gives the source sheet contribution as

$$q_\zeta = \frac{(\lambda - 1)S}{2\pi} \log \frac{r_1}{r_2} \quad [25]$$

$$q_\eta = \frac{-(\lambda - 1)S}{2\pi}(\phi_1 - \phi_2) \quad [26]$$

where $\zeta$ and $\eta$ are coordinate directions, and $\phi_1$ and $\phi_2$ are angles as specified in Appendix 1. The equation for the streamlines in the flow field is

$$\frac{\psi}{\Gamma} = (x\cos\theta + y\sin\theta)\left(\log\frac{r_1}{r_2} - \frac{q_\infty}{\Gamma}\cos\theta\right) + (x\sin\theta - y\cos\theta)\left[(\phi_1 - \phi_2) - \frac{q_\infty}{\Gamma}\sin\theta\right] - (x_1\cos\theta + y_1\sin\theta)\log\frac{r_1}{r_2} + (x_2\sin\theta - y_2\cos\theta)\phi_2 - (x_1\sin\theta - y_1\cos\theta)\phi_1 \quad [27]$$

$\psi$ is the stream function, and the subscripts 1 and 2 indicate the end points of the source sheet. Since lines of constant $\psi$ are streamlines, Equation [27] permits mapping the entire flow field by specifying the values of $S/q_\infty$ and $\lambda$. Such a flow field has been mapped out and is shown in Fig. 4. This represents a flow for $S/q_\infty = 0.1$, and $\lambda = 7$; values which are common for deflagration.

At the discontinuity, the tangential component of velocity $q_\zeta$ is small compared with usual values of $q$, except for points close to the ends of the source sheet. Here, the solution has singular points and the values of $q$ become very large. This of course violates the low Mach number restriction and the solution is not valid in the near neighborhood of the end points of the discontinuity. The pressure distribution is given by

$$\frac{q^2}{2} + \frac{\gamma}{\gamma - 1}\frac{p}{\rho} = h_0 \quad [28]$$

since the stagnation enthalpy is constant in either the reactant or product flow field. However, the value of $h_0$ changes across the flame discontinuity as indicated by Equation [11]. By the nature of the solution, $\vec{q}$ is continuous across the free streamline which bounds the products and the secondary air. However, $h_{0_2} > h_{0_1}$, and this results in the difficulty previously mentioned, namely, that these two bounding streamlines have a resulting pressure drop across them and hence could not be steady. This results in an error in the position of the streamlines. The magnitude of this error will be compared with experiment in a later section.

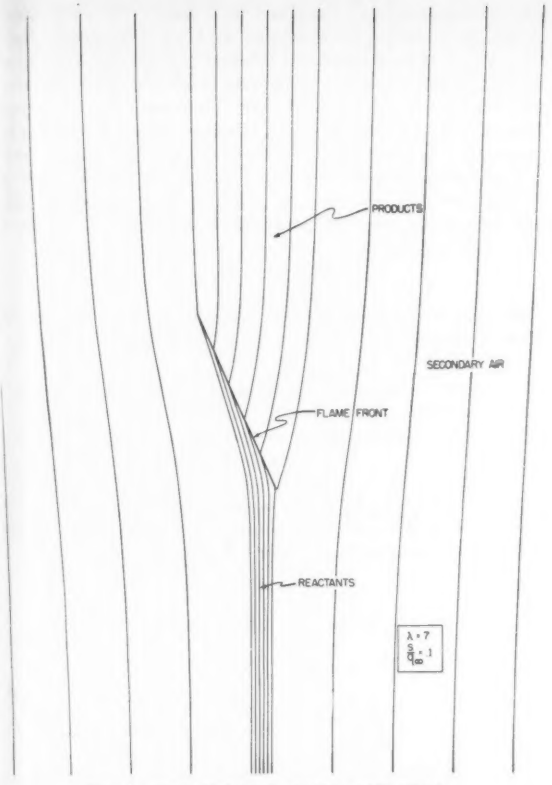


FIG. 4 STRAIGHT-LINE FLAME FLOW FIELD

Examining Fig. 4 shows some interesting features. The streamlines which pass through the ends of the source sheet are considered to be boundaries of the combustible core. The flow outside this core is assumed to be noncombustible secondary air. The effect of the flame front on the remainder of the flow field is evident. The entire combustible core is deflected from its initial path because of the presence of the flame front. Such stream deflections are evident in schlieren photographs of real flames. One should recall that in this analysis these effects are *not* because of such things as heat transfer, but are the aerodynamic interaction of the flame front and the flow field.

A commonly observed flame is the so-called V-flame. Such a flame is shown in Fig. 2. Since this appeared so similar to the straight-line solution already given, it was hoped that we could generate simply a solution to this V-flame by reflecting the first solution about its $y$-axis. Although the resulting flow field still satisfies Equations [3], [5], and [9], the flame speed constraint Equation [23] is violated because of the mutual interaction of the two sheets.

An examination of the induced normal velocity to these sheets indicated that $q_{1n}$ varies about as $l^2$ where $l$ is the length along the discontinuity, measured from the vertex. By placing a proper strength dipole at the origin, the flame speed may be made nearly constant over the major length of the V. This problem of the V has been worked out and is shown in Fig. 5. The area within the circle at the vertex contains the domain where the singularity (resulting from the dipole) violates the basic assumptions of the problem. The details of the V solution and dipole addition are given in Appendix 2. A graph of $q_{1n}$ as a function of $l$ is shown in Fig. 6.

In comparing the V solution to the single sheet, it is evident that for the same values of $\lambda$ and $\theta$, the V requires a smaller value of $S/q_\infty$. This is physically evident from the mutual interaction of the two flame surfaces. The V solution has nearly a constant flame speed except close to the apex where the solution breaks down ordinarily.

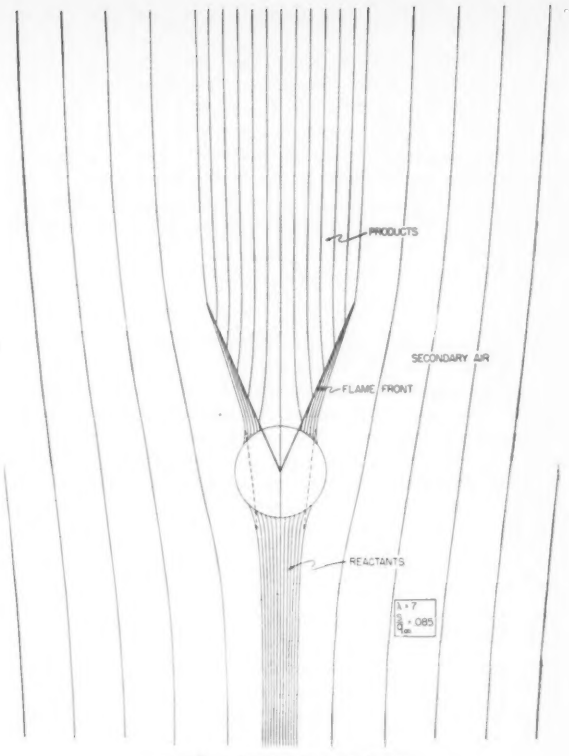


FIG. 5 V-FLAME FLOW FIELD

## Dimensional Considerations; Some Experimental Results

The previous analysis permits an interesting insight into the important physical parameters present in such aerothermodynamic problems. For those cases where the flame may be treated as a discontinuity and no solid boundaries are present, the following dimensionless groups determine the problem:

$s/q_\infty$ = flame speed/velocity at infinity
$\rho_1/\rho_2 = \lambda$ = density ratio
$M_1 = s/a$ = flame speed Mach number
$Q/c_pT_1$ = heat of reaction/enthalpy of reactants
$\gamma$ = ratio of specific heats = $c_p/c_v$

In the presence of boundaries it would appear that the vis-

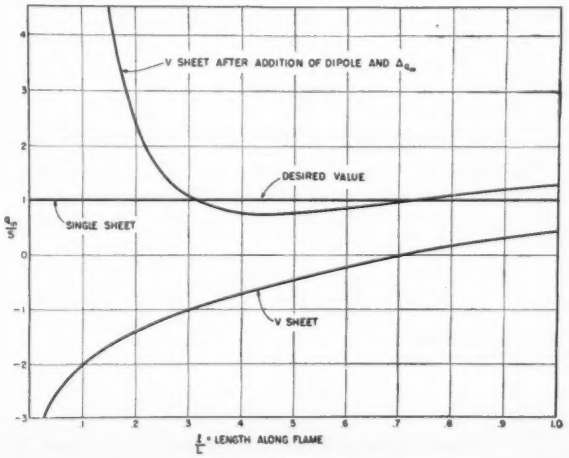


FIG. 6 NORMAL VELOCITY AT FLAME FRONT

cosity and thermal conductivity of the gases must be included.

In the development of the present problems, some interesting questions arose. In reality, the flame speed Mach number $M_1$ varies slightly and the product flow is rotational. If the flow is slightly rotational, when can this rotation be justifiably neglected? The characteristic length present in this problem is the finite length of the flame front, $L$. It would appear from dimensional considerations that the vorticity does not appreciably influence the shape of the flame front when

$$\frac{\omega L}{q_\infty} \ll 1$$

In the combustion tunnel at Harvard University it is possible to experimentally check some of the conclusions drawn from this analysis. In the presence of a thin wire flame holder held above the primary nozzle, flat sheets and V-type flames can easily be produced. The easiest quantitative prediction to check is that of Equation [24], the flame angle. This was done for propane-air flames. Some typical results are given below.

| $\lambda$ | $s/q_\infty$ | Computed | Measured |
|---|---|---|---|
| 7.30 | 0.0490 | 12° | 10° ± 2° |
| 7.23 | 0.0494 | 12° | 10° ± 2° |
| 7.00 | 0.100 | 23° | 16° ± 2° |
| 7.30 | 0.0962 | 23° | 15° ± 2° |

The above numbers represent values of $s$ and $q_\infty$ over the range $1.15 \leq S \leq 1.47$ ft/sec, and $13.8 \leq q_\infty \leq 30$ fps. The agreement appears good for small values of $s/q_\infty$ but is poor at higher values.

The neglect of the product vorticity does not appear to adequately explain the disagreement. However, the use of a single $\psi$ function for the products and the secondary air belies the fact that physically they have different densities. Thus, in our solution if we consider the density of the products and secondary air to be different, we have violated momentum conservation along the bounding streamlines. This may partially explain the difference in angles measured experimentally and predicted from our equations.

If one neglects the aerodynamic effect of the flame, the value of $\theta$ would be given by $\sin\theta = s/q_\infty$. Using the above data, this would predict values of $\theta$ less than 6°, which are far too small.

## Acknowledgments

The authors would like to express their appreciation to the Office of Ordnance Research for making this work possible, and to the Harvard Computation Laboratory for the use of the Mark IV computer. We also take pleasure in acknowledging the many stimulating discussions with Prof. H. W. Emmons, Dr. M. Mitchner, and Dr. R. E. Kronauer.

## APPENDIX 1

### Field Equations for Straight Line Source Sheet

We consider an element of length $dl$ of the source sheet, as shown for the general case in Fig. 3. The sheet extends infinitely in the direction normal to the page. The potential arising from such an element is

$$d\Phi = \Gamma \log r\, dl = \frac{(\lambda - 1)S}{2\pi} \log r\, dl$$

generating velocity

$$\vec{dv} = \nabla(d\Phi) = \frac{\Gamma}{r}\, dl\, \frac{\vec{r}}{|r|}$$

The entire potential and resulting velocity are obtained by integrating these expressions over the entire source sheet, and superimposing a constant flow field. For any flame shape, the resulting field satisfies the laws of mechanics both throughout the reactant and product regions and across the discontinuity. The one remaining condition, that the normal velocity of the reactants into the source sheet be equal everywhere to the flame speed, has been shown previously to be satisfied in particular for a finite straight line source sheet.

The integration of the above equations for this case is straightforward; it may be checked that Equations [25] and [26] result. A more convenient technique is the use of the complex potential

$$W(z) = \Phi + i\psi$$

since it gives also the stream function $\psi$, by definition related to the potential $\Phi$ by the Cauchy-Riemann conditions

$$\frac{\partial \Phi}{\partial x} = q_x = \frac{\partial \psi}{\partial y}$$

$$\frac{\partial \Phi}{\partial y} = q_y = -\frac{\partial \psi}{\partial x}$$

which, of course, imply that $\psi$ is a solution of $\nabla^2\psi = 0$. Since $\nabla\Phi \cdot \nabla\psi = 0$, the lines $\psi$ = constant are everywhere normal to the equipotential lines, hence being streamlines.

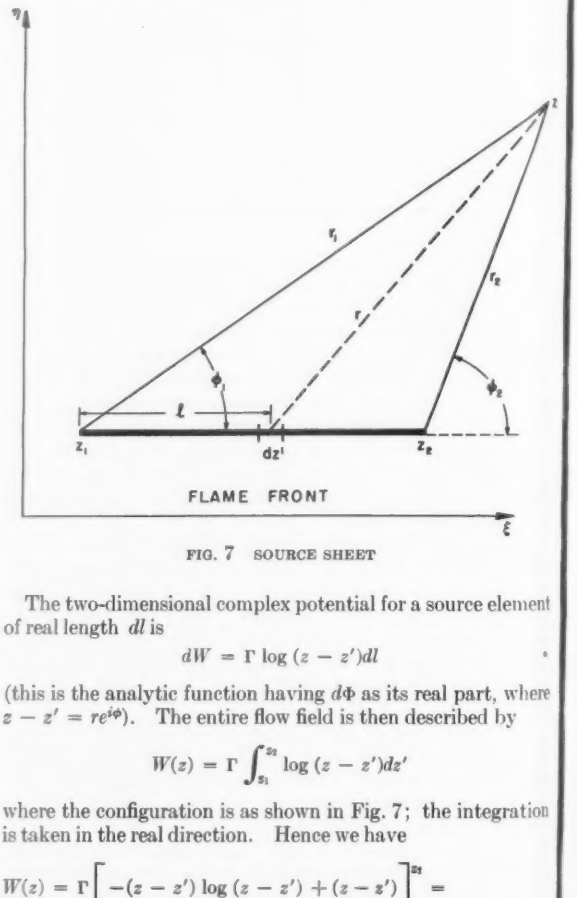


FIG. 7 SOURCE SHEET

The two-dimensional complex potential for a source element of real length $dl$ is

$$dW = \Gamma \log (z - z')dl$$

(this is the analytic function having $d\Phi$ as its real part, where $z - z' = re^{i\phi}$). The entire flow field is then described by

$$W(z) = \Gamma \int_{z_1}^{z_2} \log (z - z')dz'$$

where the configuration is as shown in Fig. 7; the integration is taken in the real direction. Hence we have

$$W(z) = \Gamma\left[-(z - z') \log (z - z') + (z - z')\right]_{z_1}^{z_2} =$$

$$\Gamma\left[z \log \frac{(z - z_1)}{(z - z_2)} + z_1 - z_2 + z_2 \log (z - z_2) - z_1 \log (z - z_1)\right]$$

As shown in Fig. 7, we define $z = \xi + i\eta$

$$z - z_1 = r_1 e^{i\phi_1}$$

$$z - z_2 = r_2 e^{i\phi_2}$$

hence

$$\frac{z - z_1}{z - z_2} = \frac{r_1}{r_2} e^{i(\phi_1 - \phi_2)}$$

giving the real and imaginary parts of $W(z)$

$$\frac{\Phi}{\Gamma} = \zeta \log \frac{r_1}{r_2} - \eta(\phi_1 - \phi_2) + \zeta_1 - \zeta_2 + \zeta_2 \log r_2 - \zeta_1 \log r_1 + \eta_1(\phi_1 - \phi_2)$$

$$\frac{\psi}{\Gamma} = \eta \log \frac{r_1}{r_2} + \zeta(\phi_1 - \phi_2) + \eta_1 \log \frac{r_2}{r_1} + \zeta_2\phi_2 - \zeta_1\phi_1$$

where we use $\eta_2 = \eta_1$.

By differentiation of either of these (expressing $\phi_1$, $\phi_2$, $r_1$, and $r_2$ in terms of $\zeta$ and $\eta$), we find

$$q_\zeta = \Gamma \log \frac{r_1}{r_2} \quad \ldots\ldots\ldots\ldots\ldots\ldots [25]$$

$$q_\eta = -\Gamma(\phi_1 - \phi_2) \quad \ldots\ldots\ldots\ldots\ldots\ldots [26]$$

and finally, by a counterclockwise rotation of the coordinate system by $(\pi/2 - \theta)$ (see Fig. 8), and by adding $-xq_\infty$, the stream function of a constant velocity in the $y$ direction, we obtain the final stream function

$$\frac{\psi}{\Gamma} = (x \cos\theta + y \sin\theta)\left(\log \frac{r_1}{r_2} - \frac{q_\infty}{\Gamma} \cos\theta\right) + (x \sin\theta - y \cos\theta)\left[(\phi_1 - \phi_2) - \frac{q_\infty}{\Gamma} \sin\theta\right] - (x_1 \cos\theta + y_1 \sin\theta) \log \frac{r_1}{r_2} + (x_2 \sin\theta - y_2 \cos\theta)\phi_2 - (x_1 \sin\theta - y_1 \cos\theta)\phi_1 \ldots [27]$$

We may check that this solution has the properties claimed; thus, examining Equations [25] and [26], we see that the induced velocity goes to zero as $r$ grows large in any direction. Further, the normal velocity $q_\eta$ is constant along the source sheet, and discontinuous by the constant amount $(\lambda - 1)\, S = 2\pi\Gamma$ across the source sheet, as desired.

## APPENDIX 2

### V-Sheet Equations

Making use of the line of symmetry, we put the origin at the vertex of the V. Let $\psi(x,y)$ be the stream function for the single sheet (forming one leg of our V), as derived in Appendix 1. Then $-\psi(-x,y)$ will give the stream function contribution at the point $(x,y)$ from the other half of the V. The minus sign arises as, in reflecting about the $y$-axis, the coordinate system becomes left-handed. Then, in order that

$$q_x = \partial\psi/\partial y$$

$$q_y = -\partial\psi/\partial x$$

still be true in the original coordinate system, we must replace $\psi(-x,y)$ by $-\psi(-x,y)$.

Hence, proceeding as before, our complete stream function is

$$\psi_v = \psi(x,y) - \psi(-x,y) - xq_\infty$$

This of course satisfies the laws of mechanics throughout the plane and across the discontinuity; however, it gives a $q_{1n}$ (normal velocity of the reactants at the source sheet) which differs badly from a constant (see Fig. 6). This discrepancy is not remedied by changing $\theta$ or our fundamental parameters $\lambda$ and $s/q_\infty$. Thus we are led to the conclusion that, for our simplified model, the V is not a possible flame shape.

The fact remains, however, that flames which are fairly two-dimensional and fairly V-shaped are observed. (See Fig. 2.) Though conditions in the Harvard Combustion Tunnel are not the ideal conditions assumed here (the secondary air region does not extend to infinity, the problem is not exactly two-dimensional, a flame holder and nozzle boundary layer have been introduced, etc.), it is felt that experimental

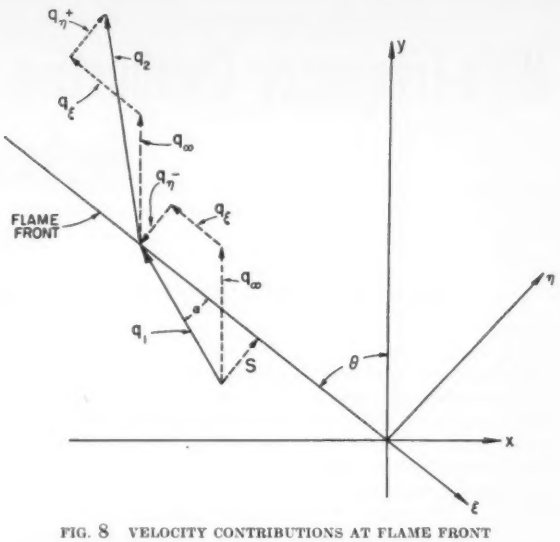


FIG. 8 VELOCITY CONTRIBUTIONS AT FLAME FRONT

perturbations do not explain the disagreement. Perhaps some assumption (such as that of constant flame speed) is unjustified, or perhaps the influence of a flame holder is important throughout the real flow field. However, as remarked above, the use of a single $\psi$ function is unrealistic, and probably this is responsible.

Putting aside for now the problem of an exact solution of the simplified problem, we seek an approximate solution to the V-flame which does not involve an exorbitant amount of computation. Let us add a dipole at the origin, oriented with source in the negative $y$ direction, which induces a velocity field with stream function

$$\mu_x/(x^2 + y^2)$$

where $\mu$ is a constant. (It may be readily verified that this is a solution to $\nabla^2\psi = 0$.) The total stream function then is

$$\psi_v = \psi(x,y) - \psi(-x,y) - (q_\infty + \Delta q_\infty)x + \mu_x/(x^2 + y^2)$$

The addition of the dipole and $\Delta q_\infty$ has introduced a change in $q_{1n}$ given by

$$\Delta q_\infty \sin\theta + \mu/(l^2 \sin\theta)$$

Choosing arbitrarily a tolerance of 25 per cent, it was found that by adjustment of the parameters $\mu$ and $\Delta q_\infty$, $q_{1n}$ could be made approximately constant over the upper three fourths of the source sheet. (See Fig. 6). The resulting approximate solution is presented in Fig. 5. Within the circle about the origin the dipole dominates the solution. The effects of the dipole are noticeable just outside of the circle; fortunately they fall off as the square of the distance from the origin.

## References


1 "Influence of Flame Front on the Flow Field," by H. S. Tsien, *Journal of Applied Mechanics*, vol. 18, June 1951, pp. 188–194.

2 "Eine neue Stromfunktion für die Erforschung der Bewegung der Gase mit Rotation," by L. Crocco, *Zeitschrift f. Aug. Math. und Mech.* vol. 17, 1937, pp. 1–7.

3 "On Rotational Gas Flows," by A. Vazsonyi, *Quarterly of Applied Mathematics*, vol. III, April 1945, pp. 29–37.

4 "Flame Stabilization and Propagation in High Velocity Gas Streams," by A. C. Scurlock, Meteor Report no. 19, Massachusetts Institute of Technology, 1948.

5 "A Study of a Two-Dimensional Flame," by George A. Ball, Combustion Laboratory Report, Harvard University, July 1951.

6 "Experimental and Theoretical Studies of Flame Front Stability," by G. H. Markstein, *Journal of the Aeronautical Sciences*, vol. 18, March 1951, pp. 199–209.

# High-Frequency Combustion Instability in Solid Propellant Rockets. Part 2[5]

SIN-I CHENG

Daniel and Florence Guggenheim Jet Propulsion Center, Princeton University, Princeton, N. J.

**A theory of unstable high-frequency oscillations in solid propellant rockets is advanced with the mechanism of self-excitation based on the following simplified model. Both the rate of primary decomposition of solid propellant element and the rate of activation of the intermediate products during the time lag are assumed to depend upon the gas oscillations. Both interactions are expressed in terms of the instantaneous pressure according to power law with exponent $n$ and $m$, respectively. The dependence of the rate of decomposition on drifting velocity is shown to be not of fundamental importance in determining the stability of oscillations in the combustion chamber. Analysis shows that a simplified over-all pressure index of interaction $S = m - (n/2)$ must be bigger than certain minimum value if unstable oscillation is to be possible. Unstable oscillation further requires the time lag to be in proper range. The most unstable mode is shown to be the fundamental spiral mode, and its tangential component with exactly the acoustical frequency is the one which is most easily observed at finite magnitudes because of its rapid amplification. Several configurations of the propellant grain with radial burning surfaces have been investigated. Rod grain becomes more stable while other grain shapes become less stable in the course of firing. Rod grain is the most stable while tubular grain is the most unstable configuration. The stabilizing effect of inserting a nonburning solid rod into tubular grain is verified by the theory. Several other aspects have also been treated. Solid rocket with end burning grain also becomes less stable in the course of operation. Both the spiral and the longitudinal modes in rocket with end-burning grain are briefly investigated.**

## Rockets with Tubular Grain

Consider first a solid propellant rocket using perforated cylindrical grain with interior burning surface, that is, the tubular grain. In this case there is no solid nonburning surface. The radial boundary condition [14] is replaced by the requirement that all disturbances must remain finite at the axis of the cylinder. Thus, the constant $c$ in Equation [8] must vanish. When the radius of the burning surface is taken as the reference length, it can be found either directly or by taking the limit of $r_1 \to 0$ with $r_2 = 1$ in Equation [20], that

$$\begin{cases} \kappa = 1 - \dfrac{\beta^2}{\eta_0^2} \\ J_\beta'(\eta_0) = 0 \end{cases} \qquad [27]$$

For the fundamental spiral mode, $\beta$ is equal to unity. Then $\eta_0 = 1.84$ which is the lowest zero of $J_1'(\eta)$. Equation [27] gives $\kappa = 0.70$ which is a constant throughout the entire period of firing of the rocket. Equation [25] for the minimum index of interaction compatible with unstable oscillations then becomes

$$S_{\min} = \frac{1}{2\gamma}\left[1 + 0.70\,\frac{\mathcal{I}(\xi^2)}{-2\,\eta_0\bar{v}_1}\right] \qquad [28]$$

During the course of firing of the solid rocket after steady state has been reached, the burning rate at stable operation is constant and, therefore, the normal velocity $\bar{v}_1$ of the burned gas at the burning surface is also constant. For the interior burning surface, $\bar{v}_1$ is negative. When the propellant burns, the radius of the burning surface is increasing. As the length of the grain is constant, the value of $\lambda$ is decreasing with time. Whether the value of $S_{\min}$ is decreasing or increasing with decreasing $\lambda$ is of particular interest because this indicates whether the system becomes more stable or more unstable in the course of firing.

By expanding the left-hand side of Equation [16] into real and imaginary parts, one obtains

$$\mathcal{R}[\lambda\xi \tan \lambda\xi] = \frac{1}{2}\,\frac{\lambda\xi_r \sin 2\lambda\xi_r - \lambda\xi_i \sinh 2\lambda\xi_i}{\cosh^2 \lambda\xi_i \cos^2 \lambda\xi_r + \sinh^2 \lambda\xi_i \sin^2 \lambda\xi_r} = -\omega A_i \lambda \bar{u}_e$$

$$\mathcal{I}[\lambda\xi \tan \lambda\xi] = \frac{1}{2}\,\frac{\lambda\xi_i \sin 2\lambda\xi_r + \lambda\xi_r \sinh 2\lambda\xi_i}{\cosh^2 \lambda\xi_i \cos^2 \lambda\xi_r + \sinh^2 \lambda\xi_i \sin^2 \lambda\xi_r} = \omega A_r \lambda \bar{u}_e \qquad [29]$$

and

$$\frac{\mathcal{R}[\lambda\xi \tan \lambda\xi]}{\mathcal{I}[\lambda\xi \tan \lambda\xi]} = -\frac{A_i}{A_r} \qquad [30]$$

The values of $\mathcal{I}[\lambda\xi \tan \lambda\xi]$ and $\mathcal{R}[\lambda\xi \tan \lambda\xi]/\mathcal{I}[\lambda\xi \tan \lambda\xi]$ for several values of $\lambda\xi_r$ and $\lambda\xi_i$ are plotted in Fig. 3.[6] Equation [30] shows that the value of $\mathcal{R}[\lambda\xi \tan \lambda\xi]/\mathcal{I}[\lambda\xi \tan \lambda\xi]$ is always negative with its magnitude equal to $A_i/A_r$ as determined from Fig. 2 by the value of the reduced frequency parameter $\Omega = \lambda\xi_r \cdot \epsilon/[(2/\gamma + 1)^{1/2} - \bar{u}_e]$ for the axial oscillation. For the fundamental mode of axial oscillation, $\lambda\xi_r$ is of the order of unity and the reduced frequency parameter is of the order of $\epsilon$ which is in practical cases a small fractional value. Consequently $A_i/A_r$ is of the order of 3 or even larger. Under such circumstances, Fig. 3 shows that the values of $\mathcal{R}[\lambda\xi \tan \lambda\xi]$ and $\mathcal{I}[\lambda\xi \tan \lambda\xi]$ can be represented by their asymptotic values $-\lambda\xi_i$ and $\lambda\xi_r$, respectively, with reasonable accuracy. Hence, using Equations [29], one obtains

$$\frac{\mathcal{I}(\xi^2)}{-2\,\eta_0\bar{v}_1} = \frac{\xi_r\xi_i}{-\eta_0\bar{v}_1} = \eta_0 A_i A_r \cdot \frac{\bar{u}_e^2}{|\bar{v}_1|} \qquad [31]$$

Since viscous effect is neglected, $\bar{u}_e$ represents the mean axial velocity at the exit $x = \lambda$, and the continuity of mass flow gives

$$\bar{u}_e = 2\lambda|\bar{v}_1| \cdot \frac{r_2^2}{r_2^2 - r_1^2} \qquad [32]$$

[5] Part I of this paper appeared in the January-February issue of JET PROPULSION, pages 27–32.

[6] Figs. 1 through 5 appeared in Part 1.

Equation [28] for the minimum value of $S$ of rockets with tubular grain, where $r_1 = 0$ and $r_2 = 1$, becomes

$$S_{\min} = \frac{1}{2\gamma}\,[1 + 5.15 A_i A_r \lambda^2 |\bar{v}_1|] \quad \ldots\ldots\ldots\ldots [33]$$

where $\eta_0 = 1.84$ for $\beta = 1$ has been substituted.

For a given solid rocket $e$, $|\bar{v}_1|$, and $\lambda$ are known. The ratio of the reduced frequency parameter $\Omega$ and $A_r$ can be directly calculated from

$$\frac{\Omega}{A_r} = \lambda \eta_0 \bar{u}_e \frac{1}{e}\left[\left(\frac{2}{\gamma+1}\right)^{1/2} - \bar{u}_e\right]$$

The values of $A_r$ and $A_i$ can thus be read from Fig. 2, and $S_{\min}$ for the particular configuration can be calculated from Equation [33]. For example, with $1/e = 7.5$, $|\bar{v}_1| = 0.01$, and $\lambda = 15$ we have for $\gamma = 1.20$

$$\bar{u}_e = 2\lambda|\bar{v}_1| = 0.30 \qquad \Omega/A_r = 1.78 \qquad A_r = 0.14 \qquad A_i = 0.30$$
$$2\gamma S_{\min} - 1 = 0.49 \qquad S_{\min} = 0.62$$

This calculation is repeated for different values of $\lambda$ of two rockets with $1/e = 7.5$ and 10, respectively, using a solid propellant with $|\bar{v}_1| = 0.01$. The results are plotted in Fig. 4. In the determination of $A_r$ from the ratio of $\Omega/A_r$, it is found that in certain range of values of the ratio $\Omega/A_r$, $A_r$ is multivalued. The lowest value is selected because we are only interested in the fundamental axial mode which gives the lowest value of $S_{\min}$ for the time being. If $\lambda$ is kept increasing, both the value of $\bar{u}_e = 2\lambda|\bar{v}_1|$ and $\Omega/A_r$ increase monotonically. When the value of $\Omega/A_r$ is sufficiently large, no solutions of $A_r$ can be found from Fig. 2. Solution, however, does exist in the region of $\Omega$ beyond that covered by Fig. 2, but this solution will give an $S_{\min}$ much bigger than unity. Furthermore, the approximate method is no longer valid in this region. Therefore, the solutions in regions of large $\Omega$ are discarded. The results of calculation as given in Fig. 4, indicate a very steep rise of $S_{\min}$ with increasing $\lambda$ before $\lambda$ is big enough to invalidate the present method of approximate calculation. The solution for $S_{\min}$ with larger values of $\lambda$ is hence of little practical interest. It is, therefore, inferred that during the course of firing of a solid rocket using tubular grain, the solid rocket destabilizes at a very fast rate in the early stage of operation until the value of $\lambda$ of the rocket becomes smaller than certain critical ranges of values which depends on the axial geometrical parameter $1/e$ ($\lambda = 15$ to 18 as shown in Fig. 4 for the cases calculated). After passing through this critical range, the rate of destabilizing becomes much slower. The small high-frequency disturbances which are stable at the earlier stage of operation may thus become unstable at a later stage when the value of $\lambda$ of the system becomes sufficiently small as to give a $S_{\min}$ lower than the value of the index $S$ of interaction of the particular propellant used. This destabilizing tendency of a solid rocket with tubular grain agrees with the fact that abnormal pressure peak occurs in the later period of operation of a solid rocket preceded by a period of smooth operation.

From Fig. 4, the importance of the axial geometry of the solid rocket is easily recognized. The destabilizing effect of using shorter "effective nozzle," i.e., larger value of $1/e$, is very significant.

Suppose an end seal of radius $r_0$ is installed at the end of the propellant grain; then Equations [32] and [33] become

$$\bar{u}_e = 2\lambda|\bar{v}_1| \cdot \frac{r_2^2}{r_0^2} = 2\lambda|\bar{v}_1|\frac{1}{r_0^2} \quad \ldots\ldots\ldots\ldots [34]$$

and

$$S_{\min} = \frac{1}{2\gamma}\left[1 + 5.15\, A_i A_r \lambda^2 |\bar{v}_1|/r_0^4\right] \quad \ldots\ldots\ldots [35]$$

since $r_0 < 1$, $\bar{u}_e$ is greater than $2\lambda|\bar{v}_1|$. For the same value of $\lambda$ the product $A_i A_r$ would change slightly from the corresponding value without end seal. However, this change of $A_i A_r$ is rather small as compared to the increase of $S_{\min}$, due to the factor $1/r_0$.[4] The use of end seal with $r_0 < 1$ is thus stabilizing, and the stabilizing effect is larger when $r_0$ is smaller. Some calculated results are shown in Fig. 5. This stabilizing effect of using end seals of smaller inside diameter as obtained from the present investigation agrees with the experimental results in (1). They find rough burning in rockets using end seal of larger inside diameter, but find smooth burning in rockets using end seal of smaller inside diameter.

Now if the end seal is nonerosible, that is, the inside radius of the end seal is constant throughout the operation, the value of $r_0$ decreases continuously with time during operation because the burning surface radius or the reference length increases with time. Hence, the stabilizing effect of the nonerosible end seal increases with time. Whether this stabilizing effect can offset the destabilizing effect of decreasing $\lambda$ toward the later stage of operation can be determined by further calculations for the particular geometrical configuration. If the end seal is erosible the value of $r_0$ decreases less fast than that for nonerosible end seal and, in extreme cases, $r_0$ may even increase depending upon the rate of erosion of the end seal. The rocket with nonerosible end seal is thus more stable than a similar rocket with erosible end seal of the same initial inside diameter.

Now we investigate the stability of the fundamental nonspiral mode in rockets with tubular grain as compared to the stability of the fundamental spiral mode. For nonspiral mode $\beta = 0$, and the first or the lowest nonzero value of $\eta_0$ that makes $J_0'(\eta_0) = 0$ is 3.83 and $\kappa = 1$. The expression for $S_{\min}$ for the fundamental nonspiral mode becomes

$$S_{\min} = \frac{1}{2\gamma}\,[1 + 15.3 \cdot A_i A_r \lambda^2 |\bar{v}_1|] \quad \ldots\ldots\ldots [36]$$

which is considerably larger than the values of $S_{\min}$ for fundamental spiral mode as given by Equation [33] under any circumstances. This shows that the fundamental high-frequency radial mode of oscillation with no circumferential component and small axial component is much more stable than the fundamental spiral mode where circumferential component is predominating with negligible axial component. (The case of $\beta = 0$ and $\eta_0 = 0$ is essentially an axial mode which cannot be analyzed with the approximate scheme used in the present investigation.) The relative stability of high-frequency oscillations of different modes can be compared with Equations [28] and [31]. If the axial component of an oscillation is not the fundamental mode, but a higher mode, then the value of $\lambda\xi_r$ corresponding to this higher axial mode is larger than the value of $\lambda\xi_r$ corresponding to the fundamental axial mode. The reduced frequency parameter for the flow in the de Laval nozzle, $\Omega = \lambda\xi_r \cdot e \Big/ \left[\left(\frac{2}{\gamma+1}\right)^{1/2} - \bar{u}_e\right]$ will also increase proportionately. From Fig. 2, it is seen that while $\Omega$ increases, both $A_r$ and $A_i$ increase so long as $\Omega$ is not too big. Equation [31] then shows that $\mathcal{J}(\xi^2)/-2\eta_0\bar{v}_1$ is bigger in the case of higher axial mode. The value of $S_{\min}$ for oscillations with nonfundamental axial component is hence larger than the value of $S_{\min}$ for oscillations with fundamental axial component. In other words, oscillations with nonfundamental axial component are more stable than the oscillation with fundamental axial component.

For oscillations with fundamental axial component and successive higher modes of circumferential component, i.e., when $\beta$ takes successive higher integral values bigger than unity, the lowest zero $\eta_0$ of $J_\beta'(\eta)$ increases with $\beta$. Thus, the ratio $\Omega/A_r$, the reduced frequency $\Omega$, the product $\eta_0 A_r A_i$, and ultimately $S_{\min}$, increase with increasing $\beta$. Oscillations with nonfundamental circumferential component are, therefore, more stable than the oscillation with fundamental cir-

cumferential component. Likewise, oscillations with non-fundamental radial components, i.e., when the zeros of $J_\beta'(\eta)$ larger than $\eta_0$ are taken, can be shown to be more stable than the oscillation with fundamental radial component. It is, therefore, concluded that the high-frequency oscillation composed of the three fundamental components in the circumferential, the radial, and the axial directions is the most unstable mode. Let us call this mode the fundamental spiral mode. The investigation of the relative stability of this fundamental spiral mode alone in different rockets will indicate the relative liability of the occurrence of large amplitude oscillations in these rockets.

## Rockets with Different Radial Configurations

If a nonburning rod is installed axially inside a solid rocket with tubular grain, the expression for $S_{\min}$, as given in Equation [25], is more conveniently written with $r_1 = a$ and $r_2 = 1$ as

$$S_{\min} = \frac{1}{2\gamma}\left[1 + 4\lambda^2|\bar{v}_1|\cdot\zeta\cdot\sigma\right] \quad \ldots\ldots\ldots\ldots [37]$$

where $\sigma = -(\bar{u}_e/2\lambda\bar{v}_1)\kappa$ which is a parameter of radial dimensions only. $\kappa$ is given by Equation [20], and $\bar{v}_1$ is negative on an interior burning surface and is positive on an exterior burning surface.

$\zeta = \eta_0 A_i A_r/(1 - a^2)$ is the parameter critically dependent on the axial boundary condition at $x = \lambda$.

$\eta_0 \cong \omega$ is given by the solution of the equation

$$\frac{J_\beta'(\eta_0)}{J_\beta'(\eta_0 a)} = \frac{Y_\beta'(\eta_0)}{Y_\beta'(\eta_0 a)}$$

For the case of fundamental spiral mode where $\beta = 1$, the smallest positive values of $\eta_0$ for different values of $a$ are determined graphically, based on the tabulated values of Bessel's functions in (7). They are presented in Fig. 6 with $\eta_0$ and $Y_1'(\eta_0)/Y_1'(\eta_0 a)$ plotted against $a$. It should be noted that when $a$ approaches zero the function $Y_1'(\eta_0)/Y_1'(\eta_0 a)$ behaves like $a^2$. The parameter $\sigma$ is also calculated and plotted as shown in Fig. 7. When the radius of the nonburning rod increases, $\sigma$ increases monotonically and is, therefore, stabilizing. The actual value of $S_{\min}$ further depends on the parameter $\zeta$, which depends on a number of factors involved in the boundary condition at the axial exit; for example, the nozzle geometry, the extent of the stagnant gas region, the shape of the end seal, and so on. Suppose the approximate boundary condition is taken and $A_i$ and $A_r$ are determined from Fig. 2 in the manner explained in previous section, it is found that when $a$ increases from zero, the value of $\zeta(a)/\zeta(0)$ shows a slight decrease and then increases rapidly, as shown in Fig. 8 for the particular case of $|\bar{v}_1| = 0.01$ and $1/e = 10$ with three different values of $\lambda$. The value of $\sigma(a)/\sigma(0)$ is also plotted in Fig. 7 which shows a rapid increase when $a$ begins to increase from zero, but becomes nearly constant when $a$ is bigger than 1/2. The product of the two parameters $\zeta\cdot\sigma$ for given value of $\lambda$ and, therefore, the value of $S_{\min}$ will increase steadily with increasing radius of the nonburning rod. In Fig. 9 the value of $S_{\min}$ is plotted against $\lambda$ for $a = 0$, $a = 1/4$, and $a = 1/2$. Therefore, by inserting a nonburning rod into the tubular grain of a solid rocket, the system is stabilized. The stabilizing effect expressed as the increase in $S_{\min}$ is larger if the radius of the nonburning rod as a fraction of the burning surface radius is larger. From Fig. 9 it is seen that the increase in $S_{\min}$ when $\lambda$ is less than 15 is rather small, and the destabilizing effect does not seem to be significant. However, if we look for the critical value of $\lambda$ corresponding to a given value of $S$ of the propellant, the stabilizing effect is considerable in reducing the maximum value of $\lambda$ compatible with unstable oscillations. In practical cases, the critical value of $\lambda$ is only reached near the final configuration of the tubular grain. The reduction of $\lambda$ by 1 or 2 can easily suppress the instability completely. The stabilizing effect of the insertion of a nonburning rod into a tubular grain has long been confirmed by experiments and experience.

Consider now, solid rockets using rod grain with exterior burning surface of radius $a$ which decreases continuously in the course of operation. The radius of the combustion chamber is taken as reference length so that $r_2 = 1$ and $r_1 = a$. $\lambda$ is constant throughout the operation and $\bar{v}_1$ is positive. Thus, one obtains from Equation [20]

$$\sigma = -\frac{a^2}{1 - a^2}\left\{\left(1 - \frac{\beta^2}{\eta_0^2 a^2}\right) - \left(1 - \frac{\beta^2}{\eta_0^2}\right)\left[\frac{Y_\beta'(\eta_0 a)}{Y_\beta'(\eta_0)}\right]^2\right\} \quad \ldots\ldots [38]$$

where $\eta_0$ is determined by $J_\beta'(\eta_0 a)/J_\beta'(\eta_0) = Y_\beta'(\eta_0 a)/Y_\beta'(\eta_0)$. The values of $\eta_0$ for fundamental spiral mode with $\beta = 1$ are given in Fig. 6. The values of $\sigma$ calculated from Equation [38], are plotted in Fig. 7. It is seen that $\sigma$ is always bigger than unity and increases monotonically without limit as $a$ approaches zero. During the period of operation of a rocket with rod grain, $\lambda$ is constant but $a$ decreases from the initial fractional value toward zero. The decrease of the

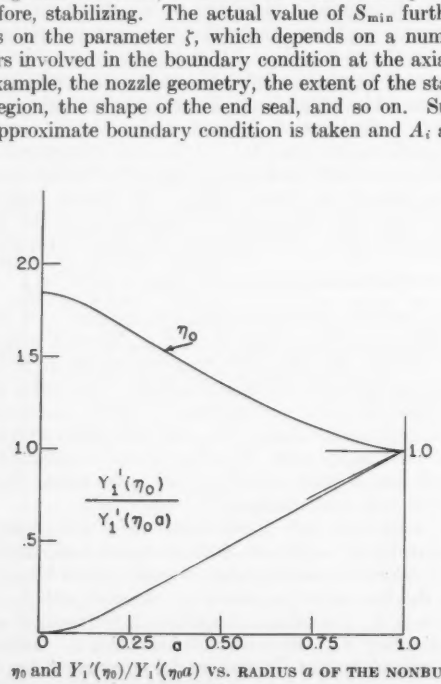


FIG. 6 $\eta_0$ and $Y_1'(\eta_0)/Y_1'(\eta_0 a)$ VS. RADIUS $a$ OF THE NONBURNING SURFACE

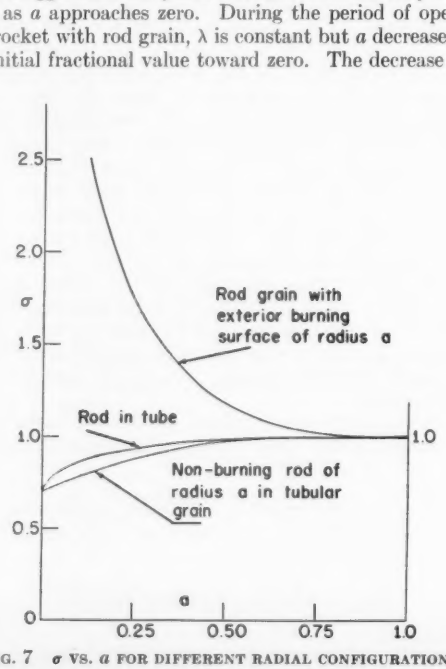


FIG. 7 $\sigma$ VS. $a$ FOR DIFFERENT RADIAL CONFIGURATIONS

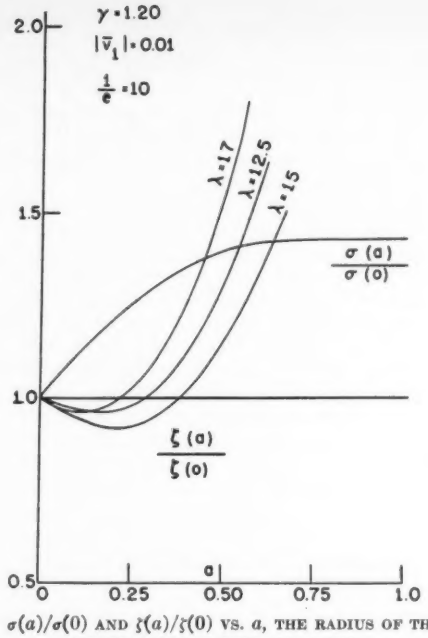


FIG. 8 $\sigma(a)/\sigma(0)$ AND $\zeta(a)/\zeta(0)$ VS. $a$, THE RADIUS OF THE NONBURNING ROD IN TUBULAR GRAIN

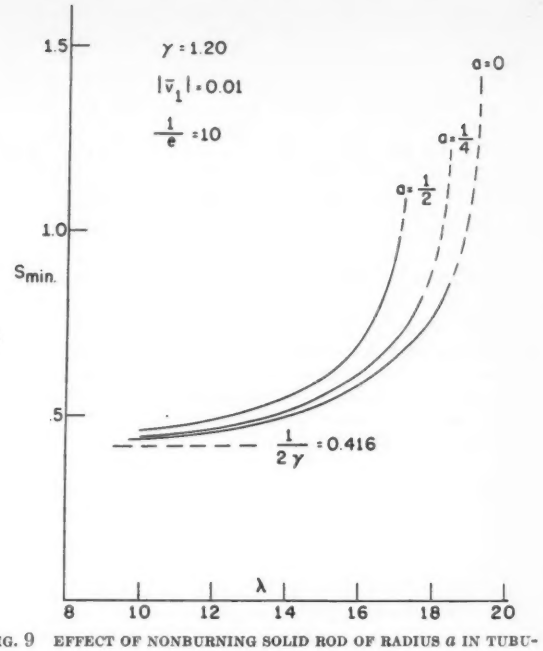


FIG. 9 EFFECT OF NONBURNING SOLID ROD OF RADIUS $a$ IN TUBULAR GRAIN

parameter $\zeta$ as given in Fig. 8 may decrease the value of $S_{min}$ when $a$ is reasonably large during the initial stage of operation, but is very soon overbalanced by the rapid increase of the parameter $\sigma$ toward the later stage of operation. Some calculated results are shown in Fig. 10 with $S_{min}$ plotted against $a$ for several values of $\lambda$. Rockets with rod grain will hence become much more stable toward the later stages of operation, and if a rocket with rod grain is stable during the initial and the early stage of operation, it will remain stable throughout the operation. In Fig. 10, it is seen that the value of $S_{min}$ during the early stage of operation, for the value of $\lambda$ as low as 12.5, remains bigger than unity, which is twice the value of $S_{min}$ for rockets with tubular grain of equal $\lambda$ and stabilized by nonburning axial rod. Therefore, it seems that a rocket with rod grain is unlikely, even if not impossible, to become unstable. So far as it is known, abnormal pressure peak has not been demonstrated in rockets with rod grain.

Now consider solid rockets using rod-in-tube grain with both exterior and interior burning surfaces at $r_1 = 1$ and $r_2 < 1$. The boundary condition given by Equation [14] is dropped and the boundary condition as given by Equation [15] is applied at both $r_1 = 1$ and $r_2 = a < 1$. Thus

$$\eta \frac{J_\beta'(\eta) + cY_\beta'(\eta)}{J_\beta(\eta) + cY_\beta(\eta)} = -\eta \frac{J_\beta'(\eta a) + cY_\beta'(\eta a)}{J_\beta(\eta a) + cY_\beta(\eta a)} = i\omega B\bar{v}_1 \ldots [39]$$

where $\bar{v}_1$ is the normal velocity of the burned gas on the interior burning surface $r_2 = 1$ and is, therefore, negative. Let $c_0 = J_\beta'(\eta_0)/Y_\beta'(\eta_0) = -J_\beta'(\eta_0 a)/Y_\beta'(\eta_0 a)$ and $c = c_0 + (dc/d\eta)_{\eta=\eta_0} d\eta$. Using the scheme of finding approximate solutions in previous sections, we can solve Equation [39] simultaneously with Equations [13] and [16]. The expression of $S_{min}$ is

$$S_{min} = \frac{1}{2\gamma} [1 + 4\lambda^2 |\bar{v}_1| \cdot \zeta \cdot \sigma]$$

where $\zeta = \eta_0 A_i A_r/(1 - a)$

$$\sigma = \frac{1}{1-a}\left\{\left(1 - \frac{\beta^2}{\eta_0^2}\right) \frac{aY_\beta'(\eta_0 a)^2}{Y_\beta'(\eta_0)^2 + aY_\beta'(\eta_0 a)^2} - a\left(1 - \frac{\beta^2}{\eta_0^2 a^2}\right) \frac{Y_\beta'(\eta_0)^2}{Y_\beta'(\eta_0)^2 + aY_\beta'(\eta_0 a)^2}\right. \ldots [40]$$

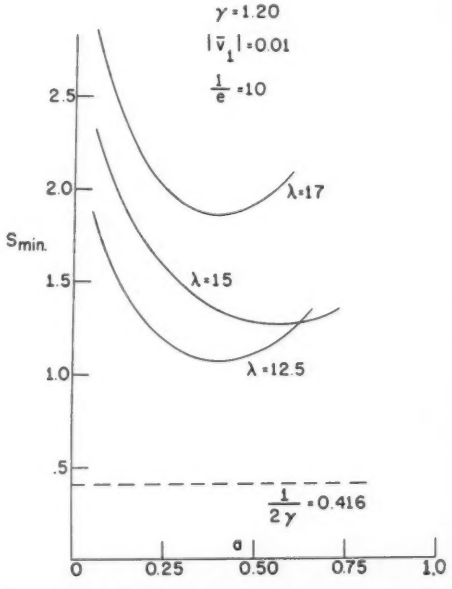


FIG. 10 MINIMUM PRESSURE INDEX OF INTERACTION $S_{min}$ FOR ROD GRAIN WITH DIFFERENT LENGTH TO RADIUS RATIO $\lambda$ OF THE NONBURNING SURFACE

Both $\lambda$ and $a$ decrease with time during the operating period of a given rocket with rod-in-tube grain. $\sigma$ is a function of $a$ only and is plotted in Fig. 7 when $\beta = 1$. We see that the value of $\sigma$ of solid rocket using rod-in-tube grain is in general slightly larger than the value of $\sigma$ of solid rocket using tubular grain with nonburning rod having the same value of $a$. This slight difference in $\sigma$ does not seem to justify a conclusion about the relative stability of rocket using rod-in-tube grain as compared to rocket using tubular grain with nonburning rod, because the variation of the parameter $\zeta$, being a function of the rather uncertain axial boundary condition at $x = \lambda$, may be a decisive factor in the comparison of these

two critical cases. But a rocket using rod-in-tube grain seems to be much more stable than the corresponding rocket using tubular grain having the same value of $\lambda$. Therefore, if the initial radius of the central rod is sufficiently larger than the thickness of the cylindrical shell, so that the shell will be burned out before the rod, the system is less likely to become unstable. On the other hand, if the radius of the central rod is smaller so that the rod is exhausted before the shell, the system will become unstable just as the corresponding rocket using tubular grain would near the end of operation.

### Rocket with Restricted End Burning Grain

It is also interesting to investigate the case of solid rockets with restricted end burning grain. This system looks very likely to be a one-dimensional system and can be analyzed by the method used in (4). We shall see whether the presence of the transversal components will be of importance in the stability analysis of such systems.

The acoustical solution satisfying the periodicity in the circumferential direction and the radial boundary conditions is given as

$$\delta^{(0)} = e^{-i\beta\theta} J_\beta(\eta_0 r)(e^{i\xi x} + ce^{-i\xi x}) \quad \ldots\ldots [41]$$

with $\alpha^2 = \xi^2 + \eta_0^2$, where $\xi$ and $\eta_0$ are the characteristic constants in $x$ and $r$ coordinates, respectively, $\beta$ = integral characteristic constant in $\theta$ direction, and $\eta_0$ = the lowest zero of $J_\beta'(\eta)$.

The boundary condition at axial exit $x = \lambda$ is

$$\left[i\alpha \frac{\mu^{(0)}}{\delta^{(0)}}\right]_{x=\lambda} = -\left(\frac{\delta_x{}^{(0)}}{\delta^{(0)}}\right)_{x=\lambda} = -i\xi \frac{e^{i\xi\lambda} - ce^{-i\xi\lambda}}{e^{i\xi\lambda} + ce^{-i\xi\lambda}} = i\alpha A \bar{u}_e \quad \ldots [42]$$

The boundary condition at burning surface $x = 0$ is

$$\left[i\alpha \frac{\mu^{(0)}}{\delta^{(0)}}\right]_{x=0} = -\left(\frac{\delta_x{}^{(0)}}{\delta^{(0)}}\right)_{x=0} = -i\xi \frac{1-c}{1+c} = -i\alpha B \bar{u}_e \quad \ldots [43]$$

Eliminating $c$ from Equations [42] and [43], one obtains

$$\frac{1 - \frac{\alpha}{\xi}\bar{u}_e B}{1 + \frac{\alpha}{\xi}\bar{u}_e B} = e^{2i\xi\lambda} \frac{1 + \frac{\alpha}{\xi}\bar{u}_e A}{1 - \frac{\alpha}{\xi}\bar{u}_e A} \quad \ldots\ldots [44]$$

By separating the real and the imaginary parts in Equation [44], one obtains for neutral oscillations

$$\begin{cases} \gamma(m-n)\sin\omega\bar{\tau} = -Y \\ \gamma(m-n)\cos\omega\bar{\tau} = \gamma m - (1-X) \end{cases} \quad \ldots\ldots [45]$$

where

$$X = -\frac{2A_r}{(1+\cos 2\lambda\xi) + (1-\cos 2\lambda\xi)\left(\frac{\omega\bar{u}_e}{\xi}\right)^2 (A_r{}^2 + A_i{}^2) - 2A_i \left(\frac{\omega\bar{u}_e}{\xi}\right)\sin 2\lambda\xi}$$

$$Y = -\frac{2A_i \cos 2\lambda\xi + \left[1 - \left(\frac{\omega\bar{u}_e}{\xi}\right)^2 (A_r{}^2 + A_i{}^2)\right]\frac{\xi}{\omega\bar{u}_e}\sin 2\lambda\xi}{(1+\cos 2\lambda\xi) + (1-\cos 2\lambda\xi)\left(\frac{\omega\bar{u}_e}{\xi}\right)^2 (A_r{}^2 + A_i{}^2) - 2A_i \left(\frac{\omega\bar{u}_e}{\xi}\right)\sin 2\lambda\xi}$$

The value of the average pressure index $S$ of interaction corresponding to neutral oscillation with axial component $\xi$ and radial component $\eta_0 = (\omega^2 - \xi^2)^{1/2}$ can be found from Equation [45] as

$$S = m - \frac{n}{2} = \frac{1}{2\gamma}\left[1 - X + \frac{Y^2}{1 - X - \gamma n}\right] \quad \ldots\ldots [46]$$

and the corresponding critical time lag $\bar{\tau}$ as

$$\bar{\tau} = \frac{1}{\omega}\sin^{-1}\frac{-Y}{\gamma\left(s - \frac{n}{2}\right)} \quad \ldots\ldots [47]$$

where the value of $\sin^{-1}$ is taken in the proper quadrant consistent with the sign of $\cos\omega\bar{\tau}$. Equations [44] to [47] are closely analogous to Equations [4.1.1] to [4.1.4] in (4) with necessary changes of notations.

If $\eta_0$ is taken to be zero, that is, if there is no radial component of oscillation,[7] one has $\alpha = \omega = \xi$ or $\alpha/\xi = 1$, and only longitudinal oscillations can exist. Equation [44] with $\alpha/\xi = 1$ can also be derived from one-dimensional consideration. Since $m - n = S(n/2)$ is of the order of unity or smaller, one sees from Equation [45], for this one-dimensional case, that $Y$ must be of the order of unity, and that $\sin\lambda\xi$ must be of the order of $\bar{u}_e$ ($\cos\lambda\xi$ must not be small because the denominator is of the order of $\cos^2\lambda\xi$). Hence, $\lambda\xi$ will be close to integral multiples of $\pi$ with a deviation of the order of $\bar{u}_e$. While $\lambda\xi$ varies in the neighborhood of $\pi$ or integral multiples of $\pi$, $S$ will have its minimum value, $S_{min}$, when $Y$ is approximately zero. Thus, $S_{min}$ is approximately given by

$$S_{min} = \frac{1}{2\gamma}(1 - X) \cong \frac{1}{2\gamma}(1 + A_r) \quad \ldots\ldots [48]$$

If the deLaval nozzle of the rocket is "very short," and the "short nozzle boundary condition" applies as explained in (4), then $A_r = (\gamma - 1)/2$ and

$$S_{min} = \frac{\gamma + 1}{4\gamma} \quad \ldots\ldots [49]$$

If the nozzle is not "very short," Equation [48] gives the value of $S_{min}$ for pure axial neutral oscillation of frequency $\lambda\xi$ with $A_r$ determined from Fig. 2. Since $A_r$ increases with $\lambda\xi$, we see that $S_{min}$ for higher axial modes are larger, that is, the higher axial modes are more stable than the lower modes. Qualitative stability behavior of pure axial mode in rockets with end burning grain is, therefore, closely analogous to that in liquid rocket of similar geometry with concentrated combustion at the injection end. However, there are two fundamental differences between the present results and those in (4). Since the length of the combustion chamber of solid rocket increases with time during operation, the effective length of the nozzle $e$ is decreasing. Therefore, the values of $A_r$ and $S_{min}$ for a given axial mode, decreases during operation. In other words, a solid rocket with end burning grain destabilizes itself. The unstable ranges of the time lag for given value of $S$ of the propellant also varies, due to the change of $\omega = \xi$ as can be seen from Equation [47]. Therefore, if the value of $S_{min}$ of the rocket with end burning grain becomes smaller than the value of $S$ of the propellant, the axial mode will very likely become unstable. Another fundamental difference is that the analysis in (4) deals with intrinsic instability only where the rate of supply of the combustible mixtures is constant, while the present analysis deals

[7] It can be shown from the solution of the wave equation, that when $\eta = 0$, $\beta$ must be zero in order that both of the two radial boundary conditions at $r = 1$ and $r = 0$ may be satisfied. Physically, this means the absence of any transversal components of oscillation or the flow is strictly one-dimensional.

with systems with varying rates of supply of the combustible gases.

Suppose now a radial mode $\eta_0$ associated with circumferential mode of order $\beta = 0, 1, 2$, etc., is superposed on the axial mode of frequency $\lambda\xi$, then $\omega/\xi = \left[1 + \left(\frac{\eta_0}{\xi}\right)^2\right]^{1/2}$ is bigger than unity. If $\eta_0/\xi$ is of the order of unity, for example, in the case of fundamental spiral mode with $\beta = 1$, $\eta_0 = 1.84$, $\lambda\xi < \pi$, and $\lambda = 0(1)$, then $\omega/\xi$ is still of the order of unity. Following the reasoning for the case of pure axial mode, one sees that $\lambda\xi$ is still close to integral multiples of $\pi$ with deviation of the order of $\bar{u}_e$. The value of $S_{min}$ for the neutral spiral mode as specified is still given by Equation [48]. However, $A_r$ is not known even approximately. Because when $\eta_0/\xi$ is of the order of unity, the time-wise variations of the flow properties due to the transversal and the longitudinal components of oscillations are also comparable. Thus, the approximation of taking over the one-dimensional results in (5) is invalid. Until an analysis of nozzle flow with transversal oscillations is made, very little can be said about $A_r$ as a function of $\lambda\xi$, $\eta$, and probably $\beta$ as well. The investigation of the qualitative stability behavior of this type of oscillation should, therefore, be studied more carefully. If, on the other hand, $\eta_0/\xi$ is large, either in the case of fundamental spiral mode with large $\lambda$ or in the case of higher members of the radial modes superposed on fundamental axial mode, then $\omega/\xi$ is much larger than unity of the order of $1/\bar{u}_e$. With $m - n$ of the order of unity, it is no longer necessary that $\lambda\xi$ is in the neighborhood of some integral multiple of $\pi$. The frequency of the axial component of the neutral oscillations and, therefore, of the unstable oscillation may be quite different from and cannot possibly be identified with any of the natural organ-pipe frequencies of the combustion system.

The simplifying scheme of calculating $S_{min}$ by Equation [48] as $1/2\gamma(1 - X)$ is no longer valid. Numerical determination of $s$ and $\bar{\tau}$ for different values of $\eta_0$, $\xi$, $\bar{u}_e$, and $n$ can however, be carried out with Equations [46] and [47] in a manner analogous to that in (4). Fig. 2 can still be used in determining $A_r$ and $A_i$ as a rough approximation. The qualitative behavior of the variation of $S_{min}$ will be expected to be not much different from that of pure axial oscillation in solid rocket with restricted end burning grain.

## Summary of Conclusions

1 High-frequency unstable oscillations in solid propellant rockets are excited by the sensitivity of the rates of the combustion processes to oscillations of the burned gas in the combustion chamber. The following simplified model is assumed. The solid propellant first decomposes into intermediate gaseous products without appreciable energy release. These intermediate gaseous products are then activated during a time lag $\tau$, near the end of which these intermediate gases undergo a series of combustion reactions at a very large rate which releases practically all the chemical energy made available through combustion. The interaction between the rates of the combustion reactions and the gas oscillations is expressed in terms of the pressure dependence of time lag $\tau$ through the following integral relation

$$\int_{t-\tau}^{t} p^m(t')dt' = \text{const}$$

where $m$ represents the average extent of interaction including temperature effects. The rate of primary decomposition of the solid propellant on the burning surface is assumed to be proportional to the $n$th power of the instantaneous gas pressure exerted on the solid surface. Both of the two constants $m$ and $n$ can only be determined by experiments at the present time. The effective over-all interaction parameter $S$ is found to be the difference between the two indices $S = m - (n/2)$. Small high-frequency oscillations of a given mode of either spiral or nonspiral type can become unstable when both the value of $S$ of the propellant is larger than a certain minimum value, and the value of $\bar{\tau}$ lies in one of the unstable ranges of $\bar{\tau}$ for that mode. The minimum value of $s$ of a given mode is in general of the order of or smaller than unity, and depends on the rocket geometry and the burning rate of the propellant. The unstable ranges of $\bar{\tau}$ of a given mode depend on the rocket geometry and the value of $S$ of the propellant.

2 For solid rockets with cylindrical burning surface or surfaces, the frequency $\beta$ of the circumferential component of the unstable oscillations of the spiral mode is always equal to the frequency of the acoustical circumferential mode of the combustion system, i.e., $\beta$ = integral values. The frequency $\eta$ of the radial component is close to the frequency $\eta_0$ of the acoustical radial mode with a fractional deviation of the order of $|\bar{v}_1|$, the dimensionless normal velocity component of the burned gas on the burning surface. The frequency $\xi$ of the axial component is, however, significantly different from the natural organ-pipe frequency $k\pi/\lambda$. The frequency $\alpha$ of the variation of flow properties at a given point is close to the frequency $\eta_0$ of the acoustical radial mode. When the unstable spiral mode of oscillation amplifies, the circumferential component amplifies at a much faster rate, and measurement of the unstable oscillations at finite magnitude may not be able to reveal the associated radial and axial components of oscillation.

3 Despite the fact that the burning surface is in the radial direction in solid rockets with cylindrical burning surface, which seems to be most susceptible to the oscillations in the radial direction, the nonspiral oscillation with predominating radial component but no circumferential component is more stable than the fundamental spiral node. Among all the possible unstable high-frequency oscillations either of the spiral or of the nonspiral mode, the fundamental spiral mode is the most unstable mode.

4 Solid rockets using tubular grain or perforated propellant grain with interior burning surface are found to be the most unstable grain shape as compared to other shapes studied in the present paper. It is shown that: (i) A solid rocket using tubular grain become more unstable, that is, it destabilized when the ratio $\lambda$ decreases with time of operation. The minimum value of $S$ of such systems decreases very rapidly when $\lambda$ decreases until certain critical range of $\lambda$ is reached, after which $S_{min}$ decreases at a much slower rate. The rocket that is stable for most part of its operation will suddenly become unstable when the value of $S_{min}$ of the system becomes sufficiently below the value of $S$ of the propellant. (ii) The rocket with tubular grain is stabilized by introducing a nonburning rod into the axial cavity. Both the value of $S_{min}$ is increased, and the critical range of $\lambda$ is reduced. If the value of $\lambda$ of the tubular grain near the end of its operation is close to the critical value of $\lambda$ of the rocket system, the introduction of a nonburning rod can suppress completely any instability. The stabilizing effect increases when the radius of the rod increases. (iii) Rockets with nonerosible end seal are likely to be more stable than those with erosible end seal of the same initial inside diameter. The effect of increasing the inside diameter of the end seal is destabilizing.

5 Rockets using rod grain with exterior burning surface is the most stable configuration among those studied here. This system becomes more stable when the radius of the burning rod decreases in the course of its operation, especially near the end of the operation.

6 Rockets using rod-in-tube grain with both interior and exterior burning surfaces are more stable than the corresponding rockets with tubular grain. If the initial radius of the central rod is sufficiently larger than the thickness of the shell, this system will remain more stable than those with tubular grain.

7 By decreasing the parameter $e$ which represents the effective length of the nozzle, the rocket system is destabilized.

8 The stability behavior of high-frequency small disturbances in restricted end burning solid rocket can be analyzed strictly by one-dimensional model only when there is no transversal component of oscillation present. The restricted end burning rocket destabilizes itself toward the pure longitudinal oscillation during the course of its operation. If the ratio of the length of the combustion chamber space to its radius is large, the frequency of the axial component of the unstable fundamental spiral mode will not necessarily be close to the fundamental natural organ-pipe frequency of the combustion system.

## APPENDIX 1

Postulate series solutions in terms of the mean exit velocity $\bar{u}_e$ as follows

$$\frac{\varphi}{\gamma} = \delta = \delta^{(0)} + \bar{u}_e\delta^{(1)} + \bar{u}_e{}^2\delta^{(2)} + \dots$$

$$\mu = \mu^{(0)} + \bar{u}_e\mu^{(1)} + \bar{u}_e{}^2\mu^{(2)} + \dots \quad \dots\dots [A1]$$

Substitute these into Equations [7] and equate terms of the same power of $\bar{u}_e$. The ratios of the steady-state velocity components to $\bar{u}_e$ are less than unity and are considered as terms of the order of unity or smaller. The equation for the 0th order solutions are

$$i\alpha\delta^{(0)} + \mu_x{}^{(0)} + \frac{1}{r}\frac{\partial}{\partial r}(r\nu^{(0)}) + \frac{1}{r}\chi\theta^{(0)} = 0$$

$$i\alpha\mu^{(0)} = -\delta_x{}^{(0)}$$
$$i\alpha\nu^{(0)} = -\delta_r{}^{(0)}$$
$$i\alpha\chi^{(0)} = -\frac{1}{r}\delta_\theta{}^{(0)} \quad \dots\dots [A2]$$

Equation [A2] can be reduced to the single partial-differential equation

$$(\alpha^2 + \nabla^2)\delta^{(0)} = \alpha^2\delta^{(0)} + \delta_{xx}{}^{(0)} + \frac{1}{r}\frac{\partial}{\partial r}(r\delta_r{}^{(0)}) + \frac{1}{r^2}\delta_{\theta\theta}^{(0)} = 0 \quad \dots [A3]$$

where $\nabla^2$ is the Laplacian operator in cylindrical coordinates. The solution of Equation [A3] is easily obtained by the method of separation of variables and is well known as the cylindrical acoustical wave solution. This solution satisfying particular sets of boundary conditions are given as Equation [8] and Equation [41], respectively.

The differential equation for the first correction $\delta^{(1)}$ is obtained as

$$(\alpha^2 + \nabla^2)\delta^{(1)} = i\alpha\left\{\left(\frac{\bar{u}}{\bar{u}_e}\right)_x + \frac{1}{r}\frac{\partial}{\partial r}\left[r\frac{\bar{v}}{\bar{u}_e}\right] + \frac{\bar{u}}{\bar{u}_e}\frac{\partial}{\partial x} + \frac{\bar{v}}{\bar{u}_e}\frac{\partial}{\partial r}\right\}\delta^{(0)} - \frac{\partial}{\partial x}\left\{\left[\left(\frac{\bar{u}}{\bar{u}_e}\right)_x + \frac{\bar{u}}{\bar{u}_e}\frac{\partial}{\partial x} + \frac{\bar{v}}{\bar{u}_e}\frac{\partial}{\partial r}\right]\mu^{(0)}\right\} - \frac{1}{r}\frac{\partial}{\partial r}\left[r\left(\frac{\bar{v}}{\bar{u}_e}\right)_x\mu^{(0)}\right] -$$
$$\frac{1}{r}\frac{\partial}{\partial r}\left\{r\left[\left(\frac{\bar{v}}{\bar{u}_e}\right)_r + \frac{\bar{u}}{\bar{u}_e}\frac{\partial}{\partial x} + \frac{\bar{v}}{\bar{u}_e}\frac{\partial}{\partial r}\right]\nu^{(0)}\right\} - \frac{\partial}{\partial x}[\bar{u}_r\nu^{(0)}] - \frac{1}{r}\frac{\partial}{\partial\theta}\left\{\left[\frac{1}{r}\left(\frac{\bar{v}}{\bar{u}_e}\right) + \frac{\bar{u}}{\bar{u}_e}\frac{\partial}{\partial x} + \frac{\bar{v}}{\bar{u}_e}\frac{\partial}{\partial r}\right]\chi^{(0)}\right\} \dots [A4]$$

The inhomogeneous part of Equation [A4] is a known function of $x$, $r$, and $\theta$ with a magnitude of the order of $|\xi|$ or $\left|\frac{\bar{v}_1}{\bar{u}_e}\right|$ which is considered as small compared to unity. Call this known function $F(x, r)e^{i\beta\theta}$ and expand it into Fourier series whose $j$th term is $e^{i\beta\theta}\,F_j(r)\exp\left[i\frac{j\pi x}{\lambda}\right]$. The solution $\delta^{(1)}$ can be obtained from Equation [A4] in the form of infinite series

$$\delta^{(1)} = e^{i\beta\theta}\sum_{j=1}^{\infty} K_j(r)\exp\left(i\frac{j\pi x}{\lambda}\right) \quad \dots\dots [A5]$$

where

$$K_j(r) = \frac{r}{2}\left[Y_\beta(r\eta')\int J_\beta(r\eta')F_j(r)\,dr - J_\beta(r\eta')\int Y_\beta(r\eta')F_j(r)\,dr\right]$$

with

$$\eta' = \left[\alpha^2 - \left(\frac{j\pi}{\lambda}\right)^2\right]^{1/2}$$

$J_\beta$ and $Y_\beta$ are $\beta$th-order Bessel functions of the first and the second kind, respectively.

Consequently, the first-order corrections $\bar{u}_e\delta^{(1)}$ can be found at least numerically after the determination of the steady-state solution and the acoustical solution of the particular system.

## APPENDIX 2

It is experimentally found that the rate of regression of the solid propellant surface during the rough combustion period is abnormally high even if the increase of burning rate due to the increase of mean chamber pressure is taken into account. This phenomenon is hardly compatible with any linearized small perturbation theory. For example, if the burning rate is sensitive to the pressure variation, then a small sinusoidal pressure disturbance will decrease the burning rate during pressure defect period to such an extent as will cancel to a large part the increase of the burning rate during pressure excess period. The mean burning rate and the mean combustion chamber pressure should not increase. If the oscillation is of sufficiently large amplitude, the nonlinear effect may produce significantly larger increase of burning rate in pressure excess period than the decrease in pressure defect period, and result in an increase in mean burning rate and mean chamber pressure. An alternative explanation of the increase of mean burning rate is the dependence of the burning rate on drifting velocity along the burning surface. Under the same pressure, the burning rate is smallest when there is no drifting velocity along the surface. If an oscillation of the drifting velocity is introduced into the gas system, the burning rate will be increased both in the velocity excess and in the velocity defect period. It seems, therefore, that a small perturbation analysis based upon this velocity mechanism can result in increasing mean burning rate and mean chamber pressure. However, the drifting velocity in the axial direction along the burning surface is not zero in steady-state operation. It is only the circumferential velocity component that vanishes in steady state and only a small velocity oscillation in circumferential direction that can possibly increase the mean burning rate. Since the burning rate depends on the magnitude of the drifting velocity, i.e., $(u^2 + w^2)^{1/2}$, and since $\bar{u}$ is not zero while $\bar{v} = 0$, the instantaneous drifting velocity is $[\bar{u}^2 + 2\bar{u}u' + u'^2 + w'^2]^{1/2}$ where prime indicates small perturbations. Both of the two nonlinear terms $u'^2$ and $w'^2$, which are independent of the sign of the perturbations, contribute to the increase of the mean burning rate and, consequently, the mean chamber pressure, just like the nonlinear terms of the pressure perturbation do. These terms of nonlinear character should not be considered in a linearized stability analysis of small disturbances because they are small quantities of higher order.

It is, therefore, inferred that the increase of the mean burning rate and the mean chamber pressure is a "nonlinear" property and should not be considered in the linearized analysis for the stability of small perturbations superposed on the steady flow.

A stability analysis based on the exciting mechanism as represented by Equation [4] can, of course, be made without much complication in analytical procedure. But due to the introduction of a second empirical interaction parameter $b$, the ultimate stability limit would involve two parameters, $S$ and $b$, which have to be presented in a plane, and the determination of such stability limit would involve much more numerical work than is intended in the present analysis. The following analysis indicates that the velocity mechanism alone is not very likely to induce instability and, therefore, the stability analysis is made on the pressure mechanism only as given in Equation [5].

When the velocity mechanism only is considered, the instantaneous burning rate $\dot{m}_b(t)$ is

$$\dot{m}_b(t) = \dot{m}_{b0}(1 + b\bar{V}) = \bar{\rho}\bar{v}_0(1 + b\bar{V}) \quad \text{[A6]}$$

where $\dot{m}_{b0} = \bar{\rho}\bar{v}_0$ is the burning rate at zero drifting velocity, and $\bar{v}_0 = |\bar{v}_1|/(1 + b\bar{V})$ under the approximation $\bar{u}^2 \ll 1$. The boundary condition at the burning surface $r_2 = 1$ in the case of a rocket with tubular grain is

$$\frac{\nu}{\delta} = \bar{v}_0\left[1 + b\bar{u} - b\frac{\mu}{\delta}e^{-i\alpha\bar{\tau}}\right] \quad \text{[A7]}$$

Equation [14] is replaced by $c = 0$, and Equation [15] by

$$\eta\frac{J_\beta'(\eta)}{J_\beta(\eta)} = -i\alpha\bar{v}_0\left[1 + b\bar{u}(x) - b\bar{u}(x)\cdot\frac{\bar{u}_e\tan\xi x}{\bar{u}\tan\xi\lambda}\cdot A\cdot e^{-i\alpha\bar{\tau}}\right]$$

It is interesting to note that $\eta$ is now a function of $x$. This indicates that the method of separation of variables is not applicable to the solution of the problem. To avoid the mathematical complications arising from this situation, we shall assume that so far as the over-all effect is concerned, the propellant elements distributed over the entire burning surface respond to the same axial velocity variation at the mean station $\bar{x}$. In actual situation each propellant element responds to the local velocity variation. These local velocity variations are of different amplitudes and are in general out of phase. Therefore certain cancellations of the exciting contributions of different propellant elements exist. The total amount of excitation in the actual system will be less than that in the assumed system if $\bar{x}$ is selected as the position where the amplitude of the axial velocity variation is the largest. In other words, the actual system will always be more stable than the most unstable one of the idealized systems with arbitrary $\bar{x}$ from 0 to $\lambda$. Thus we write

$$\eta\frac{J'_\beta(\eta)}{J_\beta(\eta)} = -i\alpha\bar{v}_0\left[1 + b\bar{u}_e\left(1 - \frac{\tan\xi\bar{x}}{\tan\xi\lambda}\cdot A\cdot e^{-i\alpha\bar{\tau}}\right)\right] \quad \text{[A8]}$$

Equation [A8] is solved simultaneously with Equations [13] and [16], with the approximate procedure as explained previously. The critical values of $b\bar{u}_e$ corresponding to neutral oscillations of frequency $\omega$ is given as

$$b\bar{u}_e = \frac{G \pm [G^2 + (|AH|^2 - 1)(G^2 + F^2)]^{1/2}}{|AH|^2 - 1} \quad \text{[A9]}$$

where

$$G = 1 + \frac{2\omega - \eta_0}{\omega}\cdot\frac{\vartheta(\xi^2)}{2\omega\bar{v}_0}\left(1 - \frac{\beta^2}{\eta_0^2}\right)$$

$$F = \left[\frac{\omega - \eta_0}{\omega} - \frac{2\omega - \eta_0}{\omega}\cdot\frac{\Re(\xi^2)}{2\omega\bar{v}_0}\right]\left(1 - \frac{\beta^2}{\eta_0^2}\right)$$

$$A = A_r + iA_i$$

$$H = \tan\xi\bar{x}/\tan\xi\lambda$$

The complex quantity $\xi = \xi_r + i\xi_i$ is still determined by the axial boundary condition, Equations [29] and [30]; and the magnitude of $A$ for the fundamental spiral mode of oscillation is considerably less than unity.

The magnitude of $H$ depends on the position $\bar{x}$ where the generation of the burned gas is assumed to be concentrated in the evaluation of the variation of the rate of burned gas generation. If $\bar{x} = \lambda$ we have $H = 1$, and if $\bar{x} = 0$ we have $H = 0$. For arbitrary values of $\bar{x}$

$$|H| = \frac{\sin^2\xi_r\bar{x} + \sinh^2\xi_r\bar{x}}{\cos^2\xi_r\bar{x} + \sinh^2\xi_r\bar{x}}\Big/\frac{\sin^2\xi_r\lambda + \sinh^2\xi_i\lambda}{\cos^2\xi_r\lambda + \sinh^2\xi_i\lambda}$$

Since $\xi_i/\xi_r$ is of the order of 2 or 3 or even larger, $|H|$ will remain very close to unity and become very small when $\bar{x}$ approaches zero. The magnitude of $AH$ is thus given by $|A|$ which is considerably less than unity.

Now Equation [A9] shows that if $|AH| < 1$ the right-hand side is negative no matter whether the upper or the lower sign before the bracket is taken. Since $b\bar{u}_e$ of the solid propellants are positive, we conclude that the fundamental spiral mode would be always stable if the velocity mechanism were the only exciting agent. Physically this means that the velocity mechanism is not able to supply sufficient amount of energy to the disturbance to compensate the energy dissipation due to the outflow through the nozzle associated with the velocity oscillation. The disturbance will lose its energy and die out eventually.

Even if we consider the extreme case where $|AH| > 1$, the minimum value of $b\bar{u}_e$ compatible with any unstable oscillations is given by

$$(b\bar{u}_e)_{\min} = \frac{G}{|AH| - 1} = \frac{1 + \eta_0 A_i A_r\dfrac{\bar{u}_e^2}{|r_1|}\left(1 - \dfrac{\beta^2}{\eta_0^2}\right)}{|AH| - 1} \quad \text{[A-10]}$$

Sample calculations show that $(b\bar{u}_e)_{\min}$ remains considerably bigger than unity while the magnitude of $b\bar{u}_e$ for solid propellants is in general considerably less than unity, even for those propellants that exhibit instability in tubular grain. It is therefore inferred that the velocity mechanism is not the essential mechanism in exciting instability, at least for the cases that are considered in the present investigation.

Finally it should be emphasized that this velocity mechanism can be neglected without seriously affecting the qualitative results only in the analysis of the stability of small disturbances, that is, the analysis of the behavior of the initial phase of the development of the large oscillations in solid rockets. Once the unstable small disturbances have grown up to considerable magnitudes, the velocity mechanism will become important and even may be the predominating mechanism, as is in the case of unstable spiral modes at large amplitudes.

# Technical Notes

## Excitation of Oscillations by Chemical Reaction[1]

JACK LORELL[2] and HENRY WISE[3]

Jet Propulsion Laboratory, California Institute of Technology, Pasadena, Calif.

SEVERAL theoretical treatments (1–5)[4] have recently dealt with the problem of combustion instability in the rocket motor. These analyses have shown that inherently unstable (oscillatory) systems may result from the interaction of the hydraulic, mechanical, and hydrodynamic components of the rocket motor. The purpose of this paper is to suggest that, in addition to the factors named, the chemical kinetics of the combustion process may also be a source of excitation for pressure oscillations.

In an open reaction system, such as a rocket motor, in which there exist a continuous supply and removal of reactants, the concentration changes which occur are governed by the rate processes of mixing, phase change, and chemical reaction. For the present discussion, the system oscillations caused by variations in physical parameters are separated from the fluctuations which may originate within the chemical system as a result of the interplay of the reaction kinetics. Such time-dependent kinetic variations in the concentration of a particular molecular or atomic species can couple with the hydrodynamics of a system such as a rocket motor. In general, chemical systems do not fluctuate about their equilibrium because chemical energy is normally transformed irreversibly into heat, not into some form of potential energy as experienced in a mechanical vibration.

In considering only the chemical kinetics of a system made up of a series of consecutive first-order reactions, the possibility of true time-dependent oscillations in the concentration of a given reactant is ruled out (6). However, it has been shown that the differential rate equations applicable to an idealized open reaction system of two autocatalytic reactions can give rise to undamped oscillations in the concentration of intermediate species (7). Such a system of equations has been employed by Walsh (8) and Frank-Kamenetsky (9) in the treatment of the periodicity of cool flames operative in the mechanism of two-stage ignition of hydrocarbons (10). Other periodic chemical reactions have recently been reviewed (11). The analysis has been extended to a chain of autocatalytic reactions in which the precursor is introduced by a first-order process and the other substances are removed by first-order processes (12). Such a system exhibits almost undamped oscillations under certain conditions.

Since the study of the transient behavior of nonlinear systems (such as are encountered in many chemical reactions) involves a complex mathematical treatment, the analysis suggested herein deals with isothermal, closed (with respect to the concentration of reactants) systems involving kinetics of first and second order. It is obvious that, in a reaction proceeding along the sequence, reactants → intermediates → products, the rate of this over-all reaction is governed by the slowest step in the mechanism. In such a system characterized by the absence of a feedback loop, the concentration of each species does not display oscillations but rises or falls monotonically to the equilibrium value. On the other hand, in the presence of a chain or an autocatalytic mechanism as exhibited by some chemical reactions of interest in combustion (13), periodic variations in the concentration of some of the species cannot be ruled out.

The oscillatory behavior of such a system may be analyzed by linearizing the reaction-rate equations about the equilibrium point, resulting in a system of linear differential equations with constant coefficients. If, for such a system of linear differential equations in the displacements from equilibrium of the various chemical species, the characteristic complex frequencies are all real and negative, the system is nonoscillatory. However, a resulting complex frequency with nonzero imaginary part indicates oscillatory behavior. An oscillating system is of particular interest since it contains a natural frequency which, upon excitation by an external disturbance, may result in an observable resonance.

As an example of an oscillation induced by the kinetics of a reacting system, a reaction involving two consecutive autocatalytic reactions may be considered. Such a system is of particular interest since it has been applied in the analysis of ignition of hydrocarbons (10). This system in which the formation of the intermediates $A$ and $B$ (whose respective concentrations are given by $r_1$ and $r_2$) exhibits autocatalysis may be represented by the rate equations

$$-\dot{r}_1 = -k_1 r_1 + k_2 r_1 r_2 \quad [1]$$

$$-\dot{r}_2 = -k_2 r_1 r_2 + k_3 r_2 \quad [2]$$

These equations lead to a periodic time dependence of $r_1$ and $r_2$ about their equilibrium values

$$\bar{r}_1 = k_3/k_2$$
$$\bar{r}_2 = k_1/k_2$$

For small displacements $x_1$ and $x_2$ from their equilibrium values, one obtains from Equations [1] and [2]

$$-\dot{x}_1 = k_3 x_2 \quad [3]$$

$$-\dot{x}_2 = -k_1 x_1 \quad [4]$$

where

$$x_1 = r_1 - (k_3/k_2) \text{ and } x_2 = r_2 - (k_1/k_2)$$

This set of simultaneous, first-order, differential equations may be solved directly, resulting in an expression for $x_1$ and $x_2$ which has the characteristics of a harmonic oscillator. The nature of the oscillation is also apparent from an examination of the characteristic equation of the differential expressions [3] and [4]

$$\phi(\lambda) = \begin{vmatrix} \lambda & k_3 \\ -k_1 & \lambda \end{vmatrix} = 0 \quad [5]$$

which is a quadratic equation having for its discriminant

$$\Delta = -4k_1k_3 \quad [6]$$

Received February 1, 1954.

[1] This paper presents the results of one phase of research carried out at the Jet Propulsion Laboratory, California Institute of Technology, under Contract No. DA-04-495-Ord 18, sponsored by the Department of the Army, Ordnance Corps.

[2] Senior Research Engineer, Research Analysis Section. Mem. ARS.

[3] Senior Research Engineer, Chemistry Section.

[4] Numbers in parentheses refer to References at end of paper.

EDITOR'S NOTE: This section of JET PROPULSION is open to short manuscripts describing new developments or offering comments on papers previously published. Such manuscripts are published without editorial review, usually within two months of the date of receipt. Requirements as to style are the same as for regular contributions (see first page of this issue).

Since the discriminant is negative, the solution of Equation [5] contains purely imaginary roots. Consequently this system exhibits undamped oscillations with a frequency $\nu$ equal to

$$\nu = (k_1 k_2)^{1/2}/2\pi \quad [7]$$

Further analysis shows that $x_1$ and $x_2$ are out of phase by 90 deg. It should also be noted that the rate constants are exponential functions of temperature. Therefore the frequency of the oscillation rises exponentially with temperature, according to Equation [7]. The order of magnitude of this frequency at 1000 K is from 10 to $10^3$ $sec^{-1}$ for a reaction with an activation energy of 50 to 60 kcal and a pre-exponential factor of $10^{13}$.

### References


1 "Self-Excited Oscillations in Dynamical Systems Possessing Retarded Actions," by N. Minorsky, *Journal of Applied Mechanics*, vol. 9, 1942, pp. 65–71.

2 "Stability of Flow in a Rocket Motor," by D. F. Gunder and D. R. Friant, *Journal of Applied Mechanics*, vol. 17, 1950, pp. 327–333.

3 "A Theory of Unstable Combustion in Liquid Propellant Rocket Systems," by Martin Summerfield, JOURNAL OF THE AMERICAN ROCKET SOCIETY, vol. 21, 1951, pp. 108–114.

4 "Aspects of Combustion Stability in Liquid Propellant Rocket Motors. Part I. Fundamentals. Low Frequency Instability with Monopropellants," by L. Crocco, JOURNAL OF THE AMERICAN ROCKET SOCIETY, vol. 21, 1951, pp. 163–178.

5 "Aspects of Combustion Stability in Liquid Propellant Rocket Motors. Part II. Low Frequency Instability with Bipropellants. High Frequency Instability," by L. Crocco, JOURNAL OF THE AMERICAN ROCKET SOCIETY, vol. 22, 1952, pp. 7–16.

6 "Kinetics of Open Reaction Systems," by K. G. Denbigh, Margaret Hicks, and F. F. M. Page, *Transactions of the Faraday Society*, vol. 44, 1948, pp. 479–494.

7 "Undamped Oscillations Derived from the Law of Mass Action," by Alfred J. Lotka, *Journal of the American Chemical Society*, vol. 42, 1920, pp. 1595–1599.

8 "Processes in the Oxidation of Hydrocarbon Fuels," by A. D. Walsh, *Transactions of the Faraday Society*, vol. 43, 1947, pp. 305–313.

9 A. A. Frank-Kamenetsky, *Journal of Physical Chemistry (USSR)*, vol. 14, 1940, p. 30.

10 "Combustion, Flames, and Explosion of Gases," by B. Lewis and G. von Elbe, Academic Press, 1951.

11 "A Periodic Chemical Reaction. The Reaction Between Hydrogen Oxide and Iodic Acid," by M. G. Peard and C. F. Cullis, *Transactions of the Faraday Society*, vol. 47, 1951, pp. 616–630.

12 "Kinetics of Open Reaction Systems. Chains of Simple Autocatalytic Reactions," by Margaret J. Moore, *Transactions of the Faraday Society*, vol. 45 (No. 324), 1949, pp. 1098–1109.

13 "Chemical Kinetics and Chain Reactions," by N. Semenoff, Clarendon Press (Oxford, England), 1935.


## Production of Chemicals by Gas-Dynamical Methods[1]


GORDON J. MacLEOD[2]

**Daniel and Florence Guggenheim Jet Propulsion Center**
**California Institute of Technology**
**Pasadena, Calif.**


SEVERAL proposals for the production of chemicals by the use of gas-dynamical methods have been advanced in recent years. Briefly, these methods involve (a) the utilization of the possibility of "freezing" equilibrium gas compositions by very rapid chilling (as by expansion through a de Laval nozzle), or (b) the production of chemicals under nonequilibrium conditions, for example, by rapid heating and cooling through proper exposure to compression and rarefaction shocks.

It is the purpose of this letter to call attention to a study entitled "Some Considerations in the Application of a Gas Turbine Cycle to the Manufacture of Nitric Oxide," which was carried out by the author in 1951 and 1952 at the California Institute of Technology, in partial fulfillment of requirements for the degree of mechanical engineer. The abstract of the thesis (146 pages) is given below in order to indicate the scope of the work:

"Problems associated with the application of a gas turbine cycle to the manufacture of nitric oxide have been investigated. The feasibility of quenching the nitric oxide decomposition reaction with a de Laval nozzle is demonstrated. Thermochemical studies show that yields of nitric oxide approaching one per cent are attainable in a gas turbine cycle. It may be possible to overcome the serious problem of blade cooling by using either transpiration cooling or film cooling. Transpiration cooling appears to be the more promising method. The coolant requirements amount to approximately one per cent of the main stream mass flow per cooled turbine-blade row. The effect of transpiration and film cooling upon cycle performance is negligible. Although all of the problems associated with the application of a gas turbine cycle to the manufacture of nitric oxide appear to be surmountable, it has not been demonstrated conclusively that the turbine cycle will be competitive with conventional methods for nitrogen fixation."


Received January 4, 1954.

[1] The study of the production of chemicals by gas-dynamical methods was initiated by Professor H. S. Tsien. The author is indebted to both Drs. H. S. Tsien and S. S. Penner for helpful suggestions.


[2] Formerly graduate student in Jet Propulsion at the California Institute of Technology. Present address: Propulsion Research Corporation, Santa Monica, Calif.

## Ethylene Oxide as a Monopropellant[1]


WILLIAM CLAY ROBISON[2]

**Daniel and Florence Guggenheim Jet Propulsion Center**
**California Institute of Technology**
**Pasadena, Calif.**


THERMODYNAMIC calculations to determine the theoretical performance of ethylene oxide as a monopropellant have been carried out for various possible decomposition reactions. The performance calculations were carried out, by using standard evaluation procedures,[3] for two possible exothermic decomposition reactions, one of which leads to the formation of CO and $CH_4$, whereas the other leads to the production of CO, C, and $H_2$. For the process leading to carbon formation, two limiting cases were considered: (a) no slippage between the carbon particles and the gases during expansion with thermodynamic equilibrium being maintained at all times; and (b) complete deposition of carbon in the combustion chamber. The results of calculations, for a chamber to exit pressure ratio of 20.42:1 and injection of the liquid monopropellant at its normal boiling point of 10.7 C, are summarized in Table 1, where $T_c$ and $T_e$ denote the adiabatic flame temperature and the nozzle exhaust temperature, respectively, $c^*$ is the characteristic gas velocity, $C_f$ represents the nozzle thrust coefficient, and $I_{sp}$ denotes the specific impulse.


Received January 4, 1954.

[1] Supported in part, by the Office of Ordnance Research under Contract DA 04-495-Ord-446.


[2] Lt., U. S. Navy. This letter is abstracted from a thesis submitted to the graduate school of the California Institute of Technology, in partial fulfillment of requirements for the degree of Aeronautical Engineer, June 1953. Details concerning the work described in this letter may be found in the thesis.

[3] "Quantitative Evaluation of Rocket Propellants," by S. S. Penner, *American Journal of Physics*, vol. 20, 1952, pp. 26–31.

TABLE 1 SUMMARY OF PERFORMANCE CALCULATIONS FOR $C_2H_4O$ MONOPROPELLANT

| Decomposition reaction | $T_c$ (°K) | $T_e$ (°K) | $c^*$ (m/sec) | $C_f$ (−) | $I_{sp}$ (sec) |
|---|---|---|---|---|---|
| $C_2H_4O = CO + CH_4$ | 1430 | 908 | 1230 | 1.295 | 162.2 |
| $C_2H_4O = CO + 2H_2 + C$ (carbon in equilibrium with gas) | 638 | 304 | 891 | 1.400 | 127.6 |
| $C_2H_4O = CO + 2H_2 + C$ (carbon deposited in rocket chamber) | 638 | 270 | 1025 | 1.385 | 105.4 |

The factors leading to carbon formation in combustion are not clearly understood, although a considerable amount of work has been done on this subject in recent years. An extensive literature survey on the kinetics of ethylene oxide decomposition has been carried out. The results of this study are summarized in the thesis from which this letter is abstracted.

## Experimental Measurement of the Heats of Dissociation of Hydrazine-Water and Hydrazine-Methyl Alcohol Systems[1]


WILLIAM CLAY ROBISON[2]

Daniel and Florence Guggenheim Jet Propulsion Center
California Institute of Technology
Pasadena, Calif.


ALTMAN and Adelman[3] have studied the equilibrium between hydrazine and water in the vapor phase by following the pressure change in a constant-volume apparatus. They found the heat of dissociation of hydrazine hydrate to be 13.97 Kcal/mole. Their data on hydrazine hydrate have been checked within the limits of our experimental error. Furthermore, the heat of dissociation of $N_2H_4 \cdot CH_3OH$ has been found to be 8.6 ± 0.3 Kcal/mole, using essentially the same experimental technique as Altman and Adelman.


Received January 4, 1954.
[1] Supported in part, by the Office of Ordnance Research under Contract DA 04-495-Ord-446.

[2] Lt., U. S. Navy. This letter is abstracted from a thesis submitted to the graduate school of the California Institute of Technology, in partial fulfillment of requirements for the degree of Aeronautical Engineer, June 1953. Details concerning the work described in this letter may be found in the thesis. The author is indebted to Dr. S. S. Penner for helpful suggestions.
[3] "Measurements on the Equilibrium Between Hydrazine and Water in the Vapor Phase," by D. Altman and B. Adelman, *Journal of the American Chemical Society*, vol. 74, 1952, pp. 3742-3744.

### Ramjet Diffusers at Supersonic Speeds


(*Continued from page 94*)


#### Collateral Reading


4. "The Dynamics and Thermodynamics of Compressible Fluid Flow," vol. 1, by A. H. Shapiro, The Ronald Press, New York, 1953, pp. 147–152 (sections on supersonic inlets and diffuser efficiency).
5. "Aerodynamics of Propulsion," by C. Kuchemann and J. Weber, McGraw-Hill Book Co., Inc., New York, 1953, chap. 7 (section on the ramjet engine).

# Jet Propulsion News

**ALFRED J. ZAEHRINGER, Thiokol Chemical Corporation,** ***Associate Editor***

**JOSEPH C. HOFFMAN, General Electric Corporation,** ***Contributor***

## Rockets and Guided Missiles

ADDITIONAL details of the Nike guided missile system have been made available. The Nike is a ground-to-air missile which was developed jointly by Army Ordnance, Douglas Aircraft, Bell Telephone Laboratories, Western Electric Company, and Aerojet-General Corporation. Nike is about 20 ft long and 12 in. in diam. A solid propellant booster is used for launching while an acid-aniline rocket engine provides sustaining thrust for the missile. Range is stated to be from 10 to 20 miles with 30,000 to 50,000 ft altitude. Guidance is by a beam rider system. It was announced that the Nike system will be used for the air defense of Washington, D. C. Other U. S. cities are scheduled to be protected by Nike batteries in the near future. (See Figs. 1 to 5.)

LOKI is a new member of America's guided missile family to be announced. Loki is a solid-propellant barrage-type antiaircraft missile based on the Taifun rocket developed in Germany during World War II.

THE Air Force has released preliminary flight information on the Rascal, a Mach 1.5, air-to-surface missile developed by Bell Aircraft. Completely rocket-propelled, the Rascal is designed to be launched from the bomb bay of a B-36 or a B-50 bomber. The launching gear is said to be similar to that used for the X-1A, Bell's rocket-powered aircraft. To keep the mother ship well out of the range of antiaircraft missile defenses, the Rascal is launched about 100 miles from its surface target. After the drop, initial guidance comes from a preset programming device within the missile.

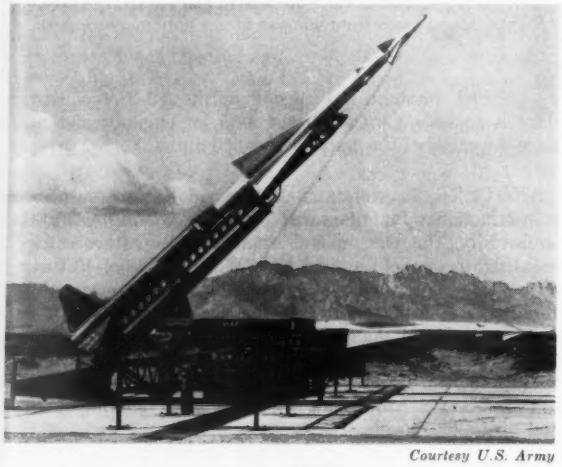

*Courtesy U.S. Army*

FIG. 1 NIKE

This remotely controlled U. S. Army Ordnance launcher poises a partially erected Nike missile against the New Mexico sky. When the launcher has reached an 85-deg angle, the missile will be in position to fire

*Courtesy U. S. Army*

FIG. 2 NIKE

A booster charge has started the Army's antiaircraft Nike on its supersonic quest for a flying target. The lower portion is expended after an initial thrust, and the guided missile proper continues toward its target, guided by an electronic "brain"

EDITOR'S NOTE: The information reported in this Section has been selected from approved news releases originating with the Department of Defense, private manufacturers, universities, etc., and from published news accounts in journals and newspapers. The reports are considered generally reliable, although no attempt has been made to verify them in detail.

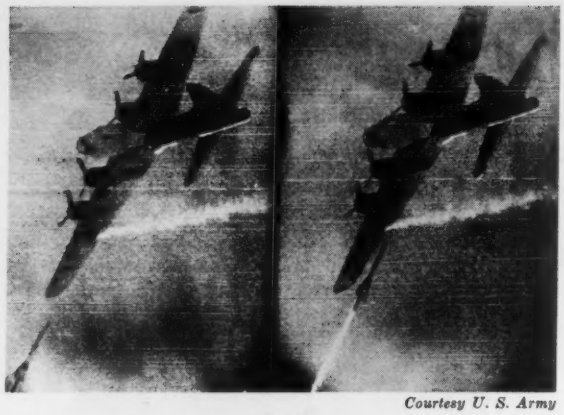

*Courtesy U. S. Army*

FIG. 3

*Left:* Nike nears the target plane. A smoke pot under wing enabled the photographer to follow the action
*Right:* Nike flashes beneath the target's wing

Midcourse and terminal guidance is provided by radar from the mother plane. The Rascal uses its rocket engine to accelerate in level or climbing flight, reaching its maximum speed when the propellants are exhausted. Terminal portion of the flight is said to be either a long glide or a quick push-over into a steep glide.

TWO other British rocket engines have been disclosed by the Royal Aircraft Establishment. One, a 900-lb thrust unit, with an over-all diameter of 18 in., was used to power the transonic research model aircraft produced by Vickers. The propellants, hydrogen peroxide and methanol, were fed into the uncooled combustion chamber by high pressure gas at 500 psi. Although single-shot performance (70 sec) of the rocket motor was considered good, the British found that it was not suitable for repeated use. The RAE has had marked success with the Beta 2 rocket engine. One of the Beta's main features is its turbopump propellant feed system. Driven by steam generated from hydrogen peroxide, which is used as the oxidizer, the turbine is of simple construction and said to be extremely reliable.

ENGINEERS of the Cook Research Laboratories, Chicago, Ill., are testing parachutes at near supersonic speeds on the rocket track at Edwards AFB, Calif. The sled (Figs. 6, 7) is powered by a North American Aviation rocket motor and is capable of being accelerated from standstill to 1500 mph in 4.5 sec. As the sled nears the end of the 10,000-ft long precision-aligned track, a brake scoops up water from a trough between the tracks and throws it out into the airstream, thus utilizing the energy of the moving water to stop the sled. Cook engineers are also conducting near supersonic tests on parachutes with its "Skokie Missile" (Fig. 8) which is dropped from aircraft at high altitudes. The pods at the tail of the missile house cameras which record the action of the parachute during drop conditions. The use of a landing spike (Fig. 9) facilitates recovery after the test.

## Aircraft

ON DECEMBER 12, 1953, Major Yeager of the USAF flew the Bell X-1A at a speed of 1600 mph. The flight took place over Edwards AFB, Calif. Powered by an RMI rocket engine, the X-1A differs from the X-1 in having a turbine-driven propellant pumping system.

THE U. S. Navy has awarded North American Aviation a contract for the production of FJ-4 carrier-based jet fighters. Called an improved version of the FJ-3, the power plant is to be a Curtiss-Wright J-65 jet engine which will place the speed of the craft "above 650 mph."

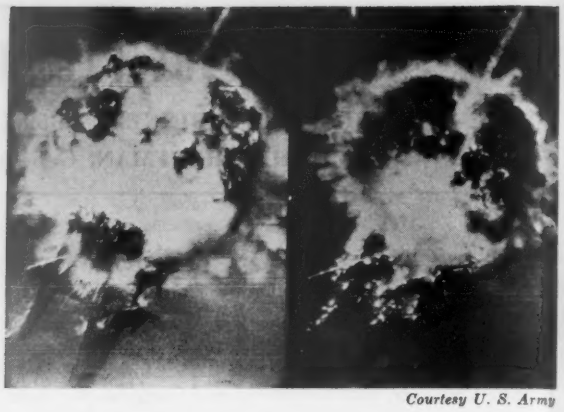

*Courtesy U. S. Army*

FIG. 4

*Left:* Nike explodes at microsecond of intercept
*Right:* Firey fragments of exploded Nike missile rip target

*Courtesy U. S. Army*

FIG. 5

*Left:* Wing shattered and afire, target plane starts final plunge
*Right:* Motor tears from wing as target plummets to earth

ANOTHER Navy craft, the F3H Demon, has been placed in production. Manufactured by McDonnell Aircraft, St. Louis, Mo., the Demon is a single-jet, all-weather carrier-based fighter model powered by a Westinghouse J-40 turbojet engine. Later models are scheduled to be powered by an Allison J-71 power plant. The Demon combines interceptor speed and maneuverability with the payload of an attack bomber. Specifications: wing span, 35 ft 4 in.; length, 59 ft.; height, 14 ft. Top speed was not disclosed by the Navy. Armament is to consist of 20-mm cannon and air-to-air rockets.

THE de Havilland Corporation stated that jet-powered Comets will be placed on the trans-Pacific and trans-Atlantic passenger runs. The Comet 2, seating 44 to 48 passengers, operating at nearly 500 mph at ranges of over 2000 miles, will be delivered to Canadian Pacific Airlines during 1954 for the Vancouver-Sydney run. The Comet 3, cruising at better than 500 mph, at ranges of 2500 miles, will carry 58 passengers in the trans-Atlantic run for British Overseas Airways Corporation.

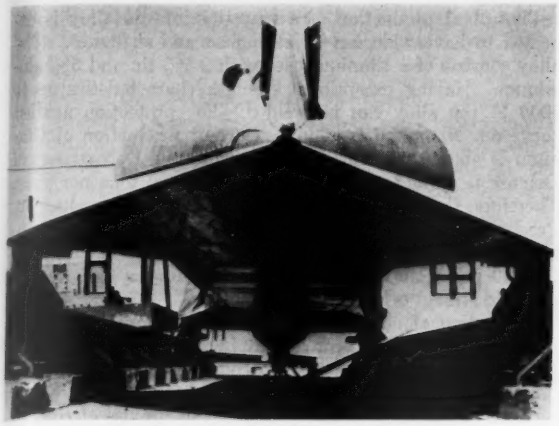

FIG. 6 ROCKET-PROPELLED TEST SLED

## Jet Propulsion Engines

A RAMJET engine that needs no boost to reach its operating speed is under development at Rensselaer Polytechnic Institute. Mechanical inlet valves and explosive ignition are said to be the basis for the RPI design. The information available indicates that the operating cycle of the ramjet will resemble a pulsejet engine.

RYAN Aeronautical Company has received production orders for components on the General Electric J-57 jet engine and for afterburners on the newest model of the Wright turbojet.

JAPAN soon expects to complete its first postwar turbojet engine, the Omiya Fuji JO-1, produced by Omiya Fuji Industries. The JO-1 is essentially an improved Ne-20 (a Japanese version of the German BMW 003) which powered the "Kikka." The engine is of the axial-flow type and features a single-stage turbine and 8-stage compressor, delivering two thrusts around 2200 lb.

FRENCH jet-engine development was given a substantial boost with the announcement that the Snecma Vulcan turbojet completed qualification test at 10,000-lb sea-level thrust. The single-compressor axial-flow turbojet is expected to qualify as an 11,000-lb thrust production unit in 1955. Other jet engines developed by the French Snecma firm include the Atar 101D and 101E. The 101D produces 6600-lb thrust from a 1900-lb engine. With an afterburner, the 101D will give close to 8500-lb thrust. A later modification of the 101D, the 101E is rated at 7270-lb thrust and can produce 9400-lb thrust when equipped with an afterburner.

SEVERAL reverse-thrust devices have been in the news lately. The French firm of Snecma has announced a reverse-thrust device that utilizes 20–30% of full-stage forward static thrust. The unit is claimed to have been test proved on five types of jet engines and that it has been used in place of air brakes up to Mach 0.9. Total running time of 150 hr is claimed. Boeing is said to be conducting extensive reverse-thrust tests for the all-jet B-52. The 150-ton aircraft is thought to require braking power considerably greater than that offered by more conventional methods (viz., wheel brakes and parachutes) to land on present airstrips. Although the work is classified, Boeing has reported "real progress" in their reverse-thrust development. The de Havilland Comet, Britain's all-jet transport, will have reverse-thrust devices on the Model III series, according to a recent press note. De Havilland, like Boeing, is said to be conducting an extensive reverse-thrust development program.

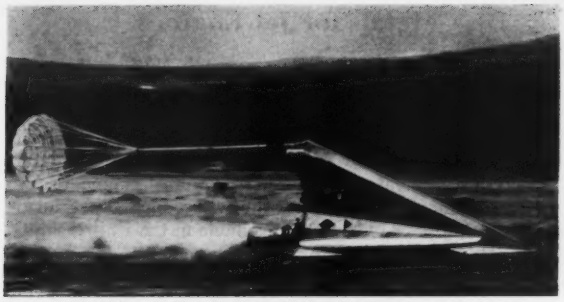

FIG. 7 PARACHUTE TEST AT SUPERSONIC SPEED

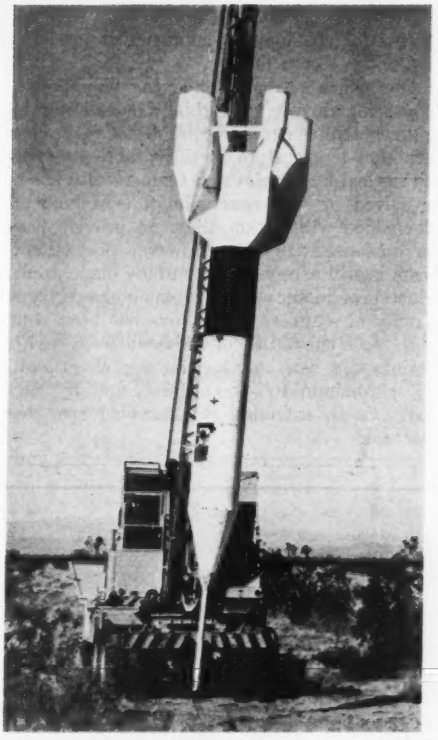

FIG. 8 SKOKIE MISSILE FOR TESTING PARACHUTE RECOVERY FROM HIGH-ALTITUDE DROPS

FIG. 9 SKOKIE MISSILE LANDED WITH PARACHUTE

## Metals for Jet Engines

A LARGE portion of metals research during the past year has been concerned with developing alloys for use at very high temperatures in corrosive atmospheres. Also pressing is the need for low-weight alloys of high strength in modern aircraft where weight must be kept at a minimum. Several developments are of interest in the jet engine field.

New aluminum powder-metallurgy products, first introduced in Europe, have become available in the United States for limited experimental use. One such new alloy has a tensile strength at 900 F equivalent to the best existing high-temperature aluminum alloys at 600 F. It is hoped that this high-tensile strength feature can be yet extended.

Production increases in jet engines have used large amounts of nickel; however, the amount of nickel per plane has been decreasing despite the change from cobalt to nickel alloys. Replacements for cobalt-type "superalloys" used in jet engines have not yet been found.

One factor which has prohibited the widespread use of molybdenum for aircraft gas-turbine blades is the high oxidation rate. Meanwhile, such problems as production of large pieces, low-temperature ductility, fabrication, and good load-carrying features at elevated temperatures are reported as being solved or very near solution. Molybdenum has been roll-cladded with nickel alloys to provide flat-surface oxidation resistance at 1900 F. However, protection of edges and corners is still a problem in turbine blade applications. The production of ductile welds still remains largely unsolved.

The family of stainless steel alloys has been continually increasing. As a substitute for the familiar 18–8 chromium-nickel stainless, a new stainless low-nickel austenitic steel with 16% chromium, 16% manganese, and 1% nickel was developed. As an extender, stainless-clad steel has come into wider use.

Pilot plant production of a new titanium-tin alloy is expected to have wide use in jet engines and airframes. The alloy consists of a titanium base with 2.5% tin and 5% aluminum. Having exceptional strength characteristics up to 1000 F, the alloy can be welded. For protection against corrosion, zirconium is added. Current production of titanium is about 2000 tons per year, while the Department of Defense is aiming at a production of 25,000 tons per year. Therefore, the present emphasis is on increasing production. Progress is being made in welding and production techniques. Alpha-phase alloys have given yield strengths of 110,000 psi, while some alpha beta-phase alloys of 180,000 psi yield strengths have been produced.

Production of zirconium, with high-temperature and corrosion resistance, has been begun by several private firms. Current price of zirconium metal sponge is about $15 per pound.

Much attention also has been given to the use of cermets for blade materials in turbojets. Titanium carbide base cermets have shown good properties at 1800 F. Main avenues of research have been to improve creep and oxidation qualities. The low ductility has remained a serious problem in jet engine applications.

## Instrumentation and Equipment

GENERAL Electric Company has announced development of its FC5 flight control system to be used in production models of supersonic aircraft coming down the production line in 1955. Functioning as a fully automatic relief and maneuvering system, the FC5 consists of three basic units: a rate gyro, an amplifier, and an actuator. The rate gyro detects and accurately measures spurious attitude rates and sends signals to the amplifier which discriminates the signals and amplifies them to a level suitable for control of the actua-

tor. The actuator in turn moves the aircraft's control surfaces to oppose the unwanted attitude rates.

THE extreme heat generated by jet engines and guided missiles calls for a new approach to temperature measurement. A promising new thermometer contains paint which changes color with variations in temperature. Scientists at the Naval Research Laboratory have been able to establish a series of compounds that will record temperatures from 50 to 278 C. It is expected that future compounds will indicate temperatures in the higher ranges.

THE temperature distribution in a rocket flame can be determined by a new gage developed at the General Electric Research Laboratory. Based on the use of a sodium-vapor lamp as a standard for comparison, the gage uses an interferometer which magnifies the radiated spectrum coming from the lamp for a more detailed analysis. The new gage can be used to survey the temperature structure in a large section of a flame, in contrast to earlier methods which permitted temperature measurements at one point only. Study of the rocket exhaust helps determine the efficiency of the rocket motor and tells how much energy is being converted into thrust.

THE Hycon Manufacturing Company has announced production of its Submicrosecond Camera which enables exposure times of one ten-millionth of a second. There are no moving parts to the shutter which operates on the Kerr effect. An electric potential causes realignment of nitrobenzene molecules placed between two polarized screens, thus allowing light to pass onto the film. The camera is being used by Aberdeen Proving Grounds for ballistic research work.

## Upper Atmosphere Research

A PROJECT is being conducted by the USAF Air Research and Development Command to shed some light on the tremendous potential—upward of 100,000 volts—that exists between our earth and the upper stratosphere, a problem pertinent to long-range communications today and one that may affect future extraterrestrial flight. Balloons are carrying aerial electrometers to altitudes of 100,000 ft above Holloman AFB, New Mexico. This upper stratosphere project is a part of a continuing study being made on the terrestrial electrical field existing between the earth and the ionosphere. For over 50 years, science has been trying to discover the source of the 1800-amp current constantly flowing toward the earth.

THE "Jet Stream" is another upper atmosphere phenomenon being studied by the Air Force. The aim of "Project Jet Stream" will be to study the air current that ranges over the northern hemisphere at altitudes between 30,000 and 40,000 ft, and sometimes reaches speeds of 300 mph. A B-47 and a B-29 will be used to measure winds, temperatures, humidity, and turbulence. Air Force scientists agree that the jet stream will be of considerable aid to both military and commercial planes that can take advantage of this super tailwind which travels from west to east.

A NEW parachute jump record is claimed for the Navy pilot who recently bailed out of his all-jet F9F at 33,000 ft while cruising at 450 knots. Forced to abandon his craft because of an explosion his parachute opened after he had fallen 25,000 ft; he landed safely.

FAST service in the overhaul and testing of fuel control systems for jet engines manufactured by Pratt & Whitney (J-48 and J-57) is now available to West Coast manufacturers. Pacific Airmotive Corporation will operate the jet testing equipment at its Burbank, Calif., plant.

## Facilities

THE El Segundo Division of Douglas Aircraft announced completion of a new $1.5 million hangar and flight test building at Los Angeles International Airport to house final test installation work on production models of the bat-winged F4D Skyray.

A NEW rocket facility to be constructed by the Navy Department and operated by Reaction Motors at Rockaway, N. J., was announced. The construction program will include modern research and development laboratories, a fabricating facility for experimental units, project engineering facilities, a cafeteria and supporting facilities, comprising about 150,000 sq ft. It is expected that the $3.5 million facility will be completed in 1954.

MACH number 13 has been attained in a wind tunnel designed by Cornell Aeronautical Laboratory for the Air Force's Arnold Engineering Development Center. With a Mach 20 capability, the tunnel is of the hypersonic impulse type. The driving force of the tunnel comes from a detonation of a helium-hydrogen-oxygen gas mixture. The luminous gases may reach 7000 F during the 1-millisec run at a 10,000 mph test.

BOEING Airplane has announced that it is operating the only privately sponsored wind tunnel capable of speeds in the transonic zone. This tunnel, originally designed for subsonic air speeds, was modernized by a completely new test section, a new fan, a new cooling system, and reinforced walls. Horsepower has been increased from 18,000 to 54,000. The new test section is 8 ft high and 12 ft wide. For tests at high speed it can accommodate models with wing spans as great as 9 ft. At lower speeds, larger models can be tested.

# News In Pictures

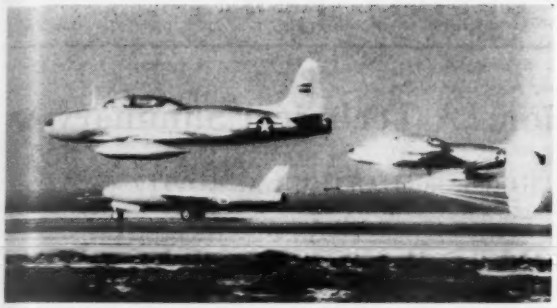

**Regulus Lands After Tests . . .** Although tactical missiles are intended for one-way flight only, considerable savings are realized in tests by being able to recover the particular unit. The landing here is monitored by a mother control plane and a photographic jet as the Regulus opens its tail parachute to slow down the run at Edwards AFB, Muroc, Calif.

**Newest Jet Trainer . . .** The latest jet trainer to be placed in operation is this North American TF-86, a two-place version of the Air Force F-86 Sabre Jet. The "hot" trainer is similar to the F-86 but has a tandem cockpit, dual controls, and is about 5 ft longer than the Korea-famed version. The speed is rated at over 650 mph, a service ceiling of 45,000 ft, and a combat radius of 600 miles. The trainer is to be used for advanced pilot training in high-speed flying, gunnery, and dive bombing

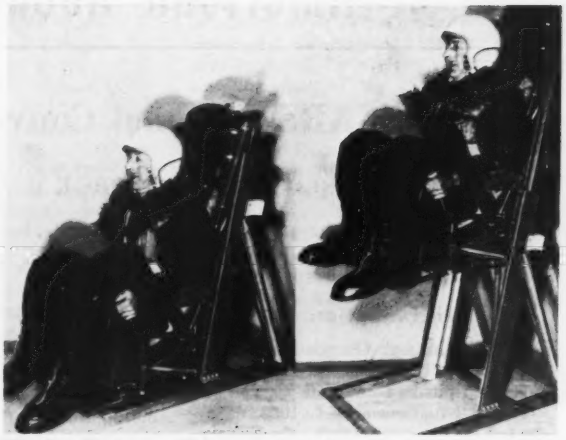

**Ejection Seat . . .** This newest ejection seat is currently being installed in the F-94C Starfire jet interceptor. At left, the seat is in the down position and ready for ejection. By squeezing a lever on the right side of the seat activates the ejection propellant. At right, the seat is shown as it would appear in the process of being ejected. The guide rails steer the seat well above the top of the cockpit sill and give it a high trajectory after ejection

**Regulus Gets Rocket Boost . . .** Rocket boosters enable the Regulus to get quickly into the air from a short ramp or launching platform on a submarine or surface ship

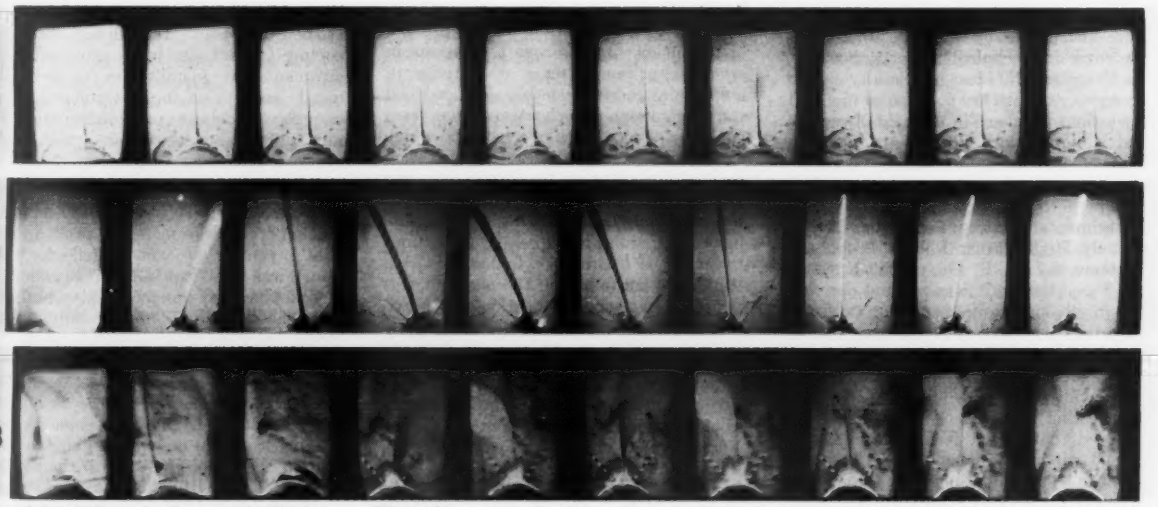


**Aeroelastic Effects in Supersonic Flight . . .** These film strips, shot by automatic rocket-borne camera, illustrate the reaction of high-speed flight on different wing designs. The photographs were made in tests carried out by the Lockheed Aircraft Corporation. Strip 1 shows a thin, straight wing in supersonic flight. Strip 2 shows a straight wing made deliberately flexible. The wing in strip 3 was a swept wing derived by sweeping back the straight wing in strip 2 and increasing the stiffness about 20 per cent. The reaction to high-speed flight was violent before failing

# American Rocket Society News

## The 8th ARS National Convention: A Technical Summary

JOHN E. SCOTT, JR.,[1] GEORGE B. MATTHEWS,[2] and ARTHUR A. KOVITZ[2]

Forrestal Research Center, Princeton University, Princeton, N. J.

### Introduction

THE 8th Annual Convention of the American Rocket Society, held at the Hotel McAlpin in New York City from December 2 to December 4, 1953, again reflected the rapid growth of the Society with the presentation of a record number of twenty-one papers. The broadening interests of the Society were expressed in the wide diversification of the topics presented. Fundamental research was represented by the theoretical aspects of ignition and the aerodynamics of combustion; development activities were represented by such topics as the testing of large-thrust rocket propulsion systems; and the Space Flight Symposium provided a fitting climax to the Annual Convention. In addition, the subject of the Honors Night Dinner, Long Range Applications of Rocket Power, provided an opportunity for speculation as to the ultimate position of rocket propulsion in the power plant spectrum of the future. A large attendance representing a nationwide interest assured the most effective exchange of technical information on a nonsecurity basis, both through formal and informal discussions. A good many of the papers were well worth listening to, and some of them provoked spirited and informative discussion from the floor. Some other papers, however, did not seem to awaken the interest of the audience.

It is to be hoped that in future years, more open discussion can be stimulated on controversial technical subjects, because, the interchange of ideas in this way can go a long way toward the solution of many of the serious problems in the field of rockets and jet propulsion.

### Session I

**Experimental Testing Techniques of Extremely High Thrust Rocket Propulsion Systems,** by R. F. Gompertz, Edwards Air Force Base. It was pointed out that the increasing requirements for extensive experimental testing of long-range guided missile rocket engines have severely taxed the capacity of available test facilities in this country. The requirements for system testing were outlined in which it was stressed that rocket test facilities be designed with the weapon system in mind; i.e., the test facility should be designed to reflect the ultimate mission of the rocket propulsion system.

Several solutions to the problem of optimum test installations design which are currently under consideration were outlined by the author. An analysis was given comparing the simultaneous utilization of one single test cell for more than one large test article versus utilization of multiple noninterfering preparation areas supporting a single test stand. Test readiness and compartmentation of instrumentation, propellant lines and other test connections were major factors in this analysis. It was concluded that multiple-use test stands or preparation areas are the possible solution. At the conclusion of the paper, a color movie was presented showing the test facilities at Edwards AFB.

A prepared discussion of Mr. Gompertz' paper by R. F. Rose of the Jet Propulsion Laboratory, CalTech, was read. It expressed the opinion that simultaneous occupancy of the test stand by more than one project should be rigorously avoided, since the possibility of mutual damage is too high a price to pay for the time saved. Development of proper handling gear and preparatory areas should eliminate the necessity for multiple occupancy. Mr. Rose felt that the paper was too superficial an analysis of the problem, and that more could have been said about test stand design.

**Multidirection Vibration Tester,** by A. Bohr, Reaction Motors, Inc. Present-day military considerations, particularly in missile equipment installations, have led to the need for vibration testers capable of producing simultaneous oscillations in several directions over a wide range of amplitudes and frequencies. He described the construction of such a test system from commercially available parts in which electrically excited vibration shakers were used to vary the stem position in four-way valves and thus oscillate a load to a maximum of approximately 50 cycles per second in both horizontal and vertical directions by means of hydraulic cylinders. During the discussion following the paper, it was pointed out that qualification test specifications for aircraft instruments require systems capable of producing frequencies as high as 500 cycles per second.

**Structural Design Considerations for a High Altitude Sounding Rocket of the Viking Type,** by R. C. Lea, Glenn L. Martin Co. The need always exists for improvement in mass ratio by reduction of rocket empty weight. Among many problems are the evaluation of aerodynamic heating effects at presently attainable Mach numbers above 4.0, and the development of quantitative design criteria for shock and impact loads. In addition, structural feedback of operating control frequencies to the control system by heavy oscillating masses appears to be one of the more difficult problems of structural design.

### Session II-A

**Introduction to the Analysis of Supersonic Ramjet Power Plants,** by G. Sears and B. March, Marquardt Aircraft Co. The effects of the various ramjet power plant components, altitude, Mach number, etc. upon ramjet engine performance were analyzed. The problems and limitations which determine the region of application of ramjet engines were also discussed. The equations necessary for the calculation of thrust and fuel consumption were derived. Simple charts were presented for the rapid estimation of ramjet engine performance.

**The 350,000 Pound Rocket Test Stand at Lake Denmark, N. J.,** by B. N. Abramson, D. S. Brandwein, and H. C. Menes, Naval Air Rocket Test Station. The test stand, whose basic structure is a steel cantilever, is constructed of steel and concrete. The firing attitude range in this stand is from vertical to horizontal with controls of operations being effected from the underground level in a blockhouse 250 feet away. The test stand itself is located on a steep hill such that the vertical distance from the firing mount to the ground is 60 feet. This provides protection from the effects of the exhaust jet. In addition, water for cooling the exhaust jet is provided. Instruments are installed to measure the usual rocket engine parameters, and enough channels are provided to allow for any additional measurements which might be needed for a complete engine test.

**The Problem of Cooling a Rocket Flame Deflector,** by T. F. Reinhardt, Naval Air Rocket Test Station. The problem was that of cooling a rocket jet deflector plate which was to be exposed to the exhaust of a rocket having a possible maximum thrust of 100,000 lb and located only 51 in. away. Several possible solutions to this cooling problem were considered, and four of these were discussed by the author. The methods considered were as follows: 1 Utilization of the heat capacity and thermal conductivity of the plate to keep the surface temperature below the melting point. 2 Provision of a cooling water source beneath the deflector plate to absorb the heat. 3 Flooding of the plate with water on its upper surface. 4 Cooling of the exhaust jet by water injection through high pressure nozzles.

Each of these methods was explained in

[1] Research Assistant. Stud. Mem. ARS.
[2] Research Assistant. Mem. ARS.

detail, and a comparison of the advantages and disadvantages of each was made. Experimental test results were presented to illustrate the major factors involved in each method.

## Session II-B

**Some Aspects of Design and Fabrication of Liquid Propellant Engines,** by H. Davies, Reaction Motors, Inc. Such topics as the choice of materials for particular applications and the problems of sealing against high temperature, high pressure gases were stressed in this paper. Strength-to-weight ratio, high and low-temperature strength properties, machinability, and compatibility with various propellants are involved in the selection of materials. The presentation concluded with a comparison of various types of static and sliding seals now in use and a short discussion of the major factors which affect serviceability and ease of maintenance. A comment prepared by C. E. Hawk of the Aerojet-General Corporation emphasized the implication of the paper that rocket engines have reached a stage of development so advanced that designers concern themselves less with the problems of explosions or burnouts than with the more sophisticated questions of ease of production, durability, and field servicing. Mr. Hawk also noted the increasing importance of control systems and their integration into over-all rocket motor designs.

**Rocket Preliminary Design and Proposal Preparation,** by S. Lehrer, Reaction Motors, Inc. The author outlined the organization of his company's proposal effort, with particular details on the interaction between various departments. He also discussed the mechanics of proposal writing and the structure of a special proposal report.

**Stability of Ethylene Oxide,** by E. M. Wilson, Aerojet-General Corp. This paper was a supplement to several existing reports on the stability of ethylene oxide under normal operational hazards. It reported the results of detonation tests under conditions of sharp restriction in flow passages. Detonation did not take place in any of the pressurization tests. Similar stability and conspicuous absence of detonation was observed in the ejection tests. In an additional series of tests, ethylene oxide at temperature up to 150° F was splashed against a stainless-steel block heated to temperature from 400 to 1000° F. Again no detonations were present. However, experiments with nitromethane produced immediate detonations under similar pressurization and splashing conditions. An interesting discussion followed the presentation in which such factors as time of contact with heated surfaces, contamination of such surfaces, and incompatibility (when heated) of metals other than stainless steels were mentioned as important considerations in determining the stability of this compound.

## Session III-A

**The Isothermal Compressibilities of Some Rocket Propellant Liquids and the Ratios of Specific Heats,** by G. Kretschmar, USNOTS, Inyokern. The author described a method for the determination of the isothermal compressibility in which a thin glass capsule containing the liquid was pressurized inside a thermostated glass vessel (or piezometer) that is filled with mercury up to a fiducial point. With a knowledge of the adiabatic compressibility, obtained by the use of an ultrasonic interferometer, the author obtained the specific heat ratio simply by dividing the isothermal into the adiabatic compressibility.

**One-Dimensional Steady Adiabatic Flow in a Constant Area Channel with Mass Addition at Constant Enthalpy and Negligible Kinetic Energy,** by E. W. Price, USNOTS, Inyokern. Five equations, including continuity, momentum, energy, heat capacity, and state are written in terms of the six variables, pressure, density, velocity, temperature, enthalpy, and mass flow. When one of these variables is assumed known, then the other five may be determined. In this paper, the independent variable was chosen as the mass flow. Finally, application of the results to a solid propellant rocket was discussed briefly.

**Investigation of Boiling Heat Transfer and Burnout to JP-4,** by C. M. Beighley and L. Dean, Bell Aircraft Corp. A transparent annular test section surrounding an electrically heated stainless-steel tube was used to obtain heat transfer data in the nonboiling, nucleate boiling, and film boiling regions, heat flux values being increased until the test section burned out or the limit of the power generator was reached. The nonboiling heat transfer data were correlated by the Seider-Tate equation with a constant of 0.0213 instead of 0.023. It was observed that a sand-blasted tube caused approximately 50 per cent increase in the heat transfer coefficient over the regular and polished tubes in the nonboiling region. The nucleate boiling range was investigated quite thoroughly up to the point where film boiling begins and the wall normally fails. In the film boiling region, the authors found that it was possible to obtain a 200 per cent increase in heat flux with less than a 20 per cent increase in wall temperature. Finally, the formation of coke on the heater tube surface was discussed. It was concluded that coke deposition did not occur below a given heater tube surface temperature, that temperature depending upon the constituents in the fuel.

## Session III-B

**Study of the Combustion of Fuel Droplets Descending Through an Oxidizing Atmosphere,** by D. Charvonia, Purdue University, and H. Wood, Virginia Polytechnic Institute. The studies were made with three organic fuels, namely, triethylamine, allylamine, and cyclohexene, descending through decomposition vapors of white fuming nitric acid. Interruption of a light beam by the falling droplet starts operation of a Fastax camera photographing the descent of the droplet. It was found from these photographic records that ignition is initiated in the vapor region in the wake at a considerable distance behind the droplet, producing a flame front which propagates at a speed greater than droplet velocity, and hence overtaking the droplet. Ignition delays were measured for a wide range of conditions for each of the three fuels mentioned. Increasing vapor temperature decreased the ignition lag of two of the fuels, leaving the third relatively unaffected; a fuel temperature increase showed a tendency to decrease the ignition lag; and fuel droplet size was found to have a marked effect on ignition delay, appearing to give a minimum ignition delay at some definite drop size. Attempts to explain these variations from a theoretical approach have thus far proved unsuccessful.

**Ignition and Combustion in a Laminar Mixing Zone,** by F. E. Marble and T. C. Adamson, California Institute of Technology. This paper considered the theoretical approach to the problem of ignition and combustion in a laminar mixing zone between two parallel streams, one of which consists of a cool combustible mixture and the other being composed of hot combustion products. After discussion of the physical and chemical relations which apply to the problem, the initial portion of the mixing zone was investigated where the heat evolved through chemical reaction is small, and the problem is solved by consideration of a perturbation to the solution for mixing without combustion. This gives the analytical picture of the early portion of the mixing zone.

The complete course of development of a laminar flame front was then examined by means of an approximate treatment which effectively extended the solution throughout the remainder of the flame zone. This analysis indicated that a new class of combustion problems is open to investigation through application of the usual boundary layer concepts.

In a prepared comment, J. A. Bierlein pointed out that the mathematical description is in harmony with experience. He also pointed out the benefits which might be forthcoming from an extension of the analysis to consider fractional and second-order reactions in an attempt to obtain a mass of data depicting flame stand-off distance over a wide range of values for all the disposable parameters. It might then be possible to predict the complete blow-off or quenching behavior of a system on the basis of a few experimental results, without prior knowledge of the chemical kinetics or the transport properties of the system. The discussion from the floor which followed indicated a widespread interest in this paper.

**Erosive Burning of Some Composite Solid Propellants,** by L. Green, Jr., Aerojet-General Corp. The paper reported experimental data on the erosive burning characteristics of several composite solid propellants. It was found that the data were best correlated in terms of a reduced mass velocity. In discussing the existence of an apparent "threshold velocity for erosion," the author pointed out that this is probably due to the conditions at the fore end of the grain. In order to determine the best method of correlation and to resolve the question as to the existence of the threshold velocity, it was pointed out that

experiments of increased precision are necessary.

In a prepared comment by R. N. Wimpress, read by the vice-chairman, it was pointed out that the existence of a threshold velocity has been definitely shown for JPN and ballistite and must be considered in any design using these propellants. It was also mentioned that the chamber pressure and the gas velocity must be considered as being two separate effects on the "erosion ratio" $\epsilon$.

## Session IV-A

**Oxidant Pumps,** by W. Mizen, Bendix Aviation Corp. The results of development work on a positive displacement plunger-type pump for 90 per cent $H_2O_2$ were described. A single plunger test pump was built using Type 440-C steel, bright hardened to 55 $R_c$ for the plunger housing and Type 416 steel chrome-plated for the plunger. All other mechanical components were made of 18-8 stainless steel with neoprene as the O-ring seal material. This pump performed well, but failure after 9 hr of operation was caused by severe pitting of the Type 440-C discharge valve seat. To extend the life of the pump, materials such as glass, synthetic sapphire, and dry molded alumina ceramic were tried for the plunger housing and plunger materials. The test results which were reported evoked active discussion on the relative merits of all kinds of materials for such service.

Two prepared comments on this paper were read. The first comment, by D. Chatfield of RMI, complimented Mr. Mizen on providing a good insight into the use of some rather unusual materials in notching or moving parts. With respect to the use of ceramics or high strength glass as bearings, he felt that this application would be limited to moderate speeds and thrust loads. He also verified that the use of steels of the 400 series is usually avoided because they cannot be successfully passivated.

The second comment was prepared by David K. Hart, USNOTS, Pasadena, Calif. In discarding conventional corrosion-resistant materials, Mr. Hart felt that too much haste was shown. He pointed out that pitting occurred only in areas which were not critical. If the failure was due to pitting of the discharge valve seat, it seems reasonable to suppose that the installation of a Teflon valve seat would have solved the problem without resorting to the longer term investigation of ceramics.

**An Analytical Procedure for Mixed Acid,** by J. Clark, Naval Air Rocket Test Station. The problem of determining the composition of mixed nitric acid, a liquid that is in common use as an oxidizer for rockets, was described. Mixed acid is approximately 83 per cent $HNO_3$, 15 per cent $H_2SO_4$, plus small amounts of water and $NO_2$. The method in common use is based on three titrations, a procedure developed by Scott and modified at the author's laboratory. This method is entirely satisfactory except for the $H_2SO_4$ titration. The author's line of attack resolved itself into a conductimetric endpoint method for the $H_2SO_4$ after most of the interfering $HNO_3$ had been removed. In conclusion, it was stated that the method is probably reliable to 0.1 per cent $H_2SO_4$, which is a considerable improvement over the current procedure.

**Experience with the Application of Hydrogen Peroxide for Production of Power,** by H. Walter, Worthington Pump and Machinery Corp. The paper constituted a recounting of personal experiences in Germany with hydrogen peroxide in applications for the production of power. This historical account began in 1933 with a proposal for a submarine engine using hydrogen peroxide, and extended through World War II in which peroxide rocket engines were used to propel aircraft and guided missiles. The major emphasis of the paper was on the reliability and relative hazards involved in the handling, storage, and power applications of peroxide, and a number of interesting experiences were related to illustrate these properties. After a period of research and development on the sensitivity of hydrogen peroxide and mixtures of this oxidizer and various organic fuels, a number of peroxide-drive devices were tested, accepted, and introduced into service without a single accident directly attributable to hydrogen peroxide.

## Session IV-B

**Low-Frequency Combustion Stability of Liquid Rocket Motor With Different Nozzles,** by Sin-I Cheng, Princeton University. The paper reported the results of a theoretical investigation of the effects of the nozzle flow on the stability of low-frequency oscillations in liquid propellant rockets. The fundamental equations were developed on the basis of assumptions outlined in previous analyses of low-frequency instability. The resulting characteristic equation was solved to determine the boundaries of stable operation. These new stability boundaries thus represent a general solution for all rockets with a given combustion chamber and feed system, but with different Laval nozzles. It was generally concluded that a decrease in contraction ratio with constant length of converging section or an increase in length with constant contraction ratio would have a stabilizing effect on low frequency oscillations.

**Low-Speed Combustion Aerodynamics,** by R. A. Gross and R. Esch, Harvard University. The authors introduced the problem of the two-dimensional low-speed steady flow field containing a finite length discontinuity which represents a flame in unbounded space with uniform parallel flow at infinity. By making the assumptions that the density ratio and pressure ratio across the flame are constant, the heat of reaction is constant and the flow field is everywhere irrotational, the flow field can then be described by classical potential theory where the flame discontinuity is represented by a source sheet.

Two approximate solutions to flow fields were presented. The first was a straight line flame of finite length inclined at an angle to the free stream, and the second was the V-flame shape. The experimental data showed good agreement only for small values of the ratio of flame speed to the uniform velocity at infinity.

The general discussion which followed the presentation of the paper dealt mainly with the validity of the basic assumptions and their possible verification experimentally. On the basis of the experimental data obtained by the author, it was pointed out that the source sheet is a powerful tool for use in solving problems of this general type.

**Instantaneous Rocket Flame Temperature Measurement,** by J. H. Hett and J. B. Gilstein, New York University. The paper described some measurements of instantaneous combustion chamber and exhaust temperatures in a 1500-lb thrust alcohol-oxygen rocket. The authors gave an account of their work while at the GE Malta Test Station from January 1950 to August 1951. The temperature instrument used was an instantaneous two-path optical pyrometer. Since the continuous background of the spectrum of a hydrocarbon flame is believed to be in thermal equilibrium with the gas, this instrument uses for temperature measurement a region of this spectrum that is free from line and band structure. Planck's radiation law and the usual negative exponential function for absorption are used for the purpose of analysis. Spectrographic data showed that the radiation was not quite Planckian so that the recorded temperatures should be considered only as "indicated" temperatures. Temperatures of about 2130° K at the first Mach cone were shown in contrast to the Bundy and Strong figure of 2360° K, using a sodium-line reversal method. The indicated average temperature was found to be 1900° K$\pm$50° with an emissivity of 0.15$\pm$0.05. A spectrographic study of the radiation from the chamber through a quartz window was undertaken to determine the departure from gray-body radiation. Because of this departure, the authors were again obliged to speak of "indicated" temperatures. An average temperature of 2750° K is presented, whereas the calculated theoretical maximum temperature for the mixture ratio used was approximately 3200° K.

---

EDITOR'S NOTE: The papers summarized in this review will appear in future issues of JET PROPULSION as space becomes available. In the meantime, preprints may be obtained from the ARS Secretary at 25 cents per copy.

## Space Flight Symposium

THE final session of the ARS 1953 Convention was a symposium on space flight held in the Ballroom of the Hotel McAlpin on Friday morning, December 4. This symposium took the form of a panel discussion followed by a formal question period. The members of the panel were: Andrew G. Haley, *chairman*, of Haley, Doty, and Schellenberg; John R. Pierce of Bell Laboratories, Inc., main speaker; J. H. DeWitt, Jr., of Stations WSM and WSM-TV; Krafft A. Ehricke of Bell Aircraft Corp.; E. E. Francisco, Jr., WSPG; R. W. Porter, General Electric Co.; Darrell C. Romick, Goodyear Aircraft Corp.; Milton W. Rosen, Naval Research Laboratory; Kurt R. Stehling, Forrestal Re-

search Center, Princeton University; A. R. Tocco, Hughes Aircraft Co.; R. C. Truax, U. S. Navy Bureau of Aeronautics; and Paul F. Winternitz, New York University.

Each of the panel members presented a short talk on a particular phase of space travel, after a brief introduction by the chairman. Col. DeWitt discussed communications between the earth and a satellite vehicle, mentioning the possible use of such a vehicle as a television transmitting station and demonstrating the ease of such transmission by the relative success of radar communication to the moon.

Mr. Ehricke spoke about a new system for supplying orbital vehicles by means of winged rockets, and discussed the problem of calculating the optimum position and direction of take-off from an orbit for interplanetary travel.

Mr. Francisco commented on the role of research in advancing the science of space flight. He emphasized the need for more fundamental work in high altitude research and mentioned the contributions made in this field by the White Sands Proving Ground.

Mr. Romick discussed control systems for space ships, stressing the importance of guidance. He suggested automatic computers feeding servo control systems as a possible method for flight correction of initial directional deviations.

Mr. Rosen then spoke on the topic, "Margin for Error," in which he pointed out a factor usually overlooked in satellite or interplanetary vehicle calculations, namely, the extreme effects which small errors or variations in specific impulse or propellant flows can produce in final velocity and altitude. He applied a reasonable value of propellant "outage" to the calculations of three satellite designs, and showed how far short of predicted performance they might fall.

Mr. Stehling spoke on the hazards of radiation in an orbital vehicle. He demonstrated how secondary emissions might produce much more harmful effects than the primary cosmic or solar radiation, and he suggested the possibilities of using water, paraffin, or electromagnetic force fields to shield human beings from such rays.

Mr. Tocco remarked on some promising new materials for rocket vehicles with regard to the problems of overheating during re-entry. He mentioned the use of titanium, porous metals, and ceramics as examples.

Dr. Winternitz gave a brief discussion on the improvement of specific impulse as a means of obtaining orbital velocities from multistage chemically fueled rockets. He was followed by Cmdr. Truax who made a plea for better economic analysis of satellite vehicle designs, illustrating the importance of such considerations by analyzing the relative costs of returnable and expendable third stages of a missile of the type suggested by von Braun.

Dr. Porter then outlined the policy of the American Rocket Society toward space flight, accentuating the importance of interplanetary exploration as a scientific challenge, independent of any military or practical applications.

Dr. Pierce, the main speaker, then addressed the audience on the over-all problem of communication in space. His analyses and conclusions were based entirely on existing equipment and techniques and indicated that, in general, transmission and receipt of information between Earth and a moving space vehicle or between Earth and a fixed interplanetary body would pose fewer problems than similar communication between two points on the earth's surface. He proposed 3-centimeter wave-length radiation and analyzed the power requirements, size of equipment, signal-to-noise ratio, and velocity corrections involved in transmitting or receiving such waves on a moving vehicle outside the earth's atmosphere. On the topic of Earth-Moon communication, Dr. Pierce was even more optimistic, declaring that telephone and telegraph contact between these two bodies would be possible with power supplies of only a few hundred watts. In conclusion, he speculated that if interfering noise can be reduced and power-to-size ratio can be increased at their present rates of development, communication with the stars may not be unreasonable.

At the close of this formal part of the session, an interesting question period was held. Written questions were submitted by those in attendance, addressed to individual panel members. Such topics as the use of solid propellants for space rockets, the minimum skin temperatures possible in descent through the atmosphere, the use of powdered metals for propellants, video communication from Earth to Mars, the technical definition of gravity, and the use of nuclear power plants in rockets were treated by the various speakers.

## Chemical Industry's Stake in Rockets

G. EDWARD Pendray, ARS Director, spoke at a dinner meeting of the Chemical Public Relations Association on February 3 at the Hotel Roosevelt in New York.

After delivering a talk on rocket history and the beginning of the ARS, Pendray told the group of some 60 public relations men from 30 major chemical companies what rocket development could mean to their industry. He contrasted the "early days" when liquid oxygen used to be "swiped by the container" to today when it moves into missile test centers by the tank carload. He also pointed out that 29 of the 79 technical papers presented in the ARS JOURNAL since September, 1951, have dealt directly or indirectly with chemicals, as well as 31 of 111 papers presented at technical meetings since January, 1949.

## ARS in Dallas Airpower Symposium

AMONG the speakers at the recent Airpower Symposium sponsored by the Dallas Council on World Affairs was Frederick C. Durant III, last year's ARS President and current President of the International Astronautical Federation. Durant's talk—on space flight—followed speeches delivered by General Nathan F. Twining, USAF Chief of Staff; James H. Smith, Jr., Under Secretary of the Army; Earl D. Johnson, and Arthur Godfrey.

## "Dream Come True" Says Mrs. Goddard at WSPG

"THIS rocket range would have been a dream come true for my husband if he had lived to see it," remarked the widow of the late Dr. Robert H. Goddard, during her recent visit to White Sands Proving Ground.

In New Mexico for the opening of an exhibit of some of her husband's work at Roswell, Mrs. Goddard was honored guest and speaker at a banquet arranged by the New Mexico-West Texas Section on January 22. She spoke on the "human aspects" of Dr. Goddard's work from 1925 to 1941 in New England and New Mexico and also showed motion pictures of static and flight tests of the rocket pioneer's experimental units, fired at Eden Valley near Roswell.

During her visit to WSPG, Mrs. Goddard was also tendered a luncheon by Brig. Gen. George G. Eddy, commanding general of WSPG.

MRS. ESTHER C. GODDARD, WIFE OF THE LATE DR. ROBERT H. GODDARD, IS SHOWN AT LUNCHEON TENDERED HER BY BRIG. GEN. GEORGE G. EDDY, COMMANDING GENERAL OF WSPG. AT RIGHT IS CAPTAIN PHILIP D. QUIRK, COMMANDER OF THE U. S. NAVY ORDNANCE MISSILE TEST STATION, WSPG; E. E. FRANCISCO AND FRANK L. KOEN, JR., PAST-PRESIDENT AND PRESIDENT, RESPECTIVELY, OF NEW MEXICO-WEST TEXAS SECTION ARE AT LEFT

# Haley Presides Over ARS-IAS Session

PRESIDENT Andrew G. Haley served as chairman of a technical session on rocket propulsion at the IAS Twenty-Second Annual Meeting on January 29 in New York.

Four papers were presented before an audience of about 60 people at the session, which was arranged by ARS.

"Ballistics of an Evaporating Droplet" by C. C. Miesse of Aerojet-General Corporation, Azusa, Calif., analyzed the behavior of droplets—particularly fuel droplets injected upstream in a ramjet burner—when droplet velocity and size, air velocity, and physical properties of the surrounding air are taken into account. Making several basic assumptions, Miesse pointed out the possibility of determining analytically the velocity profile of an evaporating droplet.

"Gas Torch Igniter for Rocket Motors" by George N. Woodruff of Reaction Motors, Inc., Rockaway, N. J., described an ignition system which promises, according to Woodruff, greater reliability in firing of rocket engines over a wide range of thrusts. Hydrogen and oxygen were the gases used principally during tests on which the paper is based.

In "Toxicity and Health Hazards of Rocket Propellants," Stephen Krop of the Army Chemical Center, Maryland, gave a detailed analysis of the characteristics and potential handling dangers of rocket fuels, oxidizers, and their decomposition products. Included were ammonia, aniline, hydrazine, JP-4, hydrogen peroxide, liquid oxygen, red fuming nitric acid and ethyl, methyl, and furfuryl alcohol.

The final paper, "A Light Weight Electric Analog Computer With no Moving Parts," was presented by Paul H. Savet of Arma Corporation, Mineola, N. Y. It described a device which performs basic calculus operations directly on a-c signals and multiplies and divides statically by means of heat transfer, eliminating the need for servomechanisms. The miniature computer was developed principally for applications in navigation and piloting of aircraft and guided missiles.

ANDREW G. HALEY ADDRESSES THE ARS-IAS JOINT MEETING

## New York Section to Sponsor Education Program

ON MARCH 24 in New York City, a group of outstanding university scientists will discuss the engineering preparation advisable for students looking forward to participation in the field of space flight.

The panel, to be moderated by Dr. Martin Summerfield, Editor-in-Chief of JET PROPULSION and Professor of Jet Propulsion at Princeton University, will include Dr. Charles L. Mantell, Chairman of the Department of Chemical Engineering, Newark College of Engineering; Prof. Charles H. Townes, Executive Officer, Department of Physics, Columbia University; Prof. William R. MacLean, Department of Electrical Engineering, Polytechnic Institute of Brooklyn; Prof. Frederick K. Teichmann, Chairman of the Department of Aeronautical Engineering, College of Engineering, New York University; and Dr. Alfred Bornemann, Professor of Metallurgy, Stevens Institute of Technology.

Undergraduate engineering and science students from colleges in the metropolitan area, as well as interested high-school science students will be invited to the meeting which will be held at the American Museum of Natural History at 8:00 p.m. Arranging the program for the New York Section is C. W. Chillson, Past-President of the ARS.

## IAF is to Award Loeser Medal

THE International Astronautical Federation announces that the subject of the competition for the first annual Guenter Loeser Memorial Medal will be "On the Economics of Space Flight."

The award, honoring Dr. Guenter Loeser, former IAF vice-president killed in 1953 in a plane crash doing consulting work for the U. S. Air Force, was established at last year's IAF Convention. Entries should be submitted to the Secretary, International Astronautical Federation, P. O. Box 37, Baden, Switzerland, in five copies, not later than December 31, 1954. They should be forwarded in two envelopes, the outer marked "Loeser Medal Competition." The inner (containing the entry) should be blank as it will be inscribed with a code mark in place of the author's name.

## Four More Corporate Members

TWO outstanding companies in the guided missile and aircraft manufacturing fields, one chemical company, and an aviation publishing company are recent additions to the ARS Corporate Member lists.

They are Lockheed Aircraft Corporation, Burbank, Calif., which just announced the formation of a Missile Systems Division; Bell Aircraft Corporation, Buffalo, N. Y., designers and producers of liquid propellant rockets and rocket engines; Linde Air Products Co., Division of Union Carbide and Carbon Co., New York, N. Y., makers of liquid oxygen; and Aeronautical Digest Publishing Co., Washington, D. C., publishers of *Aero Digest* and the *Aircraft Yearbook*.

### *Going to Innsbruck?*

Reservation forms are being circulated to all ARS Members for a 21-day tour to the 5th Annual Convention of the International Astronautical Federation at Innsbruck, Austria.

The tour will leave by plane from New York on July 25 and will include, tentatively, four days in Paris, three days in Switzerland, six days in Innsbruck for the IAF Convention, August 1–7 (with side trips optional to such places as Bolzano, Italy, Oberammergau, Garmisch-Partenkirchen), four days in Germany (including a trip up the Rhine), and two days in Belgium. Return to New York will be on August 15.

Cost of the trip to ARS members and their guests will be $750 all-inclusive (except for extras such as drinks and gifts). Seats will be assigned as reservations are received by the travel agency. Details are included in the form.

Any member who has not received a reservation form can obtain one by writing to the national office.

## ARS Fellow Honored

ON FEBRUARY 8, Dr. Theodore von Kármán was honored at a reception at the Italian Embassy in Washington, D. C. Ambassador Alberto Tarchiani, on behalf of the Italian Government, presented Dr. von Kármán with the Order "Al Merito della Repubblica" in recognition of his scientific achievement and contributions to the field of aero- and thermodynamics. In 1949, ARS honored Dr. von Kármán by awarding him its Fellow membership.

Mrs. Andrew G. Haley (in ARS President Haley's absence) and IAF President F. C. Durant III attended the reception. Others also attending included Asst. Secretary of Defense Donald A. Quarles; USAF Chief of Staff General Nathan F. Twining; and USAF Asst. Chief of Staff Lt. Gen. L. L. Craigie.

## Section Doings

**Detroit.** Results of the election of officers for this recently organized group are as follows: Laurence M. Ball, President; Fred Klemach, Vice-President; David Buell, Secretary; Dr. Richard B. Morrison, Treasurer. On the Board of Directors are Dr. Arthur B. Ash, Charles W. Williams, Dr. Leland G. Cole, and Dr. Arthur A. Locke.

**Florida.** On January 26 more than 350 persons listened to a talk on space flight by Wernher von Braun of Redstone Arsenal. This was the second public meeting of the newly formed group which is centered at Patrick Air Force Base. The first, held on November 20, 1953, had ARS Director Dr. Richard W. Porter as principal speaker. Officers of the Section are Keith K. McDaniels, President; Major Prentice B. Peabody, Vice-President; and 1st Lt. Theodore A. DeBacker, Secretary-Treasurer.

**National Capital.** Officers recently elected are: James R. Patton, Jr., President; Esterly C. Page, Vice-President; Ethna White, Secretary; Richard K. Neumann, Treasurer. Directors are Harry J. Archer, J. D. Gilchrist, Andrew G. Haley, Charles F. Marsh, Dr. S. F. Singer, and Richard B. Snodgrass.

The Section gave a dinner in honor of Dr. Theodore von Kármán on Friday, January 29. There were approximately 60 members in attendance. Andrew G. Haley, ARS President, discussed his program for the coming year. Dr. von Kármán gave a very interesting talk on the future of rockets and included some informative comments on foreign developments.

On Friday, February 12, a two-hour film, "History of Rocket Development," was shown to approximately 100 members and guests at the second meeting of this new section. The film, released through the British Ministry of Supply, traced the development of rockets in Germany from the very early work of Opel, Valier, Heylandt, and Zucker to the Rheinbote, Rheintochter, Wasserfall and A.4. Of particular interest were combat shots of the Me.163 rocket interceptor attacking a formation of Flying Fortresses. The film closed with the take-off of the space rocket from Fritz Lang's *Frau Im Mond*.

### JAMES J. WYLD

Announcement was made at the ARS 8th Annual Honors Night Dinner on Dec. 3, 1953, of the death of James J. Wyld, pioneer developer of rocket power, past president of ARS, and one of the founders of Reaction Motors, Inc., Rockaway, N. J.

Mr. Wyld, 41 years' old, died of a heart ailment on Dec. 1 at his home in Pompton Lakes, N. J. A graduate of Princeton University where he had achieved a brilliant scholastic career, he helped to form RMI in 1941 after having done research work on high speed aerodynamics for NACA for a time. His work at RMI established him as one of the leading figures in the rocket field and much of his research and development work has seen fruition in liquid propellant engines which power today's aircraft and guided missiles.

A member of the Board of Directors of RMI at his death, Mr. Wyld had served as a consultant to the Atomic Energy Commission in recent years. He leaves his wife, Mrs. Helen Wyld, a daughter, Marie, 4, and a son, Robert, 2.

**New Mexico-West Texas.** The first issue of *Missile Away*, published in December, 1953, was so successful that it is planned to print it quarterly. This year's officers are Frank L. Koen, Jr., President; Edward L. Brown, Vice-President; and G. Harry Stine, Secretary-Treasurer. The Board of Directors will consist of E. E. Francisco, Jr., Chairman, Clyde Tombaugh, Dr. Russell K. Sherburne, Charles W. Mansur, John D. Patrick, R. Gilbert Moore, Fred Koether, and John S. Piech. Honorary directors are Brig. Gen. George G. Eddy, commanding general of White Sands Proving Ground, and Capt. Philip D. Quirk, commander of the U. S. Navy Ordnance Missile Test Station, WSPG.

**New York.** New officers are Michael J. Samek, President; Thomas Reinhardt, Vice-President; W. Dorwin Teague, Jr., Secretary; and Robert J. Thompson, Jr., Treasurer.

On January 29 William Wright of Reaction Motors, Inc., talked to a group of about 40 members and guests at the Engineering Societies Building on "Patents and the Rocket Engineer." A film from the Glenn L. Martin Company on the Viking #1 and #2 firings was shown.

**Northern California.** C. C. Ross of Aerojet-General Corporation, Azusa, spoke on January 14 on "Combustion Instability in Rocket Motors" at a dinner meeting in San Francisco. New officers are William J. Barr, President; M. A. Pino, Vice-President; John S. Amneus, Secretary; and Carl W. Messinger, Jr., Treasurer. Directors are A. J. Eggers, Marjorie Evans, S. S. Sorem, Austin Bryant, and E. A. Quarterman.

**Southern California.** Dr. Leo Stoolman, a member of the propulsion research group at Hughes Aircraft Company, Culver City, spoke on "Ramjets" at the December 17 meeting. New officers are H. S. Seifert, President; C. M. McCloskey, Vice-President; W. D. Crossland, Secretary-Treasurer. The Board of Directors includes S. K. Hoffman, D. I. Baker, T. F. Dixon, R. D. Geckler, R. F. Gompertz, B. T. Morris, and W. L. Rogers.

### ARS SECTION PRESIDENTS

| | |
|---|---|
| *Alabama* | GEORGE HENDERSON<br>Redstone Arsenal |
| *Arizona* | ANTHONY R. TOCCO<br>Hughes Aircraft Co. |
| *Chicago* | KENNETH H. JACOBS<br>American Machine & Foundry Co. |
| *Cleveland-Akron* | DARRELL C. ROMICK<br>Goodyear Aircraft Corp. |
| *Detroit* | LAWRENCE M. BALL<br>Chrysler Corp. |
| *Florida* | K. K. McDANIEL<br>Boeing Airplane Co. |
| *Indiana* | J. M. BOTJE<br>Purdue University |
| *Maryland* | IVAN E. TUHY<br>Glenn L. Martin Co. |
| *National Capital* | JAMES R. PATTON, JR.<br>Office of Naval Research |
| *New Mexico-West Texas* | FRANK L. KOEN, JR.<br>White Sands Proving Ground |
| *New York* | MICHAEL J. SAMEK<br>American Electro-Metal Corp. |
| *Niagara Frontier* | WILLIS SPRATTLING<br>Bell Aircraft Corp. |
| *Northeastern New York* | GEORGE E. MOORE<br>General Electric Co. |
| *Northern California* | WILLIAM J. BARR<br>Detroit Controls Corp. |
| *Southern California* | H. S. SEIFERT<br>Calif. Inst. of Tech. |

DR. RICHARD W. PORTER, ARS VICE-PRESIDENT, DISCUSSES FLORIDA SECTION ACTIVITIES PRIOR TO A MEETING HE ADDRESSED RECENTLY. LEFT TO RIGHT ARE MAJOR PRENTICE B. PEABODY, VICE-PRESIDENT; 1ST LT. THEODORE A. DEBACKER, SECRETARY-TREASURER; DR. PORTER; AND KEITH K. MCDANIELS, PRESIDENT OF THE SECTION.

# Book Reviews

**H. S. SEIFERT, California Institute of Technology, *Associate Editor***

**Introduction to Aeronautical Dynamics,** by M. Rauscher, John Wiley & Sons, Inc., New York, N. Y., 1953, 664 pp. $12.

Reviewed by H. J. STEWART
California Institute of Technology
Jet Propulsion Laboratory

This book presents essentially the content of a group of courses which Prof. Rauscher taught for many years in the Aeronautical Engineering Department of the Massachusetts Institute of Technology. With this background the material obviously has the advantage of having been used many times; thus the methods of presentation and the choice of examples are well suited to the subject.

The material covered in the book consists of various topics in solid dynamics, such as motion of particles and of rigid bodies and vibrations, and topics in fluid mechanics, such as one-dimensional compressible-flow theory, and two-dimensional perfect-fluid theory and the elements of viscous-fluid theory, which are required as a background for the discussion of the dynamics of aircraft. The subject material is carried far enough to discuss two-dimensional airfoil theory, the Prandtl monoplane-wing theory and vibrations of systems with more than one degree of freedom; however, the treatment stops short of the final goal—the dynamics of airplanes in flight.

Since the subject matter covered is intended for presentation to undergraduate classes, Professor Rauscher has wisely limited the mathematical methods to the most elementary level required. In the treatment of two-dimensional airfoil theory he introduces and uses the theory of complex variables and conformal transformation in order to discuss Joukowsky airfoils and von Kármán-Treftz airfoils. He also introduces the elements of Fourier analysis in his treatment of vibrations. With these two exceptions the mathematical level is only that which should have been acquired by any undergraduate junior student.

**The Complete Book of Outer Space,** J. Logan, Editor, Maco Magazine Corp., New York, N. Y., 1953, 144 pp. $0.75.

Reviewed by A. J. ZAEHRINGER
Thiokol Chemical Corporation, Elkton, Md.

Despite the pretentious title of this magazine-style book, it represents a simple and concise picture of rocketry. Willy Ley presents a conventional picture of rocket history and in a later section discusses the possibilities of life beyond our solar system. Dr. von Braun has two sections dealing with the space station and urging standardization and immediate starts for an orbiting rocket. A very optimistic section on space medicine is discussed by Dr. Heinz Haber which essentially is a condensation of his recent book, "Man in Space." A section on space suits is given by Dr. Menzel of the Harvard Observatory in which he visualizes the space suit as a sort of manned automobile tire. Robert Haviland of the GE Project Hermes gives an interesting picture of multistage rocket development in the Bumper program. One of the most interesting and longest sections is the history of rocket motors by James Wyld. Developments from the Paulet engine to the author's experiences with early RMI rocket motors are presented. Other sections of the book are: Legal Aspects of Space Travel, by Oscar Schacter of the UN; Exploitation of the Moon, by Hugo Gernsbach; Interstellar Flight, by Dr. Leslie Shephard, a director of the British Interplanetary Society; and two sections by the editor, The Spaceship in Science Fiction, and the Flying Saucer Myth. Also presented are "charts" of Moon and Mars flights, space-ship timetables, temperatures of the planets, and a space-travel dictionary.

The publishers are to be commended for presenting an interesting book of semi-technical caliber at low cost. Although it is paper bound, the printing and illustrations (almost 200) are excellent. However, many of the illustrations of science-fiction type could have been weeded out together with many irrelevant illustrations, viz., a drawing of the F-99 Bomarc in the section on high-altitude research. Nevertheless, the general technical accuracy of the material is excellent, and the authors reflect a highly optimistic outlook toward manned space flight. Although somewhat scrambled in method of presentation, this book can be expected to give many persons a fairly accurate picture of space flight.

**Flying Saucers,** by D. H. Menzel, Harvard University Press, Cambridge, Mass., 1953, 319 pp. $4.75.

Reviewed by J. E. FROELICH
California Institute of Technology
Jet Propulsion Laboratory

Based on his own experience with optical displays in the atmosphere, Professor Menzel presents an interesting and plausible explanation of the flying-saucer phenomena. History is apparently studded with recordings of public consternation at strange visitors from the skies, and this book includes a fascinating summary of these historical events.

Flying Saucers is more than a historical summary. An adequate description of the physical concepts which explain optical displays in the skies is also given in the book. In addition, the author outlines some good fundamental rules for evaluating critically observations of any kind. Professor Menzel unfortunately makes the same error he criticizes in other treatments of the subject. Throughout the book he forces the conclusion that the flying-saucer phenomena arise from natural causes and are certainly not the result of interplanetary vehicles. It is understandable that the author is more willing to believe in optical tricks than in space ships, but his analysis of flying saucers presents no new facts to "prove" either conclusion; rather it falls into the category of hypothesis, as do other writings on this subject. Otherwise it is an excellent book, one toward which engineers and scientists will feel sympathetic.

The illusions of the atmosphere as described in this book are enough to make one cautious in accepting any explanation of flying saucers on the basis of the observations that have been reported to date.

The examples which are used to illustrate the theory are unusual for college texts and are especially suitable for modern students interested in aeronautics or in jet propulsion. For example, the author considers the motion of a rocket in a planetary gravitational field as an example in particle dynamics. He also considers the theory of a ramjet, in a low-speed zero-drag approximation, as an example in one-dimensional fluid flow. Again, in the section on dynamics of rigid bodies, he has an introduction of the effects of rotating propellers on the motion of an airplane in a spin.

**Mechanical Vibrations,** by W. T. Thomson, Prentice-Hall, Inc., New York, N. Y., 1953, 252 pp. $6.

Reviewed by R. H. BODEN
North American Aviation

This textbook covers in detail second-order linear systems. Many examples are presented of such systems and their electrical analogs, both alone and in combination as many-degree-of-freedom systems. Since it is presented clearly and in great detail, this book is a worth-while reference for the practicing engineer, although the material is not new.

The objective of presenting the fundamentals of vibration theory and providing a general background for advanced study in the field is achieved. The author does not stray from a presentation of the fundamentals of second-order linear systems. Some discussion of first-, third-, and higher-order systems, some digression into nonlinear types, to define more clearly the limits of application of the fundamental information and also some further discussion of stability, which is mentioned only briefly, would enhance the value of the text without overstepping the bounds of an introductory course in vibration analysis. Another worth-while addition would be a more extensive discussion of transient phenomena in simple systems and their relationship to steady-state performance. In general, the book appears limited but quite satisfactory as the basis

of an introductory course in vibration analysis, particularly for the mechanical engineer.

**Information Theory,** by S. Goldman, Prentice-Hall, Inc., New York, N. Y., 1953, 385 pp. $9.

Reviewed by R. M. Stewart and E. Rechtin
California Institute of Technology
Jet Propulsion Laboratory

This book is one of the first published attempts to rewrite the work of Shannon and Wiener in another author's language for textbook purposes. Because of this unique status, if for no other reason, the book will probably be very popular and certainly should be examined by all specialists in the field. These reviewers, however, were disappointed in certain aspects of the book. In particular, the rewriting of Shannon's work did not seem as successful as the original work, and that of Wiener is considerably less satisfactory than that of Bode and Shannon (*Proc. IRE*, vol. 38, 424, April 1950). The author expresses unnecessary pessimism when he concludes that "the actual design of an optimum filter in any practical case is invariably laborious."

Goldman's language differs from Shannon's in several ways. Various unusual words (quadiva, liniva, quadratic content, linear content, binits) are used for old concepts in lieu of well-established words, and some old words (random noise, ergodic) are given new meanings. Goldman's definition of "information received" is different from Shannon's in a way which may lead to considerable confusion. In the last chapter, the author delves into speculative theory of his own, usually a source of misunderstanding in a book written for instructional purposes.

The author is to be commended, however, for his effort to clear the air in a rapidly growing field; but these reviewers feel that the effort was not particularly successful.

**Meteorological Instruments,** third edition, revised, by W. E. K. Middleton and A. F. Spilhaus, University of Toronto Press, Toronto, Canada, 1953, 286 pp. $11.50.

Reviewed by B. Helfand
North American Instruments, Inc.
Altadena, Calif.

Instrumentation for the meteorologist includes an unusual assortment of devices and techniques designed to enable him to specify the weather. The devices range in complexity from a simple mercury and glass thermometer to a search radar, and it is with these instruments that he must make measurements for use in weather analysis, forecasting, and climatological work.

The book, now in its third edition, describes the state of the art as practiced on this continent and in most of the English-speaking countries and is based on Mr. Middleton's lecture course given for a number of years to graduate students in meteorology at the University of Toronto. Dr. Spilhaus, Dean of the Institute of Technology, University of Minnesota,

appears as co-author for the first time in this edition. He is well known in this country for his contributions in the field of meteorological instruments.

The book is written in an easy-to-read conversational style and is well illustrated. The content is largely descriptive, typical instruments and their usage being covered in considerable detail. Analytical treatment is provided where necessary to give an understanding of static and dynamic performance. Many references are provided to lead the reader to original sources of information and commercial sources of particular instrumentation. War-time developments in the application of radio and radar to upper-air-measurement problems constitute much of the new material added in this edition.

The introductory chapter deals with the special properties and requirements for meteorological instruments. Five subsequent chapters cover the measurement of atmospheric pressure, temperature, humidity, precipitation, and wind and ground stations. One chapter is devoted to sunshine recorders, one to instruments for investigating clouds, and two to the investigation of the upper air. The final chapter deals with special assemblies and systems including portable, mobile, and automatic weather stations.

This book is the only comprehensive source of information on meteorological instruments written in English; it is highly recommended as a text for meteorology students at both the undergraduate and graduate levels and also as a reference for practicing meteorologists and those in other fields with an interest in temperature, pressure, and flow measurements.

**Principles of Automatic Controls,** by F. E. Nixon, Prentice-Hall, Inc., New York, N. Y., 1953, 409 pp. $9.35.

Reviewed by R. J. PARKS
California Institute of Technology
Jet Propulsion Laboratory

This book was written as an outgrowth of a company training course given by the author at the Glenn L. Martin Company. In the author's words, it is intended as a reference, self-study, or undergraduate-level text. A very minimum of background training is assumed. As stated in the preface, a first-year course in physics is assumed and a course in electrical circuits would be helpful but not essential.

Consistent with this premise, the book starts out in a fairly elementary manner, discussing linear differential equations, the Laplace transform, block-diagram notation, and the theory and application of the Nyquist criteria. These topics are discussed from the applied standpoint, with a minimum of mathematical rigor. A considerable number of simple examples are discussed and, in addition, problems are included at the end of each chapter.

The book then discusses other methods of servo analysis such as the inverse open-

loop, transfer-function method, the log-decibel method, and the root-locus technique. These subjets are well discussed from the standpoint of one unfamiliar with the field. These techniques and that of the Nyquist criteria are discussed completely enough to point out the various pitfalls which sometimes occur if these procedures are applied blindly without a complete understanding of their development.

Several chapters are devoted to giving the reader a feeling for the problems encountered in the design of feedback systems together with typical solutions to these problems. Sections are included on numerical integration and the techniques of automatic computing, both analog and digital, as well as their application to servo design.

The important subject of noise and its effects on closed-loop systems is discussed only briefly and qualitatively. Six appendixes include information for reference including the Runge-Kutta integrator technique and a rather complete table of Laplace transforms.

It is the opinion of the reviewer that the book is well written and accomplishes its stated goals. It is not a high-level technical book, and many readers will want to skim over the first few chapters, but it would make excellent introductory reading for persons whose experience in the field of controls is limited.

**Weight Strength Analysis of Aircraft Structures,** by F. R. Shanley, McGraw-Hill Book Co., Inc., New York, N. Y., 1952, 394 pp. $8.50.

Reviewed by M. L. Williams
California Institute of Technology

Professor Shanley's book represents the first attempt to gather together in a comprehensive treatment a rational method for evaluating the interaction of weight and strength in aircraft structures. Analytical expressions are developed for the weights as a function of the design parameters and the strength level, or structural index. As opposed to solely statistical-trend data, the analytical formulation permits a greater understanding of the weight breakdown and contributes to more efficient design. In particular it is shown that the minimum structural weight can be separated into two parts, one depending on the loads, material properties, and load transmission path, and the other upon the size and geometrical arrangement.

The difficulties involved in the direct application of the material to aircraft design stem from the proper evaluation or prediction of certain constants in the analytical expressions which in many cases require additional statistical data.

The book is separated into three parts: (I) Principles of Optimum Structural Design; (II) Structural Weight Equations, covering shell structures and high-aspect ratio, thick- and thin-walled wings with and without sweepback; and (III) Material Properties and Behaviors, a somewhat different, although related, subject dealing with elastic and inelastic effects particularly in column behavior.

It is believed that one of the major contributions of the volume is to present the problem and recommend a formulation upon which to base future refinements and advances.

# Technical Literature Digest

M. H. SMITH and M. H. FISHER

The James Forrestal Research Center, Princeton University, Princeton, N. J.

## Jet Propulsion Engines

**Jet Propulsion for Converti-planes,** by David C. Prince, *American Helicopter*, vol. 32, Oct. 1953, pp. 6–9, 13–16.

**Supersonic Ram-jet Performance,** by J. Lukasiewicz, *Aircraft Engineering*, vol. 25, Oct. 1953, pp. 298–306.

**Small Turbines—The Heart of Modern Aircraft Accessory Power Systems,** by L. W. Bieuer and R. L. McManus, *Soc. Automotive Engrs., Prepr.* no. 159, Sept. 1953, 9 pp., 8 figs.

**The Performance of Some Typical Turbo-jet Engine Exhaust Systems with Particular Reference to the Effects of Swirl,** by P. F. Ashwood and P. J. Fletcher, *Gt. Brit. Aero. Res. Counc. Curr. Pap.* no. 130 (formerly ARC Tech. Rep. No. 14736, *National Gas Turbine Est. Rep. no.* R. 112), 1953, 13 pp.

**Compressor Testing at Ansty. (Armstrong Siddeley Motors, Ltd.),** *Aeroplane*, vol. 85, Nov. 13, 1953, pp. 658–663.

**Effect of a Turbojet Engine on the Dynamic Stability of an Aircraft,** by Hans C. Vetter, *J. Aero. Sci.*, vol. 20, Nov. 1953, pp. 797–798.

**Turboprops, What Europe Has Learned,** by James Hay Stevens, *American Aviation*, vol. 17, Nov. 13, 1953, pp. 28–29.

**A Method of Calculating the Performance of Turbojets and Turboprops, Useful Expressions for Research in Propulsion and in the Mechanics of Flight,** by Gaspar Santangelo, *L'Aerotecnica*, vol. 33, June 1953, pp. 204–219, 230 (in Italian).

**On Some Possible Development Trends in Aircraft Engines,** by Lorenzo Poggi, *L'Aerotecnica*, vol. 33, June 1953, pp. 199–204 (in Italian).

**Control for Hypothetical Ramjet Must Manage 300,000 hp, Fit in 4 cu. Ft.,** by J. C. Wise, *SAE Journal*, vol. 61, Nov. 1953, pp. 85–86.

**Some Stall and Surge Phenomena in Axial-Flow Compressors,** by Merle C. Huppert and William A. Benser, *J. Aero. Sci.*, vol. 20, Dec. 1953, pp. 835–845.

**Fairchild Monocoque Turbojet,** by Randolph Hawthorne, *Aviation Age*, vol. 20, Dec. 1953, pp. 30–31.

**Design for Turbojet Simplicity,** by A. L. Ervin, *Aviation Age*, vol. 20, Dec. 1953, pp. 28–29.

**A Slipstream View of Aircaft Propulsion, 1903–1953,** by Frank W. Caldwell, *Aero. Engng. Rev.*, vol. 12, Dec. 1953, pp. 108–117, 131–132.

**The Compound Engine,** by C. Casci, *L'Aerotecnica*, vol. 33, Aug. 1953, pp. 263–269 (in Italian).

**Pressure Ratios for Aero-Engines,** by J. M. Stephenson, *Aircraft Engng.*, vol. 25, Dec. 1953, p. 371.

**A Fuel-Air Turbine Starter,** *Aeroplane*, vol. 85, Dec. 11, 1953, pp. 796–798.

**Jet Ignition Developments Moving Fast,** by Joseph S. Murphy, *American Aviation*, vol. 17, Jan. 4, 1954, pp. 44–45.

**The Case for the By-Pass Jet Engine,** by James Hay Stevens, *American Aviation*, vol. 17, Jan. 4, 1953, pp. 28–30.

**Use of Electric Analogs for Calculation of Temperature Distribution of Cooled Turbine Blades,** by Herman H. Ellerbrock, Jr., Eugene F. Schum, and Alfred J. Nachigall, *NACA TN* 3060, Dec. 1953, 116 pp.

**Some Factors Pertaining to the Use of Air Breathing Propulsion for the Acceleration of High Altitude Sounding and Other Long Range Ballistic Missiles,** by J. W. Luecht, *Soc. Automotive Engr. Prep.*, No. 145, Sept. 1953, 5 pp., 9 figs.

## Rocket Propulsion Engines

**The Effect of Variation of Propellant Density on Rocket Performance,** by Jack Lorell and Albert Hibbs, *Calif. Inst. Tech. Jet Prop. Lab. Rep.* no. 20–66, July 1952, 33 pp.

**Some Limiting Factors of Chemical Rocket Motors,** by W. N. Neat, *J. Brit. Interplan. Soc.*, vol. 12, Nov. 1953, pp. 249–274.

**Propulsion Efficiency of a Rocket,** by Enio Mattioli, *L'Aerotecnica*, vol. 33, Aug. 1953, pp. 270–274 (in Italian).

**Flow in Injection Orifices, Application to Rocket Engines,** by R. Kling and R. Leboenf, *Recherche Aéron.*, no. 35, Sept.-Oct. 1953, pp. 35–41 (in French).

## Heat Transfer and Fluid Flow

**The Coriolis Effect,** by Paul E. Wylie, *J. Roy. Aeron. Soc.*, vol. 57, Oct. 1953, pp. 655–658.

**The Fluid Mechanics of Detonation Waves,** by L. G. Dawson, *J. Roy. Aeron. Soc.*, vol. 57, Oct. 1953, pp. 618–626.

**An Analysis of the Air Flow Through the Nozzle Blades of a Single Stage Turbine,** by I. H. Johnston, *Gt. Brit. Aero. Res. Counc. Curr. Pap.* no. 131 (formerly *ARC Tech. Rep.* no. 14300, *National Gas Turbine Est. Memo.* no. M. 108), 1953, 8 pp., 10 figs.

**The Design and Testing of Supersonic Nozzles,** by R. Harrop, P. I. F. Bright, J. Salmon, and M. J. Caiger, *Gt. Brit. Aero. Res. Counc. Reps. and Memo.* no. 2712 (formerly *ARC Tech. Reps.* nos. 12114, 13383; *Royal Aircraft Est. Reps. Aero.* 2293 2293a), 1953, 40 pp.

**Turbulence in Supersonic Flow,** by Leslie S. G. Kovasznay, *J. Aero. Sci.*, vol. 20, Oct. 1953, pp. 657–674, 682.

**Recent Developments in Convective Heat Transfer with Special Reference to High-Temperature Combustion Chambers,** by Martin Summerfield, *Heat Transfer, A Symposium*, Univ. of Mich., 1952, pp. 151–171, 25 refs.

**Evaporation and Spreading of Isooctane Sprays in High-Velocity Air Streams,** by Donald W. Bahr, *NACA RM* E53I14, Nov. 1953, 35 pp.

**Air Cooling Methods for Gas Turbine Combustion Systems,** by F. J. Bagley, *Gt. Brit. Aero. Res. Counc. Curr. Pap.* no. 133 (formerly *ARC Tech. Rep.* 14648, *National Gas Turbine Est. Rep.* R. 101), 1953, 34 pp.

**Cavitation Tests on Hydrofoils in Cascade,** by Fukusaburo Numachi, *Trans. ASME*, vol. 75, Oct. 1953, pp. 1257–1269.

**On the Propagation and Structure of the Blast Wave, Part I,** by Akira Sakurai, *J. Phys. Soc. of Japan*, vol. 8, Sept.-Oct. 1953, pp. 662–669.

**Calculation of Transpiration Cooled Gas-Turbine Blades,** by J. N. B. Livingood and E. R. G. Eckert, *Trans. ASME*, vol. 75, Oct. 1953, pp. 1271–1278.

**On the Evaluation of the Accuracy of the Coefficient of Discharge in the Basic Flow-Measurement Equation,** by A. L. Jorissen, *Trans. ASME*, vol. 75, Oct. 1953, pp. 1323–1326.

**A Rapid Method for the Determination of the Thermal Conductivity of Organic Liquids for Use in Heat Transfer Calculations,** by S. Baxter, H. A. Vodden, and Davies, *J. Appl. Chemistry*, vol. 3, part 10, Oct. 1953, pp. 477–480.

**Local Heat-Transfer Coefficients on Surface of an Elliptical Cylinder, Axis Ratio 1:3, in a High-Speed Air Stream,** by R. M. Drake, Jr., R. A. Seban, and D. L. Doughty, and S. Levy, *Trans. ASME*, vol. 75, Oct. 1953, pp. 1291–1302.

**New Aspects of Natural-Convection, Preliminary Study of Effect of Frictional Heating,** by Simon Ostrach, *Trans. ASME*, vol. 75, Oct. 1953, pp. 1287–1290.

**Flow Through Nozzles and Related Problems of Cylindrical and Spherical Waves,** by Yu Why Chen, *Comm. Pure Appl. Math.*, vol. 6, May 1953, pp. 179–229.

**On the Solution of the Differential Equation Occurring in the Problem of Heat Convection in Laminar Flow Through a Tube,** by Milton Abramowitz, *J. Math. and Physics*, vol. 32, July–Oct. 1953, pp. 184–187.

**Note on the Prandtl Number for Dissociated Air,** by C. Frederick Hansen, *J. Aero. Sci.*, vol. 20, Nov. 1953, pp. 789–790.

**Measurement of the Profile Drag of Compressor and Turbine Cascades and the Effect of Wakes in Exciting Vibration,** by J. M. Stephenson, *J. Roy. Aeron. Soc.*, vol. 57, Nov. 1953, pp. 722–725.

**Evidences of an Inherent Error in Measurement of Total-Heat Pressure at Supersonic Speeds,** by James S. Murphy, *Aero. Engng. Rev.*, vol. 12, Nov. 1953, pp. 47–51.

**Analogy Between Mass and Heat Transfer With Turbulent Flow,** Edmund E. Callaghan, *NACA TN* 3045, Oct. 1953, 19 pp.

EDITOR'S NOTE: This collection of references is not intended to be comprehensive, but is rather a selection of the most significant and stimulating papers which have come to the attention of the contributors. The readers will understand that a considerable body of literature is unavailable because of security restrictions. We invite contributions to this department of references which have not come to our attention, as well as comment on how the department may better serve its function of providing leads to the jet propulsion applications of many diverse fields of knowledge.

**The Mechanics of Film Cooling,** by Eldon L. Knuth, *Calif. Inst. Tech. Jet Prop. Lab. Memo.* 20–85, Sept. 1953, 108 pp.

**Preliminary Investigation of a New Type of Superonic Inlet,** by Antonio Ferri and Louis M. Nucci, *NACA Rep.* 1104 (formerly *TN* 2286), 1952, 19 pp.

**The Measurement of Heat Transfer and Skin Friction at Supersonic Speeds, Pt. III. Measurements of Overall Heat Transfer and of the Associated Boundary Layers on a Flat Plate at $M_1$ = 2.43,** by R. J. Monaghan and J. R. Cooke, *Gt. Brit. Aero. Res. Counc. Curr. Pap.* no. 139 (formerly *ARC Tech. Rep.* 15348, *Royal Aircraft Est. Tech. Note No. Aero.* 2129), 1953, 38 pp.

**The Measurement of Heat Transfer and Skin Friction at Supersonic Speeds, Part IV. Tests on a Flat Plate at M = 2.82,** by R. J. Monaghan and J. R. Cooke, *Gt. Brit. Aero. Res. Counc. Curr. Pap.* no. 140 (formerly *ARC Tech. Rep.* 15400, *Royal Aircraft Est. Tech. Note No. Aero.* 2171), 1953, 27 pp.

**Analogy Among Heat, Mass, and Momentum Transfer,** by Richard F. Kayser, *Ind. Engng. Chem.*, vol. 45, Dec. 1953, pp. 2634–2636.

**Heat Transfer in Forced Convection Film Boiling,** by LeRoy A. Bromley, Norman R. LeRoy, and James A. Robbers, *Ind. Engng. Chem.*, vol. 45, Dec. 1953, pp. 2639–2646.

**Velocity Distribution Between Parallel Plates,** by W. G. Schlinger and B. H. Sage. *Ind. Engng. Chem.*, vol. 45, Dec. 1953, pp. 2636–2639.

**Sweat Cooling, a Review of Present Knowledge and Its Application to the Gas Turbine,** by P. Grootenhuis, and N. P. W. Moore, *Iron and Steel Institute. Symposium on High Temperature Materials for Gas Turbine,* 1952, pp. 281–289, 47 ref.

**Surface Temperature and Pressure Distributions on a Circular Cylinder in Supersonic Cross Flow,** by L. W. Walter and H. H. Lange, *Naval Ord. Lab. NAVORD Rep.* 2854 (*Aeroballistic Res. Rep.* no. 180), June 1953, 10 pp.

**Flow Properties of Strong Shock Waves in Xenon Gas as Determined for Thermal Equilibrium Conditions,** by Alexander P. Sabol, *NACA TN* 3091, Dec. 1953, 29 pp.

**On the Stability of Isotropic Turbulence,** by Robert Betchov, *Maryland University. Institute for Fluid Dynamics and Applied Mathematics, Tech. Rep.* BT-15, Sept. 1953, 26 pp.

**Jets,** by M. Z. Krzywoblocki, *Naval Ord. Test Sta. Tech. Memo.* no. 1576, Sept. 1953, 83 pp.

## Combustion

**Application of an Electro-Optical Two-Color Pyrometer to Measurement of Flame Temperature for Liquid Oxygen-Hydrocarbon Propellant Combination,** by M. F. Heidmann and R. J. Priem, *NACA TN* 3033, Oct. 1953, 39 pp.

**Practical Application of Engine Flame Temperature Measurements,** by G. H. Millar, O. A. Uyehara, and P. S. Myers, *Soc. Automotive Engrs. Prepr.* no. 196, Nov. 1953, 9 pp. 24 figs.

**Development of an Improved Automotive Diesel Combustion System,** by Bruno Loeffler, *Society of Automotive Engrs. Prepr.* no. 188, Nov. 1953, 16 pp. 47 figs.

**Studies on Carbon Formation and Reaction in Acetylene,** by Jerry D. Frazee and Robbin C. Anderson, *Texas Univ. Dept. Chemistry Combustion Kinetics Proj. Tech. Rep.* no. 8, Aug. 1953, 17 pp.

**Burning Velocity Determinations. Part 10. Flame Propagation Along Horizontal**

**Tubes,** by M. F. Hoare and J. W. Linnett, *Trans. Faraday Soc.*, vol. 49, pt. 9, Sept. 1953, pp. 1038–1049.

**Investigation of Flame Temperatures in a Single-Cylinder Spark-Ignition Engine,** by J. H. Potter, and E. B. Dillaway, *Trans. ASME*, vol. 75, Oct. 1953, pp. 1311–1321.

**Combustion of a Low-Volatility Fuel in a Turbojet Combustion Chamber-Effects of Fuel Vaporization,** by V. V. Holmes, A. J. Pahnke, O. A. Uyeharo, and P. S. Myers, *Trans. ASME*, vol. 75, Oct. 1953, pp. 1303–1310.

**Temperature and Gas-Analysis Surveys in the Combustion Zone of a Gas-Fired Gas-Turbine Combustor,** by K. L. Rieke, *Trans. ASME*, vol. 75, Oct. 1953, pp. 1233–1239.

**The Slow Combustion of Cyclopropane. II. Analytical Results and Mechanism,** by A. C. McEwan and C. F. H. Tipper, *Proc. Roy. Soc.*, vol. 220A, Nov. 10, 1953, pp. 266–277.

**Effect of Diffusion Processes and Temperature on Smoking Tendencies of Laminar Diffusion Flames,** by Rose L. Schalla, *NACA RM* E52I22, Dec. 1953, 23 pp.

**Formation and Combustion of Smoke In Bunsen Flames,** by Thomas P. Clark, *Ind. Engng. Chem.*, vol. 45, Dec. 1953, pp. 2785–2789.

**Thermodynamic Charts of Combustion Products,** by Ernesto Macioce, *L'Aerotecnica*, vol. 33, Aug. 1953, pp. 288–290 (in Italian).

**Method of Electronic Statistical Measurement For the Study of Combustion Phenomena In Reciprocating Engines,** by R. Vichnievsky, and J. Weissmann, *Recherche Aéron.*, no. 35, Sept.–Oct. 1953, pp. 423–435 (in French), 36 references.

**A Note on Organ-Pipe Resonance in Ducted Burners,** by J. C. Truman and N. J. Lipstein, *J. Aero. Sci.*, vol. 20, Dec. 1953, pp. 846–847.

**Effects of Additives on Pressure Limits of Flame Propagation of Propane-Air Mixtures,** by Frank E. Belles and Dorothey M. Simon, *NACA RM* E53I29, Dec. 1953, 36 pp.

## Fuels, Propellants, and Materials

**Stability of Hydrazine in Liquid Ammonia,** by John A. Krynitsky and Homer W. Carhart, *Naval Res. Lab. Rep.* no. 4219, Sept. 1953, 16 pp.

**Hydrazine,** by Lawrence P. Lessing, *Sci. Amer.*, vol. 189, July 1953, pp. 30–33.

**Hydrogen Peroxide, Part One,** by W. C. Schumb, C. N. Satterfield, and R. L. Wentworth, *Mass. Inst. Tech. Depts. Chemistry and Chemical Engng., Div. Indus. Cooperation Rep.* no. 42, Sept. 1953, 247 pp.

**Hydrocarbon and Nonhydrocarbon Derivatives of Cyclopropane,** by Vernon A. Slabey, Paul H. Wise, and Louis C. Gibbons, *NACA Rep.* 1112, 1953, 18 pp.

**Formation, Stability and Crystal Structure of the Solid Aluminum Suboxides, $Al_2O$ and AlO,** by Michael Hoch and Herrick L. Johnston, *Ohio State Univ. Res. Found. Tech. Rep.* 280-10, Aug. 1953, 6 pp.

**Effective Thermal Conductivities of Magnesium Oxide, Stainless Steel, and Uranium Oxide Powders in Various Gases,** by C. S. Eian and R. G. Deissler, *NACA RM* E53G03, Oct. 1953, 18 pp.

**Hydrogen Peroxide. Part 4,** by W. C. Schumb, C. N. Satterfield and R. L. Wentworth, *Mass. Inst. Tech. Dept., Chem. and Chemical Engng., Div. Indus. Cooperation, Rep.* no. 45, Nov. 1953, 194 pp.

**Developing Aviation Fuels and Lubricants,** by C. B. Davies, *J. Roy. Aeron. Soc.*, vol. 57, Nov. 1953, pp. 700–708.

**Velocity of Sound in Liquid Propellants,** by Robert S. Wicks, Irving L. Odgers, and Rollow S. Pickford, Jr., *Calif. Inst. Tech., Jet Prop. Lab., Memo.* 20-84, July 1953, 11 pp.

**Properties, Production and Uses of Hydrazine,** by James E. Troyan, *Ind. Engng. Chem.*, vol. 45, Dec. 1953, pp. 2608–2612.

**Volumetric Behavior of Nitric Acid,** by H. H. Beamer, W. H. Corcoran, and B. H. Sage, *Ind. Engng. Chem.*, vol. 45, Dec. 1953, pp. 2699–2704.

**Hydrogen Peroxide. Part 2,** by W. C. Schumb, C. N. Satterfield, and R. L. Wentworth, *Mass. Inst. Tech., Depts. Chem. and Chemical Engng., Rep.* 43, Dec. 1953, 232 pp.

**The Anelasticity of Molybdenum. Final Report Covering the Period May 1, 1950–July 14, 1953 and 16th Quarterly Report Covering the Period March 1–July 14, 1953,** *Battelle Mem. Inst.*, 43 pp.

**The Improvement of the Ductility of Molybdenum Weldments, Summary Report Covering the Period Aug. 1, 1951–July 14, 1953 and 16th Quarterly Report Covering the Period March 1–July 14, 1953,** *Battelle Mem. Inst.*, 13 pp.

## Physical-Chemical Topics

**Minimum Spark-Ignition Energies of 12 Pure Fuels at Atmospheric and Reduced Pressure,** by Allen J. Metzler, *NACA RM* E53H31, Oct. 1953, 28 pp.

**The Oxidation of Carbon Monoxide in the Presence of Ozone,** by David Garvin, *Princeton Univ. James Forrestal Res. Cent., Chemical Kinetics Proj., Tech. Rep.* no. 5, Sept. 1953, 22 pp.

**The Reaction Between Nitric Oxide and Ammonia On Supported Catalysts,** by John R. Kelso, *Aberdeen Proving Ground, Ballistic Res. Lab. Memo. Rep.* no. 699, July 1953, 15 pp.

**Thermodynamic Properties of Boron and Aluminum Compounds.** *Progress Rep.* no. 2, *Pennsylvania State Univ., Dept. Chemistry,* Jan. 1–Sept. 30, 1953, 50 pp.

**The Viscosity of Vapor Mixtures of Hydrogen Peroxide and Water,** by C. N. Satterfield, R. L. Wentworth, and S. T. Demetriades, *Mass. Inst. Tech., Dept. Chemical Eng., Div. Indus. Cooperation, Rep.* no. 39, Aug. 1953, 36 pp.

**Kinetics of the Initial Reaction Between an Aldehyde and Hydrogen Peroxide In Aqueous Solution,** by C. N. Satterfield, and L. C. Case, *Mass. Inst. Tech., Dept. Chem. Eng., Div. Indus. Cooperation, Rep.* no. 40, Aug. 1953, 19 pp.

**A Mollier Chart for Moisture-Saturated Air,** H. Reichert, *Aircraft Engng.,* vol. 25, Oct. 1953, pp. 321–323.

**Isotherms and Thermodynamic Functions of Ethane at Temperatures between 0°C and 150°C and Pressures up to 200 atm.,** by A. Michaels, W. vanStraaten, and J. Dawson, *Maryland Univ. High Pressure Lab., Tech. Rep.* no. 1, Oct. 1953, 1 pp., 11 tab.

**The Thermal Decomposition of Organic Nitrates. III. The Effect of Additives on the Thermal Decomposition of Ethyl Nitrate,** by Joseph B. Levy, *Naval Ord. Lab., NAVORD Rep.* 2897, Aug. 1953, 20 pp.

**The Solubility of Oxygen in Nitric Acid Mixtures,** by Glenn D. Robertson, Jr., David M. Mason, and William H. Corcoran, *Calif. Inst. Tech. Jet Prop. Lab. Prog. Rep.* no. 20-176, Aug. 1953, 8 pp.

**The Heats of Mixing of Some Aromatic Hydrocarbons and Phtholates,** by P. Meares, *Trans. Faraday Soc.,* vol. 49, Oct. 1953, pp. 1133–1139.

**The Oxidation of Hydrocarbons, II. Examination of the Products of the Vapour Phase Oxidation of n-Heptane and of Methylcyclohexane,** by F. H. Garner, R. Long, and R. G. Temple, *Trans. Faraday Soc.,* vol. 49, Oct. 1953, pp. 1193–1197.

**Energy Transfer in Hydrocarbon Solutions,** by E. J. Bowen and B. Brocklehurst, *Trans. Faraday Soc.,* vol. 49, Oct. 1953, pp. 1131–1133.

**Ionization in Solutions of Nitrogen Dioxide in Nitric Acid from Optical Absorbance Measurements,** by Scott Lynn, David M. Mason, and W. H. Corcoran, *Calif. Inst. Tech., Jet Prop. Lab. Prog. Rep.* 20-175, Sept. 1953, 11 pp.

**An Approximate Theory of Inelastic Collisions,** by James F. Hornig and J. O. Hirschfelder, *Wisconsin Univ., Naval Res. Lab., Rep.* ONR-5, Oct. 1953, 31 pp.

**Calculation of the Heats of Formation of Gaseous Free Radicals and Ions,** by

J. L. Franklin, *J. Chem. Phys.*, vol. 21, Nov. 1953, pp. 2029–2033.

**Prediction of Liquid-Vapor Equilibria from an Empirical Equation of State for Mixtures,** by George Galloway Duplaise Town, *Wisconsin Univ., Naval Res. Lab., Rep.* no. ONR-4, Aug. 1953, 14 pp.

**The Intermolecular Potentials for Some Simple Non-Polar Molecules,** by Edward A. Mason and William E. Rice, *Wisconsin Univ., Naval Res. Lab., Rep.* no. ONR-6, Nov. 1953, 34 pp.

**Theory of the Formation of Bubbles,** by Shumsuke Takagi, *J. Applied Phys.*, vol. 24, Dec. 1953, pp. 1453–1461.

## Instrumentation and Experimental Techniques

**Measurement of the Size Distribution of Spray Particles,** by L. K. Wheeler and E. S. Trickett, *Electronic Engineering*, vol. 25, no. 308, Oct. 1953, pp. 402–406.

**An Investigation into the Possibilities of Adapting the Hot Wire Anemometer to Liquid Phase Measurement,** by David T. Harrje, *Princeton Univ., Dept. Aeron. Engng., Rep.* no. 237, Oct. 1953, 40 pp.

**Analysis of Transient Aerodynamic Heating Problems with GEDA Equipment,** *Goodyear Aircraft Corp., Rep. No.* GER-5434, June 1953, 17 pp.

**The Use of Radar to Measure the True Air Speed of an Aircraft,** by J. Warner, and K. J. Heffernan, *J. Roy. Aeron. Soc.*, vol. 57, Oct. 1953, pp. 653–655.

**A Thermistor Calorimeter for Heats of Wetting, Entropies from Heats of Wetting and Absorption Data,** by A. C. Zettlemoyer, G. J. Young, J. J Chessick, and F. H. Healey, *J. Phys. Chem.*, vol. 57, Oct. 1953, pp. 649–652.

**Burning Time and Ignition Temperature Apparatus for Metal Powders,** by Holger C. Andersen and Lawrence H. Belz, *Rev. Sci. Inst.*, vol. 24, Oct. 1953, pp. 1004.

**The Polarographic Determination of Tin in Propellants,** by C. Rubaudo, *Picatinny Arsenal, Tech. Rep.* 1974, Oct. 1953, 6 pp.

**Pressure Response in Supersonic Wind-Tunnel Pressure Instrumentation,** by Arnold L. Ducoffe, *J. Applied Phys.*, vol. 24, Nov. 1953, pp. 1343–1354.

**Wire Resistance Strain Gage Practice,** by Chr. Rohrbach, *Arch. Tech. Messen.* no. 213, Oct. 1953, pp. 237–240, 25 references (in German).

**Control System Requirements for Ramjet Missiles,** by James C. Wise, *Aviation Age*, vol. 2, Nov. 1953, pp. 64–70.

**A New Space Rate Sensing Instrument,** by Josseph Lyman, *Aero. Engng. Rev.*, vol. 12, Nov. 1953, pp. 24–30.

**General Theory and Operational Characteristics of the Gyratron Angular Rate Tachometer,** by Roland E. Barnaby, John B. Chatterton, and Fred H. Gerring, *Aero. Engng. Rev.*, vol. 12, Nov. 1953, pp. 31–36, 106.

**Monitor for Automatic Pilots,** by John J. Hess, Jr., *Electronics*, vol. 26, Dec. 1953, pp. 174–177.

**Guided-Weapons Telemetering, the Two Principal Systems Developed by the Ministry of Supply (Gt. Brit.),** *Flight*, vol. 64, Oct. 23, 1953, pp. 556–558.

**Radio-Frequency Mass Spectrometer for Upper Air Research,** by John W. Townsend, Jr., *Naval Research Lab., Rep. No.* 3928, Jan. 1952, 8 pp.

**High Frequency Pressure Indicators for Aerodynamic Problems,** by Y. T. Li, *NACA TN* 3042, Nov. 1953, 52 pp.

**Very Accurate Measurements of Fringe Shifts in an Optical Interferometer Study of Gas Flow,** by Ernst H. Winkler, *Rev. Sci. Instrum.*, vol. 24, Nov. 1953, pp. 1067–1068.

**A Geomagnetic Field Angular Orientation Indicator for a Rocket,** by Donald M. Packer, *Naval Res. Lab., Rep.* 4247 (*Upper Atmosphere Res. Rep.* 19) Nov. 1953, 16 pp.

**Rocket-Borne Servo Tracks the Sun,** by D. S. Stacey, G. A. Stith, R. A. Nidey, and W. B. Pietenpol, *Electronics*, vol. 27, Jan. 1954, pp. 149–151.

## Terrestrial Flight, Ballistics, and Vehicle Design

**Taking Man to Higher Altitude,** by A. M. Mayo, *Soc. Auto. Engrs., Prep.* no. 144, Sept. 1953, 8 pp., 11 figs.

**Fabrication of the Orbital Vehicle,** by K. W. Gatland, A. M. Kunesch, and A. E. Dixon, *J. Brit. Interplan. Soc.*, vol. 12, Nov. 1953, pp. 274–285.

**A Study of the Applicability of the Unsteady One Dimensional Isentropic Theory to an Experimental Gun,** by A. E. Seigel, *Naval Ord. Lab., NAVORD Rep.* 2692 (*Aeroballistic Res. Rep.* 79), July 1952, 34 pp.

**Design Trends—Guided Missiles,** by Clark B. Millikan, *Aero. Engng. Rev.*, vol. 12, Dec. 1953, pp. 82–87, 129–130.

**Douglas X-3, "The Flying Stiletto,"** *American Aviation*, vol. 17, Dec. 17, 1953, p. 17.

**Design of Military Aircraft,** by J. H. Kindelberger, *Aero. Engng. Rev.*, vol. 12, Dec. 1953, pp. 42–49, 125–126.

**A Guide to High-Altitude Rocket Design,** by Richard C. Lea, *Aviation Week*, vol. 59, Dec. 28, 1953, pp. 28–31.

## Space Flight

**Solar Space, Part I. A New Map of Solar Space,** by Wayne Proell, *J. Space Flight*, vol. 5, Oct. 1953, pp. 1–9.

**Solar Space, Part II. The Probability of Planets in Solar Space,** by Wayne Proell, *J. Space Flight*, vol. 5, Nov. 1953, pp. 1–7.

## Astrophysics, Aerophysics, and Atomic Physics

**The Propagation of Weak Spherical Shocks in Stars,** by G. B. Whitham, *Comm. Pure and Appl. Math.*, vol. 6, Aug. 1953, pp. 397–414.

**Radio Astronomy,** by Hans Herbert Klinger, *J. Franklin Inst.*, vol. 256, Oct. 1953, pp. 353–366.

**Air Force Cambridge Research Center. Geophysics Research Directorate, Geophysical Research Paper No. 19** (*AFCRC Technical Report* 59-9), Dec. 1952, 530 pp., International Symposium on Atmospheric Turbulence in the Boundary Layer, Massachusetts Institute of Technology, June 4–8, 1951.

**Radio Echo Studies of Meteor Ionization,** by T. R. Kaiser, *Advances in Physics*, vol. 2, Oct. 1953, pp. 495–544.

**V-2 Rocket in Upper Atmosphere Research,** by Charles F. Green, *Aero Digest*, vol. 67, Nov. 1953, pp. 20–26.

**Measurement of Variations in Atmospheric Refractive Index with an Airborne Microwave Refractometer,** by Howard E. Bussey and George Birnbaum, *J. Res. Nat. Bur. Stand.*, vol. 51, Oct. 1953, pp. 171–178.

**The Use of Clouds for Locating the Jet Stream,** by Vincent J. Schaefer, *Aeroplane*, vol. 85, Oct. 30, 1953, pp. 599–602.

**Astronautics,** by Antonio Eula, *L'Aerotecnica*, vol. 33, June 1953, pp. 231–244 (in Italian).

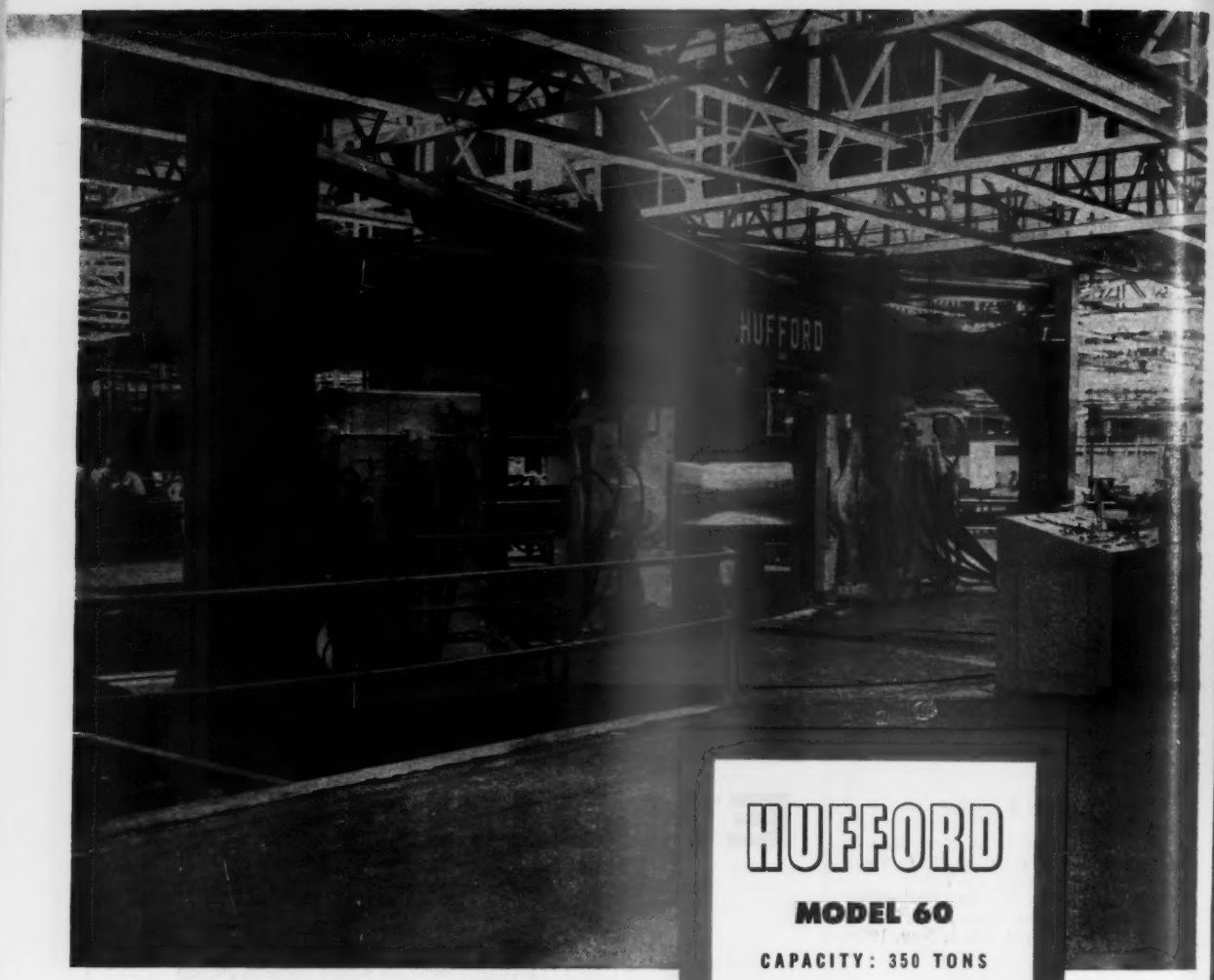


PHOTO COURTESY NORTH AMERICAN AVIATION INC COLUMBUS DIVISION.

# World's Largest Stretch-Wrap Forming Machine

## Goes to work for North American Aviation Inc., Columbus, Ohio

The Model 60 is Hufford's largest stretch-wrap forming machine to date, exceeding the capacity of all existing stretch-wrap forming machines in the world today.

With its 703,720 pounds of "pull" it is now forming stabilizer fairings, panels and fuselage skin parts for the new FJ-2 FURY. New dies will utilize its huge capacity on sheets measuring 6 feet wide by 31½ feet long. Its tremendous strength enables formation of sheet thicknesses as great as ½ inch!

The Model 60 opens another chapter in stretch-wrap forming history, *almost doubling the capacity of the largest Hufford press heretofore built.* It is Hufford's answer to unusual requirements of the present in preparation for the commonplace of the future!

Hufford

HUFFORD Machine Works Inc.
EL SEGUNDO CALIFORNIA

Manufacturers of

# moment in history

You are looking at 1/1000 of a second in the history of aviation. It occurred at a fraction past 4:31 p.m. on January 20, 1949.

This was the Zero moment which marked the official launching of the first successful pilotless bomber to be approved by the U.S. Air Force—the Martin B-61 Matador.

The picture is historic for a very significant reason: it records the tradition-shattering payoff of an entirely new development in the aircraft industry, known as Martin Systems Engineering. This is a science and a method of developing spaceborne systems as total solutions of Operations problems.

The Martin Matador is far more than the thing you glimpse here. Behind it is an integrated network of facilities designed to give this important new weapon simplicity of operation and extreme mobility. These components add up to the total solution of one of the most formidable security problems of our time.

They also add up to one of today's most important developments: the full story of Martin Systems Engineering.

*You will hear more about Martin!*

Martin AIRCRAFT

THE GLENN L. MARTIN COMPANY
BALTIMORE · MARYLAND

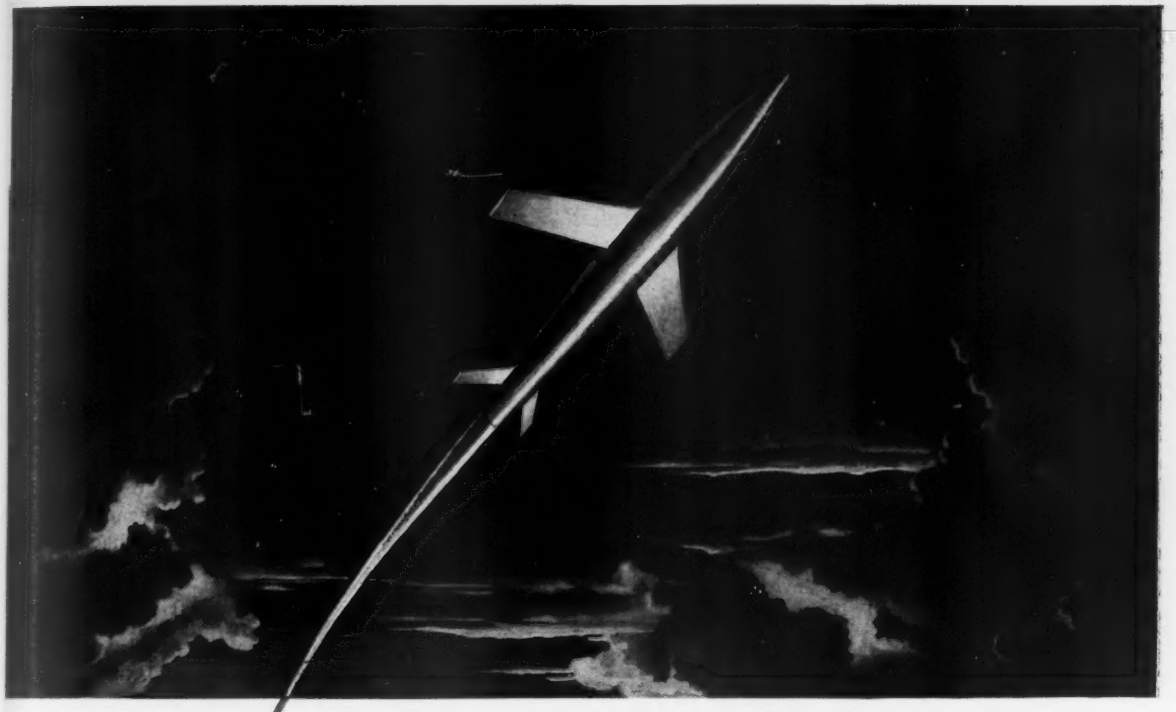

# OUTWARD BOUND · · · Controlled All the Way by—

# STRATOPOWER
## HYDRAULIC PUMPS

To the layman, the pinpointing of a destination for a guided missile is still pure magic. But to the engineer, the control and guidance of rockets and guided missiles in flight simply means another application for STRATOPOWER quality and advanced design.

The unerring performance of STRATOPOWER Pumps has been demonstrated times without number down through the years. At sea level and at heights still to be achieved these perfect examples of precision engineering provide the fluid power that positively answers the question of weight vs. horsepower as well as the equally important requirement of long-lived dependability.

In the designing of any high pressure hydraulic circuit there are definite advantages in STRATOPOWER Pumps. Whether yours is a problem for constant or variable delivery, high or low temperature operation, capacities from .25 to 30 gpm, STRATOPOWER will provide the pump to 3000 psi that will resolve that problem NOW!

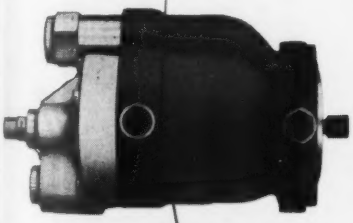

**The 66W Series of STRATOPOWER Hydraulic Pumps embrace a range of models from 2 to 10 gpm at 1500 rpm with continuous pressures to 3000 psi. Designed for maximum continuous speed of 3750 rpm... intermittent speeds to 4500 rpm.**

*Write* ***Get the full story on STRATOPOWER constant and variable delivery Pumps for your hydraulic circuits.***

**WATERTOWN** DIVISION
**THE NEW YORK AIR BRAKE COMPANY**
**STARBUCK AVENUE • WATERTOWN • N. Y.**

WATERTOWN DIVISION
THE NEW YORK AIR BRAKE COMPANY
730 Starbuck Avenue • Watertown, N. Y.

Kindly send me information on STRATOPOWER Hydraulic Pumps

☐ Constant delivery ☐ Variable delivery

Name_____

Company_____

Address_____

City_____ Zone____ State_____

## Index to Advertisers

# Extreme Temperature and Altitude Problems Solved by New Modifiable Titeflex Connector

We have the experience to solve most complex connector problems involving extreme altitudes, temperatures and pressures with space and weight limitations. And within standard design requirements, we can develop special-duty connectors as a part of complete wiring systems.

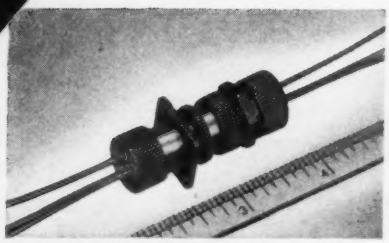

***INSTRUMENTATION*** Connector —07. For moisture and corrosion resistance, temperature ranges of −65°F. to +400°F. Made of Teflon, plug and receptacle mated weigh only ⅔ oz. Length 2". Insulation properties will permit 3500 volts at sea level, 1200 volts at 50,000 feet altitude. Can be made with 2 or 3 pins, current 7 amperes.

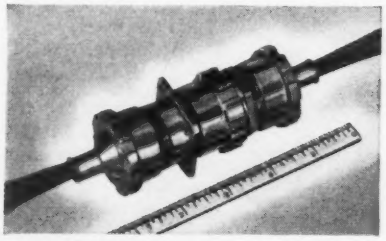

***MOISTURE-PROOF*** and resistant to synthetic lubricants. For extreme temperature changes in ranges of −65°F. to +400°F., high altitudes up to 65,000 feet. Resists salt spray, corrosion, vibration. This Titeflex Connector is radio shielded, has positive retention of pins and sockets. 5" in length. Mates with connectors that conform to MIL-C-5015.

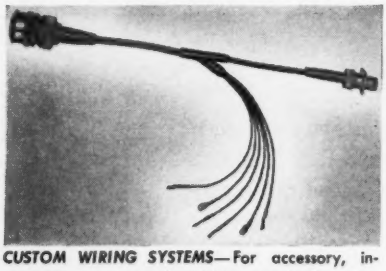

***CUSTOM WIRING SYSTEMS***—For accessory, instrumentation and radio shielded applications. Can be furnished with Titeflex or Standard AN Connectors. Can be sheathed with one or more layers of various metal braids, fiber glass or nylon, and jacketed with silicone or various other compounds. Titeflex will be glad to design, develop and produce complete wiring systems to your specifications.

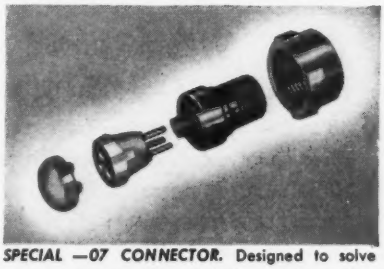

***SPECIAL —07 CONNECTOR.*** Designed to solve your connector problems in instrumentation with a real saving in space and weight since this connector has no protuberance beyond the flange. Can be designed as an integral part of your wiring or instrument components. Available in 1, 2 or 3 pin arrangements—current 7 amperes, size 1" in length. Receptacle and plug weigh only 11 grams.

**All TITEFLEX Connectors can be furnished with thermocouple pins and sockets.**

*WRITE TODAY for specific information—or send us your specifications. Whatever your requirements, we can usually provide the right answer. Our Engineering Staff will be glad to discuss your problem without obligation.*

**LET OUR FAMILY OF PRODUCTS HELP YOURS**

**Titeflex**

**TITEFLEX, INC.**
578 Frelinghuysen Avenue, Newark 5, N. J.

MAIL COUPON TODAY

Please send me your catalog on the Titeflex Connector.

Have your representative call ☐.

NAME_____

TITLE_____

COMPANY_____

ADDRESS_____

CITY_____ ZONE_____ STATE_____

# LAVOIE

## FOR THE NEWEST and BEST in ELECTRONIC EQUIPMENT

**FREQUENCY METERS**

Three frequency meters accurate to 0.001% cover ranges from 10 to 2000 MC. Model LA-5 covers the 10 to 100 MC range, LA-6, 100 to 500 MC and LA-61 500 to 2000 MC.

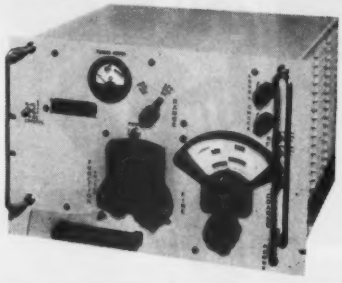

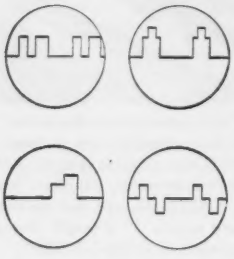

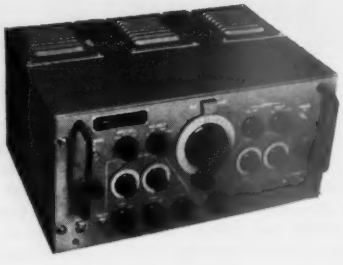

**PULSE GENERATOR—MODEL LA-592D**

A double-pulse generator with wide range control, excellent pulse shape. Eliminates necessity for many instruments usually required in an electronics laboratory.

**OSCILLOSCOPE—MODEL LA-239C**

The new and improved Lavoie oscilloscope offers wider frequency range, greater sensitivity and faster rise time. The Lavoie Camera Adapter may be added quickly and without modification.

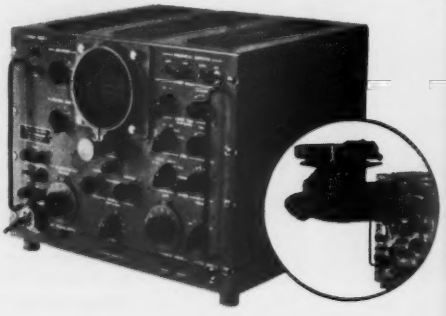

At The I.R.E. Show
BE SURE TO SEE
Low Cost Marine
Radar by Lavoie
BOOTHS 400-401-500
Production Road, Opposite Components
and Electronics Aves.

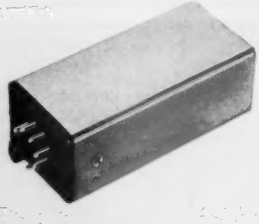

**PRECISION CRYSTAL OVEN 75° or 85° C**

Maintains crystal temperature to within 0.025° C at normal room temperature—to within .15° C over outside range from -40° F to 150° F. Available for HC 6 or HC 13 crystal units.

UHF

*Lavoie Laboratories, Inc.*

MORGANVILLE, NEW JERSEY